TRANSPORTATION RESEARCH RECORD 893

Distress Measurement and Interaction of Vehicles with Pavement Surfaces

TRANSPORTATION RESEARCH BOARD

NATIONAL RESEARCH COUNCIL

NATIONAL ACADEMY OF SCIENCES
WASHINGTON, D.C. 1982

Transportation Research Record 893
Price $9.20
Edited for TRB by Susan Singer-Bart

modes
1 highway transportation
4 air transportation

subject areas
24 pavement design and performance
51 transportation safety

Library of Congress Cataloging in Publication Data
National Research Council. Transportation Research Board.
Distress measurement and interaction of vehicles with pavement surfaces.

(Transportation research record; 893)
Reports for TRB 61st annual meeting.
1. Pavements–Addresses, essays, lectures. I. National Research Council (U.S.). Transportation Research Board.
II. Series.
TE7.H5 no. 893 380.5s [625.8'028'7] 83-8215 [TE250]
ISBN 0-309-03505-8 ISSN 0361-1981

Sponsorship of the Papers in This Transportation Research Record

GROUP 2–DESIGN AND CONSTRUCTION OF TRANSPORTATION FACILITIES
R. V. LeClerc, consultant, Olympia, Washington, chairman

Pavement Design Section
W. Ronald Hudson, University of Texas at Austin, chairman

Committee on Surface Properties-Vehicle Interaction
Don L. Ivey, Texas Transportation Institute, chairman
Glenn G. Balmer, Frederick E. Behn, Robert R. Blackburn, John C. Burns, A. Y. Casanova III, John D. Eagleburger, Robert D. Ervin, Rudolph R. Hegmon, Edward D. Howerter, Kenneth J. Law, David C. Mahone, W. E. Meyer, Thomas H. Morrow, Jr., W. Grigg Mullen, Bobby G. Page, A. Scott Parrish, Bayard E. Quinn, John J. Quinn, J. Reichert, Hollis B. Rushing, Elson B. Spangler, James C. Wambold, E. A. Whitehurst

Committee on Pavement Condition Evaluation
K. H. McGhee, Virginia Highway & Transportation Research Council, chairman
Doyt Y. Bolling, Michael I. Darter, Karl H. Dunn, Asif Faiz, Robert H. Gietz, Wouter Gulden, Lawrence E. Hart, William H. Highter, W. Ronald Hudson, Don H. Kobi, Scott A. Kutz, J. W. Lyon, Jr., Robert L. Novak, Richard D. Pavlovich, William A. Phang, Freddy L. Roberts, Albert F. Sanborn, Lawrence L. Smith, Herbert F. Southgate, Elson B. Spangler, Shiraz D. Tayabji, Loren M. Womack

Lawrence F. Spaine, Transportation Research Board staff

Sponsorship is indicated by a footnote at the end of each report. The organizational units, officers, and members are as of December 31, 1981.

Contents

Authors of the Papers in This Record

Anderson, D. A., Pennsylvania Transportation Institute, Pennsylvania State University, University Park, PA 16802
Cheng, Kuangti Ted, Pennsylvania Transportation Institute, Pennsylvania State University, University Park, PA 16802
Chong, G. J., Research and Development Branch, Ministry of Transportation and Communications, 1201 Wilson Avenue, Downsview, Ontario M3M 1J8, Canada
Garrott, W. Riley, Vehicle Research and Test Center, National Highway Traffic Safety Administration, U.S. Department of Transportation, P. O. Box 37, East Liberty, OH 43319
Guenther, Dennis A., Department of Mechanical Engineering, Ohio State University, Columbus, OH 43210
Hartgen, David T., Transportation Statistics and Analysis Section, Planning Division, New York State Department of Transportation, 1220 Washington Avenue, State Campus, Albany, NY 12232
Hayhoe, Gordon F., Pennsylvania Transportation Institute, Pennsylvania State University, University Park, PA 16802
Henry, John Jewett, Pennsylvania Transportation Institute, Research Building B, Pennsylvania State University, University Park, PA 16802
Hudson, W. Ronald, Department of Civil Engineering, University of Texas at Austin, Ernest Cockrell, Jr., Hall 6.100, Austin, TX 78712
Koeppel, K.-W. P., Transportation Statistics and Analysis Section, Planning Division, New York State Department of Transportation, 1220 Washington Avenue, State Campus, Albany, NY 12232
Lenke, Lary R., New Mexico Engineering Research Institute, Campus P. O. Box 25, University of New Mexico, Albuquerque, NM 87131
McKenzie, David W., Center for Transportation Research, University of Texas at Austin, Austin, TX 78712
Parrella, Frank T., Transportation Statistics and Analysis Section, Planning Division, New York State Department of Transportation, 1220 Washington Avenue, State Campus, Albany, NY 12232
Phang, W. A., Research and Development Branch, Ministry of Transportation and Communications, 1201 Wilson Avenue, Downsview, Ontario M3M 1J8, Canada
Shahin, M. Y., U. S. Army Construction Engineering Research Laboratory, P. O. Box 4005, Champaign, IL 61820
Shufon, John J., Transportation Statistics and Analysis Section, Planning Division, New York State Department of Transportation, 1220 Washington Avenue, State Campus, Albany, NY 12232
Spangler, Elson B., Surface Dynamics, Inc., 1465 Sodon Lake Drive, Bloomfield Hills, MI 48013
Wambold, J. C., Pennsylvania Transportation Institute, Pennsylvania State University, University Park, PA 16802
Yeh, E. C., Pennsylvania Transportation Institute, Pennsylvania State University, University Park, PA 16802

Visual Scales of Pavement Condition: Development, Validation, and Use

DAVID T. HARTGEN, JOHN J. SHUFON, FRANK T. PARRELLA, AND K.-W.P. KOEPPEL

This paper describes the procedures used by the New York State Department of Transportation to develop visual scales for assessing the condition of pavements in New York State. The paper describes the use of a psychometric scaling method known as Q-Sort to develop visual scales of pavement surface condition and the condition of base material that underlies the pavement. A panel of eight experts from the department's operating units reviewed more than 50 photographs of pavements and rated them on a scale of 1-10 for surface and base condition. Subsequent analysis produced a set of photographs representative of each position on the scales. Test-retest reliability was conducted by using the same eight judges two months later to demonstrate the replicative nature of the scales and their stability over time. These scales were then used to train scorers from the department's 11 regional offices, and scoring of the entire state highway system was conducted. Results were available within several weeks and summaries were made of the condition of the highway system in 1981. The paper concludes that the use of visual scales in highway scoring is a practical and accurate method of assessing pavement condition. It also concludes that, although the use of such scaling procedures has lagged in pavement analysis, their use should be expanded in the future as continuing assessments of highway condition are needed.

Of all the issues that confront transportation analysts in the 1980s, perhaps the most significant and possibly the most difficult to deal with is the issue of the deterioration of transportation systems. The condition of highway pavements in the United States is deteriorating as these systems age and are subjected to greater and more severe traffic loads (1). In some cases pavements constructed in the 1930s and 1940s have deteriorated to the point where their structural integrity is now impaired and traffic is slowed. To make matters worse, Interstate highways constructed in a relatively short time span in the 1950s and 1960s are now approaching the end of their design lives and will require significant rehabilitation to protect the initial investments. Funding for restoration and rehabilitation of the Interstate system is not enough to keep up with needs. This shortage comes at precisely the same time as increases in construction costs, declining revenues, and inflation have constrained governments' ability to finance the necessary improvements (2). Given projected deterioration rates of highways (1) and the likelihood that current revenues will decline as gasoline use falls (3), significant attention must be paid to this problem soon.

A periodic accurate assessment of the condition of various types of highway pavements is of critical importance in determining highway needs. The primary reason for accurate and timely information on condition is that it leads us to better decisions on investment policy. These decisions are crucial to developing a program that will provide the most service to the public per dollar invested. To achieve this goal, such assessments must be conducted periodically so that we may evaluate the changes in highway condition over time. Such assessments must be conducted and reported rapidly if their use is to be maximized.

The purpose of this paper is to describe recent activities at the New York State Department of Transportation (NYSDOT) to develop and implement straightforward windshield survey procedures for assessing pavement condition in a rapid, consistent, and accurate fashion. These procedures parallel the visual assessment procedures developed by Arizona and Ontario (4) and the federal highway performance monitoring system scoring methods (5), as well as the early American Association of State Highway Officials (AASHO) scaling procedures (6). This paper describes how such visual scales can be developed, validated, and used. Results of the 1981 survey are also presented. The primary conclusion is that such methods are reliable and capable of producing the necessary information in rapid fashion with sufficient accuracy.

DEVELOPMENT OF VISUAL CONDITION SCALES

A scale is a sequence of items such that each item, or the total group, has a specific numerical level associated with it. This is not an arbitrary assignment but one in which certain properties of the scale (e.g., origin, distance, and order) are preserved. Although we are all familiar with common examples of certain scales (e.g., rulers and thermometers) other scales can be constructed from words, photographs, and statements. Procedures for developing scales are well developed (7,8). A complete discussion of such procedures is outside the scope of this paper; the reader should realize that numerous methods of construction of such scales are treated extensively in the psychology literature.

In the area of transportation, visual and verbal scales have been used for a number of years. Verbal scales have been developed to measure the characteristics of transportation services (9), such as comfort, convenience, and cost. In a recent review of such studies, Tischer (10) found more than 100 examples of the use of transportation attitude scales constructed from verbal assessments. These scales relate primarily to public perceptions of the characteristics of transit services but have also been applied to visual assessments of highway environment, perceptions of highway impacts, and opinion studies on highway financing. The New York State Department of Transportation has also developed and used many such scales.

The procedure used to develop visual scales for highway condition is straightforward. Scales were developed by using department experts (judges). Regional personnel were then trained in their use, condition assessment was conducted, and summaries were prepared. Scales of pavement condition focused on two measures of pavement quality:

1. The condition of the pavement surface and
2. The condition of the base that underlies the pavement surface, described as the rupture and displacement rating.

The scales were developed by using a modification of a technique known as Q-sort (8). This is a standard method in psychometrics that has seen wide use in the development of visual scales. Basically, the method involves sorting or rating a number of preselected items (e.g., photographs and words) by some criteria (in this case, photographs of highway pavements are rated according to condition). The initial rating process is done by judges who apply expert knowledge to the sorting process. From a large number of sorted photographs, a few photographs are then selected, by statistical or other

Figure 1. Photographic scales of pavement condition.

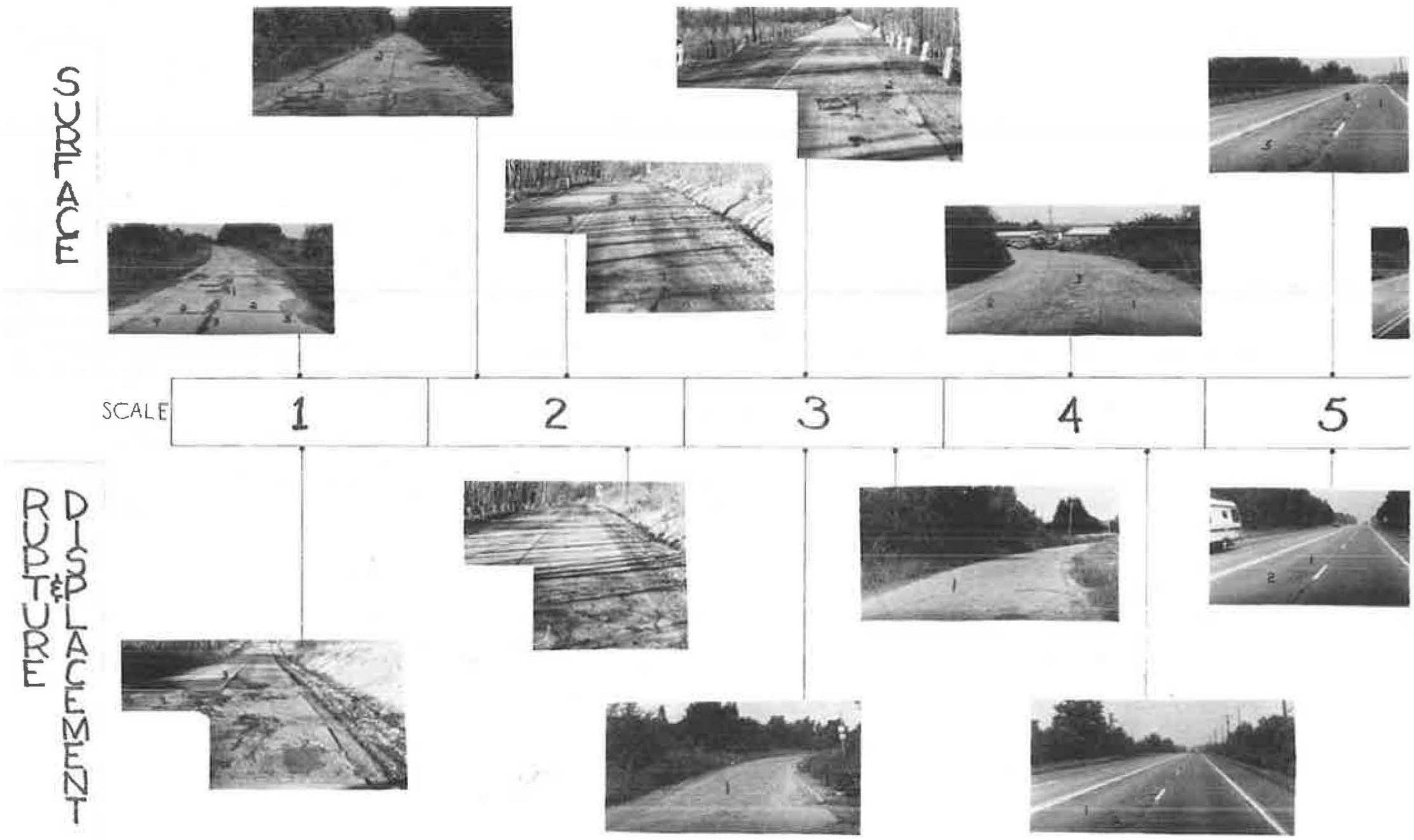

means, to form the final scale. The procedure is then repeated (usually after several months) and test-retest reliability estimates are prepared. Once developed and validated, the resulting scale, which consists of a small set of photographs to represent the scale points, is then used to train regional scorers in rating highways. If constructed carefully, the scales may then be used with confidence by others in scoring the condition of highways.

In the NYSDOT application of Q-sort, a panel of experts from the department's staff rated preselected photographs. A total of eight judges participated, representing the major program areas of the department [planning, project development, programming, soil mechanics, engineering research (2), highway maintenance, and highway construction]. The judges' qualifications included engineering degrees, engineering licenses, and 10-20 years of pavement-related experience.

The first step in the process was to develop a set of verbal scales of highway conditions. NYSDOT had previously developed 10-point verbal scales of highway condition that had been used for many years in the periodic sufficiency series of pavement condition evaluation. Through discussions with the judges and other experts, these verbal scales were carefully reviewed and refined. The results of these technical discussions are given in the list below, which gives the actual verbal descriptions prepared for surface rating.

10--Visually, pavement should show no deviations from a smooth surface. Pavement probably was recently constructed or reconstructed within the past year or two.

9--Facilities should have no cracks or patches. Pavement probably was recently resurfaced within the past year or two.

8--Pavements in this category give an excellent ride and exhibit only a few signs of surface deterioration. Flexible pavements may start to show slight evidence of rutting and fine random cracks. Rigid pavements may start to show evidence of surface deterioration such as minor cracks, slight joint spalling, or scaling.

7--Pavements in this category still give a good ride but are starting to show definite signs of surface deterioration. Flexible pavements show evidence of slight rutting, random cracking, and possibly some raveling. Rigid pavements show evidence of joint spalling, scaling, or minor cracking.

6--The riding qualities of pavement in this category are noticeably inferior to those of new pavements. Surface defects of flexible pavements may include rutting, cracking, and possible raveling; patching is also apparent. Surface defects of rigid pavements may include slight joint spalling, faulting, or cracking, and patching is apparent.

5--The riding qualities of pavements in this category are noticeably inferior to those of new pavements and may be barely tolerable for high-speed traffic. Surface defects of flexible pavements may include moderate rutting, cracking, and raveling and could have frequent patching. Surface defects of rigid pavements could include joint spalling, some faulting, moderate-to-heavy cracking, and frequent patching.

4--Pavements in this category have deteriorated to a point where resurfacing may be required. Rideability, even at slow speeds, is impaired. Surface defects of flexible pavements could include such signals as frequent rutting, cracking, raveling, and

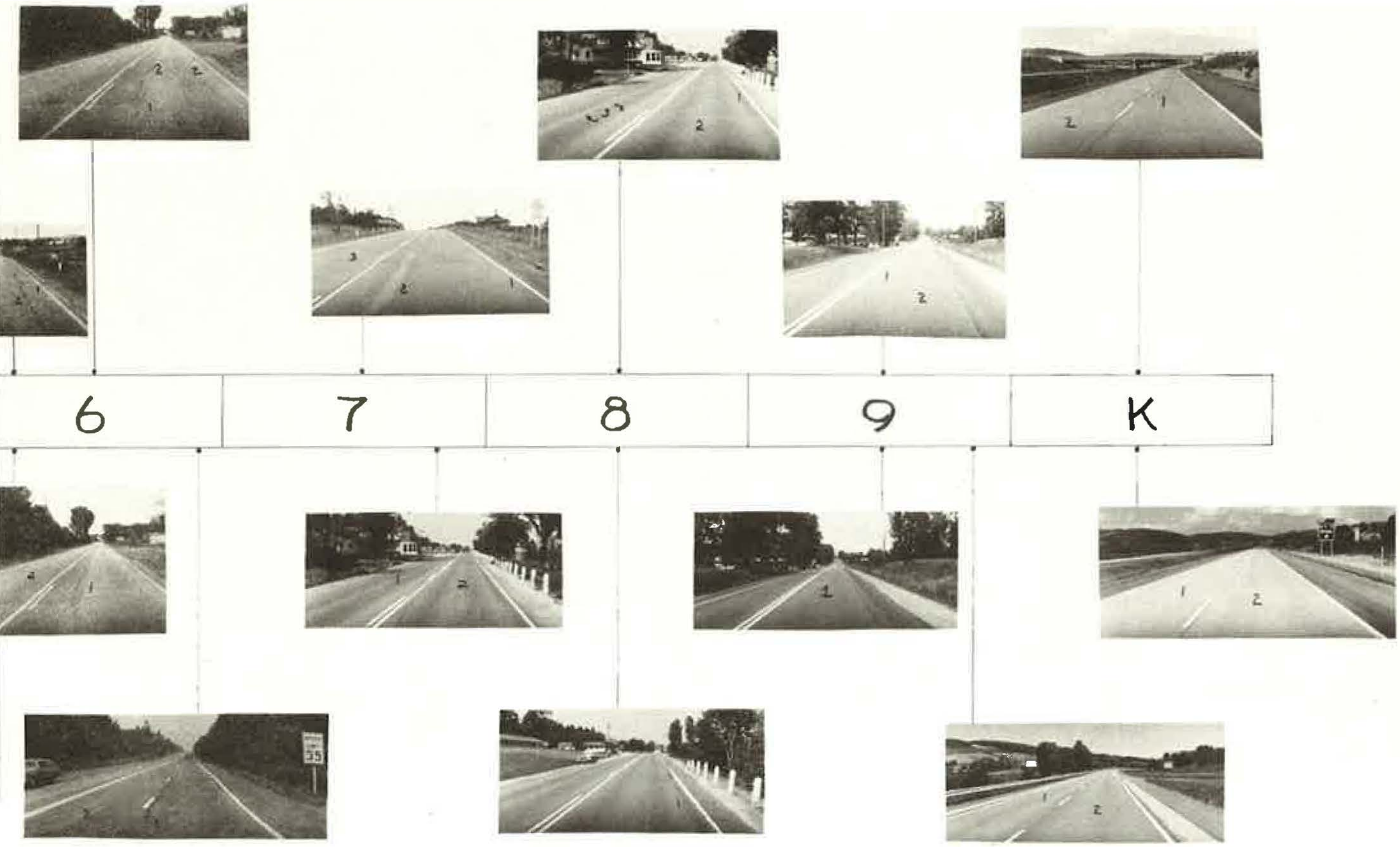

patching. Surface defects of rigid pavements might include frequent joint spalling, moderate faulting, severe cracking, and frequent patching.

3--Pavements in this category have deteriorated to a point where resurfacing is required immediately. Rideability at any speed is so impaired that the motorist will experience discomfort. Surface defects of flexible pavements may include severe and frequent rutting, cracking, raveling, and patching. Surface defects of rigid pavements will include severe and frequent scaling, joint spalling, faulting, cracking, and patching.

2--Pavements in this category are in an extremely deteriorated condition and may even require complete reconstruction. Motorists experience discomfort and traffic will slow down.

1--Pavements in this category are in an extremely deteriorated condition and are in need of some immediate corrective action. These facilities could be considered impassable at posted speeds.

The verbal descriptions of rupture and displacement rating are given in the list below.

10--Riding quality of roadways in this category should be excellent, and there will probably be no indications of any subsurface shifting. Facilities newly constructed within the last year or two generally will fall into this category. Close attention should be directed to evaluation of any riding quality that could be attributable to a displacement of the base material, which can happen even on recently constructed facilities and would preclude such a facility from receiving a 10 rating. These modifiers also apply to the 9 rating as well.

9--Riding quality is also excellent, with little or no indications of subsurface problems. Facilities reconstructed or rehabilitated within the last year or two fall into this category.

8--Facilities fall into this category if there is no evidence of base or subbase deterioration, as reflected by the pavement surface.

7--Roadways in this category are beginning to show signs of rupture and displacement caused by roadbed movement. Flexible and rigid pavements may show slight evidence of longitudinal or transverse cracking.

6--Roadways in this category show definite but infrequent signs of distress (e.g., cracks) caused by roadbed movement or inadequate roadbed support. Flexible pavements show evidence of moderate longitudinal and transverse cracking. Rigid pavements show signs of moderate longitudinal, transverse, or random cracking.

5--Roadways in this category show occasional signs of distress caused by roadbed movement or inadequate roadbed support. Flexible pavements show evidence of severe longitudinal or transverse cracking and may be beginning to show evidence of block or reflection cracking. Rigid pavements show evidence of severe longitudinal, transverse, or random cracking and may start to show signs of corner or diagonal cracking caused by a loss of the foundation material under the slab.

4--Roadways in this category show frequent signs of distress caused by roadbed movement or inadequate roadbed support. Flexible pavements may show signs of moderate block or reflection cracking and slight alligator cracking. Rigid pavements show evidence of moderate corner or diagonal cracking caused by a loss of foundation material under the slab.

3--Roadways in this category show frequent signs

Table 1. Test-retest correlations of judges' ratings of pavement condition from 50 test photographs.

	Surface			Rupture-Displacement		
Judge	r	Slope	Inter-cept	r	Slope	Inter-cept
A	0.974	0.953	0.294	0.968	1.002	−0.320
B	0.975	0.933	0.522	0.911	0.805	0.908
C	0.972	1.030	−0.287	0.784	0.741	1.240
D	0.962	1.003	0.122	0.969	0.987	−0.190
E	0.956	1.230	−2.420	0.871	0.700	2.190
F	0.953	1.024	−0.839	0.937	0.836	0.599
G	0.947	1.053	−0.365	0.852	0.901	0.874
H	0.942	0.910	0.528	0.853	0.834	0.789
Overall	0.950	0.975	0.009	0.902	0.851	0.722

Table 2. ANOVA results of test-retest of surface and base scales by expert judges.

Source of Variation	Sum of Squares	Variance (%)	df	Mean Square	F-Tests[a]	
Surface						
Photograph	5321.9	86	9	591.3	0.00	
Judges	147.0	2	7	21.0	0.00	0.01
Date	4.2	<<0.1	1	4.2	0.02	0.07
Interaction terms	234.8	4	142	1.7		
Error	520.0	8	640	0.8		
Total	6227.9	100	799			
Base						
Photograph	4353.8	67	9	483.8	0.0	
Judges	239.2	4	7	34.2	0.0	0.01
Date	4.5	<<0.1	1	4.5	0.16	0.07
Interaction terms	365.1	6	142	2.6		
Error	1479.7	23	640	2.3		
Total	6442.3	100	799			

[a]Tail probabilities.

of distress and may even show occasional roadway failures due to roadbed movement or inadequate roadbed support. Flexible pavements show signs of severe block and reflection cracking, and alligator cracking is especially visible through wheel-track rutting. Rigid pavements show evidence of severe corner and diagonal cracking and occasional pumping or faulting due to uneven roadbed support.

2--Roadways in this category are in an extremely deteriorated condition and may require complete reconstruction. Flexible pavements show frequent evidence of severe alligator cracking with rutting and possibly occasional bumping. Rigid pavements show evidence of frequent and severe cracking, pumping, and faulting.

1--Roadways in this category are in an extremely deteriorated condition. Flexible pavements show frequent evidence of severe alligator cracking with rutting or severe bumping. Rigid pavements show evidence of frequent and severe cracking, faulting, and pumping.

Technical definitions of terms (e.g., random cracks) were drawn from TRB's glossary (12); TRB's glossary was also used to illustrate specific distress signals of pavement deficiencies.

While these verbal scales were being developed, a set of photographs that represents a wide variety of highway conditions was prepared. The data base for this set of photographs is the department's photolog system, which is a visual record of the condition of state highways. Out of the very large number of photographs available for selection, 50 were selected by the researchers to span the range of highway condition, ranging from 1 to 10, as defined in the above verbal scales. No attempt was made to make the photographs representative (in a statistical sense) of the entire state highway system, since the purpose of the exercise is to develop a scale that is then used by others to score road condition.

Each of the judges was then provided with copies of the final verbal scales and copies of the 50 photographs. Each judge was asked to rank each photograph on the 1-10 scales, once for pavement surface condition and once for rupture and displacement (base) condition. No instructions were provided concerning how this ranking or scoring should be done other than that each photograph must be assigned a position on the scale. The resulting distribution of the photographs for each judge represents his or her perception of the degree to which the technical descriptors of highway conditions, as described in the verbal scales, are reflected in the visual photographs that represent the pavements. On completion of this assignment by each judge, the assigned category for each photograph was recorded.

The photographs were then reviewed by the analysis team and arranged according to the score position in which the greatest number of judges ranked the photograph (i.e., modal score). This resulted in each of the 10 categories containing a small group (3-7) of candidate photographs. The photographs within each category were then carefully reviewed by the analysis team for consistency of rating, low variance of rating, as well as an ability to show clearly typical problems with the pavement. Based on this assessment, the analysis team selected final photographs to best represent the categories. The positioning of the photographs and the final layout of the scales are shown in Figure 1.

VALIDATION

The scale established in this way needs some further analysis before it can be applied with confidence in the field. Questions to be answered include,

1. Are eight judges sufficient to establish a scale?
2. Are there significant differences between judges? and
3. Are the scales stable over time; i.e., are the judges able to reproduce their original ratings some time after the pictures were rated initially?

Research in psychology has shown that the number of judges required to establish a scale is surprisingly small. A recent study of highway condition in England (11) tested scales developed by different numbers of judges and found that scales developed with as few as 8 judges were capable of estimating the position of a given highway pavement to within one scale position on a seven-point scale with 95 percent confidence. Further, it was shown that once the number of judges exceeds about 15, little improvement in reliability is subsequently obtained.

To answer the questions concerning scale reliability over time and differences between judges, the eight experts were asked to rescore the 50 selected photographs two months after the initial scoring. The exact same procedures were used in this retest. A simple correlation-regression analysis of the two scoring results is given in Table 1 (a perfect line would have a correlation of 1.0, a slope of 1.0, and an intercept of 0.0). The overall correlation coefficient (r) for both retests is high, 0.95 for surface, 0.90 for base (rupture-displacement). The linear regressions show a good

Table 3. New York State touring routes, 1981 system condition.

Condition	Level	Surface Lane-Miles	Surface Percent	Base Lane-Miles	Base Percent
Excellent	10	1 188		1 115	
	9	1 439	6.6	1 442	6.4
Good-to-fair	8	8 381		6 473	
	7	13 487	80.4	10 610	72.6
	6	10 012		11 712	
Poor	5	3 828		5 641	
	4-1	1 325	13.0	2 668	21.0
Total		39 661		39 661	

degree of conformity among judges. The consensus of literature in psychological scaling (8) is that such results are considered excellent and indicate high reliability in the use of the final scales.

Table 1 also shows that the correlations are generally higher and more consistent for the surface ratings than for the rupture and displacement ratings. This suggests that it is more difficult to infer the state of the base from a photograph that primarily shows the surface. Therefore, judgment and experience would enter more heavily in assessing base conditions than surface ratings. In view of these concerns, a second analysis of the ratings was performed to test for differences attributable to differences among judges. This analysis was conducted by using analysis of variance (ANOVA), and the results are given in Table 2. Quite clearly, for both surface and base ratings, we find (expectedly) that most of the variance is explained by the photographs themselves. The variation attributable to judges or to time between tests (date) is considerably smaller. A standard F-test for the comparison of sources of variation shows all three sources to be significantly larger than the residual variation left unexplained. The same test shows that the variation between photographs, in turn, is significantly larger than the variation attributable to judges or time elapsed. Finally, for both scales the level of significance of other sources of variation drops off sharply. These results mean that, in actual use, the differences among scorers is likely to be small and can probably be eliminated with joint training of field scorers. The scales are also stable over time, and hence can be used (with training) in subsequent scoring with confidence that changes of pavement condition with time will not be confused with changes in the scale itself.

The first of these implications was fully addressed through training. The potential time consistency problem has not been fully addressed yet; however, it appears that this problem is slight for the eight expert judges undertaking this effort as a two-times only event. We are thus led to believe that it may be even slighter for the scoring teams that actually rate the state's road system, as these teams often have several years of experience at this task.

USE OF VISUAL SCALES IN HIGHWAY SCORING

The primary purpose of these visual scales is to enable a rapid and consistent assessment of the condition of New York State's highways. It was important, therefore, to ensure that all individuals conducting the 1981 scoring, from each of the department's 11 regional offices, be trained to assess highways in a consistent manner. To achieve this, a training session was held in the main office of NYSDOT in late April 1981. As part of the training, personnel were instructed in scoring by actually working with films of highways in various stages of condition.

A series of photolog films were shown that simulated travel over routes of the state highway system. Each film was scored and then discussed, and the individual scorers were then instructed on how to improve their ability to make judgments by using the visual scoring materials. Additional films of highways were then shown, and convergence of scoring among the different regional individuals was then evaluated. Training was repeated until convergence of scoring was reasonable.

At the conclusion of the training session each survey team was given computer-generated field sheets with locational information and physical characteristics of each highway link to be assessed listed contiguously by route. The raters traveled each highway section and coded the appropriate surface and base scores on the preprinted forms. Once completed, the field scoring sheets were transmitted to the main office for processing. Although the regional offices were given 14 weeks to complete the inventory (May-mid-August 1981) most of the regional administrators allowed the scoring crews about a one-month window in existing workloads to perform the survey.

Regional staff cooperation was excellent in reporting the results of the survey. In return, main office staff edited, processed, and tabulated the data as they came in and immediately provided each region with computer printouts in various formats. Statewide summaries were available by October 1981.

SURVEY RESULTS

Table 3 gives the results of the 1981 scoring. The overall pavement condition of the state touring route system is generally quite good, and road surfaces are in better condition (an average of level 6.82) than road bases (an average of level 6.53). Approximately 87 percent of road surfaces are in fair or better condition compared with about 79 percent of road bases. This is expected because recent department focus has centered on resurfacing projects rather than on more costly reconstruction activities. Of particular concern are highways in the lower end of the good-to-fair category. About 26 percent of the system is at level 6, just above the poor level. Without adequate attention, these highways will soon deteriorate to the poor range. Thus, although the overall system is in good shape, a significant share of facilities needs attention. Rigid pavements are in better shape, on the average, than flexible or overlay pavements (Table 4). The Interstate system is in the best overall condition (Table 5). The surfaces of the Interstate system average 7.51, bases 7.34, about a point above averages for the other federal-aid systems. Most of these Interstate highways (Thruway is excluded) are rigid and were constructed more recently than roads in the other systems. The average condition of urban roads is slightly better than that of rural roads.

CONCLUSIONS

The use of visual scales for assessing pavement condition is both practical and feasible. The development of such scales is straightforward and scoring may be completed rapidly. When constructed according to psychometric methods, the reliability of such scales is generally good.

Training is an integral part of the development and use of such scales. Training can be organized in such a way that the individual scorers from

Table 4. Condition of New York State touring routes by pavement type, 1981.

		Flexible		Overlay		Rigid	
Condition	Level	Surface	Base[a]	Surface	Base[a]	Surface	Base[a]
Excellent	10	345	313	420	388	423	415
	9	561	549	696	699	183	193
Good-to-fair	8	2 911	2 143	3 397	2 464	2072	1867
	7	4 158	3 153	5 998	4 822	3330	2635
	6	3 363	3 797	4 753	5 494	1896	2421
Poor	5	1 178	1 966	1 774	2 481	876	1184
	4-1	460	1 056	551	1 232	313	380
Total lane-miles		12 976	12 976	17 589	17 589	9093	9093
Mean score		6.83	6.46	6.77	6.44	6.90	6.73

[a]Differences in base lane-mile totals are due to rounding.

Table 5. New York State touring routes—1981 condition by federal-aid system.

			Avg Condition	
System	Roadway	Lane-Miles	Surface	Base
Interstate	Urban	2 155	7.46	7.34
	Rural	1 917	7.56	7.34
	Avg		7.51	7.34
Primary	Urban	6 251	6.69	6.55
	Rural	14 132	6.85	6.50
	Avg		6.80	6.52
Federal-aid urban system	Urban	4 645	6.80	6.56
Secondary	Rural	8 574	6.62	6.25
	Avg		6.68	6.35
Non-federal-aid	Urban	155	6.89	6.72
	Rural	1 831	6.49	6.02
	Avg		6.52	6.07
All urban		13 207	6.85	6.68
All rural		26 454	6.80	6.44
Overall		39 661	6.82	6.53

different regions of the state can use the scales with consistency over time.

The application of such methods to visual assessment of highways can be conducted in rapid fashion, thereby speeding up quantification of rehabilitation needs. Summarization of the results can provide a quick means of assessing network-level condition of pavements at the statewide, regional, or county level.

The condition of New York State's touring route system is generally good--87 percent of road surfaces and 79 percent of road bases are in fair or better shape. However, a significant portion of roadway is in poor condition and must be given attention in the near future. Rigid pavements in New York State are generally in better condition than flexible or composite pavements. The Interstate system is in significantly better condition than other federal-aid systems. The non-federal-aid rural portion of the system is in the worst condition.

REFERENCES

1. The Status of the Nations Highways: Conditions and Performance. Office of the Secretary of Transportation, U.S. Department of Transportation, Jan. 1981.
2. Price Trends for Federal Highway Construction. Federal Highway Administration, April 1981.
3. A.T. Reno, B.J. Ritchey, and J.R. Stowers; System Design Concepts, Inc. State Transportation Finance Within the Context of Energy Constraints. NCHRP, Rept. 231, April 1981, 86 pp.
4. Collection and Use of Pavement Condition Data. NCHRP, Synthesis of Highway Practice 76, July 1981, 74 pp.
5. Highway Performance Monitoring System (HPMF): Analytical Process and Applications. Office of Highway Planning, Federal Highway Administration, 1981.
6. The AASHO Road Test. HRB, Spec. Rept. 73, 1962, 438 pp.
7. W.S. Torgerson. Theory and Methods of Scaling. Wiley, New York, 1963.
8. J.C. Nunnally. Psychometric Methods. McGraw Hill, New York, 1967.
9. Charles River Associates. Data Inventory of Attitudes Toward Transportation Systems. Transportation Systems Center, U.S. Department of Transportation, Cambridge, MA, CRA Rept. No. 347, Oct. 1977.
10. M.L. Tischer. Attitude Measures: Psychometric Modeling. Paper presented at 4th International Conference on Travel Modeling, Grainau, West Germany, 1979.
11. A.O. Grigg. Rating Scales--Central Tendency and Sample Sizes. Transport and Road Research Laboratory, Crowthorne, Berkshire, England, Supplemental Rept. No. 647, 1981.
12. Standard Nomenclature and Definitions for Pavement Components and Deficiencies. HRB, Special Rept. 113, 1970, 29 pp.

Publication of this paper sponsored by Committee on Pavement Condition Evaluation.

Roughness Computer Program for Engineers and Management

KUANGTI TED CHENG, JAMES C. WAMBOLD, AND JOHN JEWETT HENRY

In this paper, a computer program developed to analyze pavement profile data is reported. The main functions of the program are to determine the present serviceability index and to analyze ride quality, either by use of the International Organization for Standardization (ISO) standard 2031 or the University of Virginia (UVA) model. The primary input is the pavement profile data. The present serviceability index analysis gives the user a value for every 0.1 mile, or any interval up to the total length of the pavement profile, at a user-specified vehicle velocity. The ride-quality analyses give the user the estimated exposure time of reduced comfort or fatigue if the ISO weights are used; if the UVA model is used, a ride quality index is given. For either model, the user can select the vehicle type, a linear or nonlinear transfer function, and the vehicle velocity. The program also includes some auxiliary functions, such as a paver-grinder simulator and a profilometer simulation that can produce, from the raw profilometer signals, a digital file of the profile as a function of distance. This paper discusses the models and simulations used. Although some of the analysis methods have been discussed in the literature, they have not previously been integrated into a single versatile package. Thus, a complete pavement surface analysis program (including several methods not reported in the literature) is available for pavement management.

Two major functions of a highway department are the planning of maintenance schedules for a system of existing roads and the acceptance of newly built or resurfaced roads. The decision to resurface a particular section of road in preference to others is not a simple one, for many factors must be taken into consideration. A large quantity of information is available to support an objective evaluation, and research is under way to permit the development of pavement management systems that use this information. The purpose of the program described here is to process and analyze the highway profile data collected by a profilometer or other road roughness measurement system.

PAVEMENT ROUGHNESS

The measurement of road roughness is of importance to the maintenance manager in determining pavement safety and serviceability. Recent developments in measuring equipment and data reduction systems will greatly expand the available data base. For example, at the present time, skid resistance and roughness are measured with operational equipment that collects data at a rate adequate for routine surveys. Research now in progress should make the measurement of pavement texture operational in the near future and thus provide additional information on skid resistance. Similarly, several noncontact sensors for roughness measurement are operational. Currently, most states that have General Motors Research Laboratories (GMR) profilometers use them to calibrate other road meters rather than as a tool for measuring surface conditions directly.

Both the type and the quantity of pavement condition data available to the management engineer will increase dramatically in the near future. These data must be analyzed and made available in a format that is compatible with maintenance management systems. For years a number of data formats, such as pavement power spectrum, seat acceleration, and vehicle roll rate, have been either directly or indirectly related to the pavement profile. Pavement profile can be measured by an inertial type of profilometer that sums the double integration of profilometer body acceleration and the relative displacement between body and test wheel (_1_-_3_).

Compared with the results of other road meters, the profilometer produces the profile as a description of the pavement. The profile is not affected by differences in measurement technique or by the use of different types of vehicles to make the measurement. Because of this reliability, profiles have been considered the most basic input to a pavement analysis system.

To avoid much of the work in processing profile data, the handling of each analysis program, and the matching of input-output data structure with other programs, a package of programs has been developed to give the user greater simplicity and flexibility in the reduction and analysis of profile data.

PROGRAM OVERVIEW

The simplicity of the program is achieved by a control program that links various analysis programs according to the user's input command and by an internal handshake of each analysis program, which frees the user from most input-output considerations. The package can be easily modified, and modules can be exchanged to fit particular needs. The purpose of this package is to enhance the use of pavement profile data.

The package includes a collection of programs that encompass the various practical methods used in analyzing pavement profile data. The overall program flowchart is shown in Figure 1. These programs were either developed by Pennsylvania State University or taken from work published by other universities or by state highway departments. The functions of these programs are in both the cascade and the parallel form. Some programs are in parallel to provide different methods of data analysis; other programs are cascaded to reach a final result. This package unifies the input-output section of all programs by using a standard 1024-points buffer for all time-based data, a 512-points format for all frequency spectrums and linear transfer functions, and a 51x51 matrix format for all the amplitude-frequency distribution (AFD) format (_4_,_5_) and nonlinear transfer functions. Sets of data that take up a large volume are stored on tapes or disks and are divided into blocks. The user need not be concerned with their length; the program handles this function automatically.

The package can be divided into six branches--three major paths [one for the analysis of present serviceability index (PSI) and two for ride quality], two minor paths (two auxiliary support paths, a pavement paver-grinder simulator, and a profilometer simulator), and a branch to make pavement signature comparisons. A path is any path that links through the data to the final results (see Figure 1). A branch is a collection of paths that lead to a single result.

PSI

From the pavement profile data, a quarter-car or half-car model (see Figure 2) simulation is performed to obtain the relative displacement between vehicle body and axle. This relative displacement

Figure 1. Flowchart for a roughness program for engineers and management.

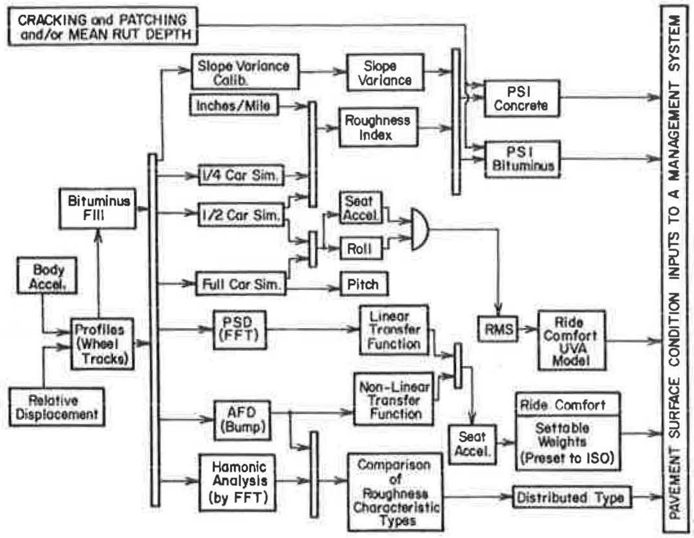

Figure 2. Quarter-car and half-car models.

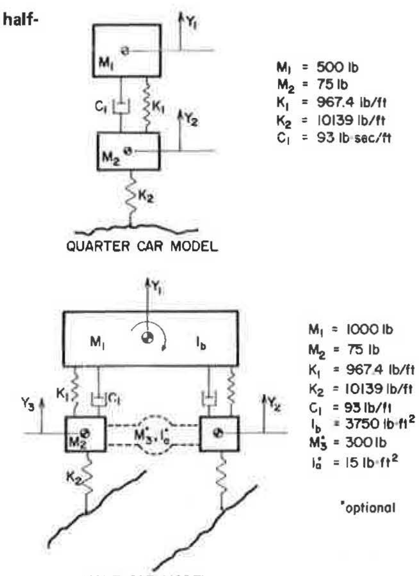

Figure 3. Ride quality path, ISO method.

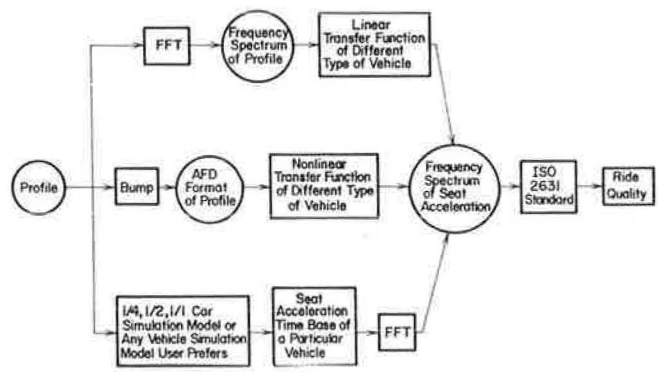

is then used as an input to a Mays meter simulator to obtain the roughness index in inches per mile (see Figure 1). A set of American Association of State Highway Officials (AASHO) regression equations (6) is selected to yield PSI. For concrete pavement,

$$PSI = 5.03 - 1.11 \log_{10} (1 + SV) - 1.38 \text{ Rut} - 0.01 \sqrt{C + P} \tag{1}$$

For bituminous pavement,

$$PSI = 5.41 - 1.78 \log_{10} (1 + SV) - 0.09 \sqrt{C + P} \tag{2}$$

where

SV = slope variance,
Rut = mean rut depth, and
C+P = measures of cracking and patching in the pavement surface.

The user can change the regression equations in the program. The program is set up to report the PSI value for every 0.1-mile pavement until the end of data.

Ride Quality Model I

The International Organization for Standardization (ISO) standard 2031 (7), a data set in tabular form that relates the endurance time of a human body to the vibration, is used to evaluate ride comfort objectively. This model determines the exposure time of reduced comfort boundary or fatigue of a human body from the frequency spectrum of the seat acceleration. The ISO data tables are reduced to two regression equations,

$$t_c = 2.980\,11 (-0.117\,78 - \ln a)^{0.621\,37} + 1.4 \tag{3}$$

and

$$t_f = 3.0 (1.03 - \ln a)^{0.6177} + 1.38 \tag{4}$$

for the frequency components from 4 to 8 Hz,

where

t_c = exposure time for reduced comfort boundary (min),
t_f = exposure time for fatigue (min), and
a = acceleration frequency component (m/s^2 Hz).

For the frequency component above 8 Hz or below 4 Hz, the equations are converted to the equivalent strength in the 4-8 Hz range by 20 dB down per decade and 10 dB down per decade, respectively.

Three paths can be used to obtain the seat acceleration frequency spectrum (see Figure 3, the

Figure 4. Full-car model, 7 df.

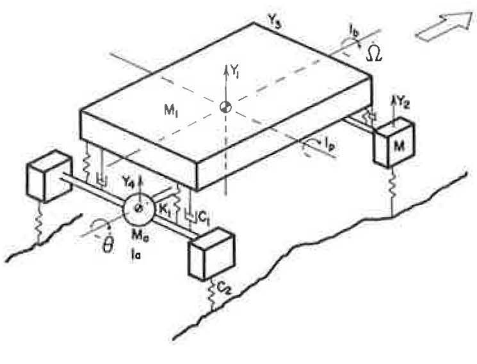

Figure 5. Ride quality path, UVA method by using RMS.

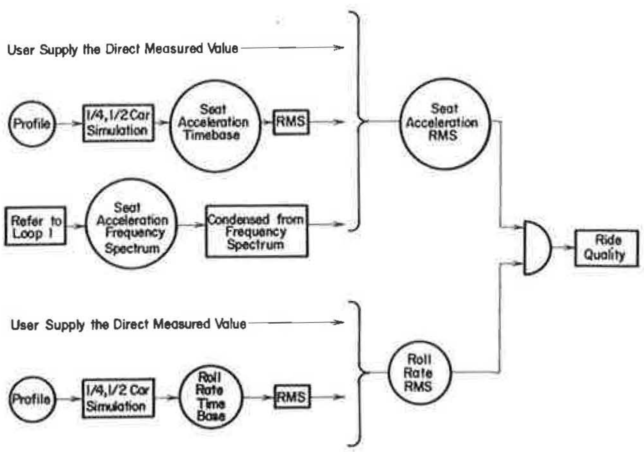

structure of path 2). The first method uses the Fast Fourier transform of the profile time base data to obtain the space frequency spectrum of the profile. The user selects the vehicle speed and one of the several types of vehicle transfer functions, and the frequency spectrum of seat acceleration is determined by the fact that the power spectral density (PSD) of the response is equal to the PSD of the input times the square of the transfer function. This is the conventional and most commonly used method.

The second method uses the AFD Bump analysis on the profile data to obtain the AFD format of the profile (8). The Bump analysis breaks the data into components of frequency and amplitude domain. The profile AFD format is then multiplied by a predetermined nonlinear transfer function (from a selection of different vehicle types stored in the program data bank) to obtain the AFD format of seat acceleration. This seat acceleration AFD format is further condensed into frequency spectrum by summing the components vertically (5). This method is different from the frequency-oriented linear transfer function method and the employment of a nonlinear transfer function is an advantage. The main shortcoming of this method is that the nonlinear transfer functions are valid only over the range of vehicle speed and amplitude levels at which the functions were established. The nonlinear transfer functions are determined by direct measurement of the seat acceleration and profile (4). The user can replace nonlinear transfer function data to fit his or her own case. Similarly, the user can easily change the equations in the linear transfer function.

The third method uses a vehicle simulation model to generate the seat acceleration time base from the profile. A quarter-car, half-car (Figure 2), or full-car model (Figure 4) can be used, or any other model can be added in the program. Then a Fast Fourier transform is used to obtain the seat acceleration frequency spectrum. The disadvantage of this method is that lengthy computation is required in the simulation of the vehicle. The time depends on the length of the profile data and the complexity of the vehicle simulation model. For example, on a given length of road, the full-car model takes about 12 times longer than the quarter-car model, and the half-car model takes 4 times as long.

Ride Quality Model II--UVA Method

This model, which uses a set of regression equations for different types of vehicles such as a bus, small, medium, or large automobile, and so on, was developed at the University of Virginia (6). The dependent variable of this model is the so-called ride quality index, which ranges from 1 (very comfortable) to 7 (very uncomfortable). The independent variables in this model include the root mean square (rms) values of the accelerations in three dimensions--roll, pitch, and yaw. Currently, only the equations for the automobiles are included in this package, and the independent variables used are the rms values of vertical acceleration and roll rate. The equation is

$$C' = 1.43 + 0.41\,\omega r + 11.84\,A_v \quad (5)$$

where

C' = comfort scale,
ωr = rms of roll rate (degrees/s), and
A_v = vertical acceleration (g's).

The rms value of seat vertical acceleration can be obtained in many ways (see Figure 5). The user can supply the measured value directly to the program or can supply the measured vertical acceleration time base and let the program calculate the rms value. If the program is required to calculate the rms values of seat acceleration, it first tries to condense the seat acceleration frequency spectrum; then, if the frequency spectrum is not available, the program calculates the seat acceleration spectrum by the method of path 2. However, if the vehicle simulation model has been run in the previous step, the program calculates the rms values directly from seat acceleration.

The rms value of roll rate is supplied to the program by the user or calculated from the roll rate time base, which can be obtained from the profile data of the two-wheel tracks via the half-car or full-car simulation model. Again, the user can replace any vehicle simulation model and can add equations for buses and trucks, or include the pitch as the third independent variable. The program structure has reserved space for expansions.

Paver-Grinder Simulator Branch

The paver-grinder simulator branch (see Figure 1) is an auxiliary program based on a program developed by the Michigan Department of Transportation that simulates the motion of an asphalt paver. The user can specify up to five different repavement thicknesses. The paver simulator will generate five sets of simulated profiles from the actual profile data. These simulated profiles are then used on other branches to obtain an estimate of improvement in

Figure 6. Sample control input.

```
                              INPUT CONTROL CARD DECK

     0         1         2         3         4         5         6         7         8
Col. 12345678901234567890123456789012345678901234567890123456789012345678901234567890

     PSIØ

                         QCAR                CONCrete pavement

                                             END

     DATA

                         VARB    2

                         CVEL  65.0

                         PSAD  0.1016
------------------------------------------------------------------------------------
     RIDE quality

                         LINEAR transfer function
------------------------------------------------------------------------------------
     RIDE

                         UNAM                ROLU

     DATA

                         VARB    2

                         ACCU  2.0

                         RROL  0.8
------------------------------------------------------------------------------------
     FINISH
```

ride quality or PSI. The paver simulator also reports the amount of material needed to repave the section studied. A user can check the estimates of improvement and the cost of various asphalt repaving thicknesses to decide which is the most cost-effective way to improve the pavement.

Profilometer Simulator

The profilometer simulator program was developed by the Federal Highway Administration (FHWA) (7) to solve the scale and filter problem in analog computation in a profilometer. The profilometer is a complex instrument to maintain and operate; it records the body acceleration of the vehicle and the body-test wheel relative displacement. The acceleration is double integrated and summed with the relative displacement by an on-board analog computer to yield the profile data. Because of the integration process, all instruments located upstream of the integrators need very accurate balance to prevent the signal from going out of bounds on integration.

The profilometer simulator takes digitized body acceleration and body-test wheel relative displacement as inputs, performs second finite difference on relative displacement, sums the second finite difference with acceleration, and then double integrates the summation digitally to yield the profile data. It includes a filter with selectable cutoff wavelengths to remove the terrain effect from the profile; unlike the analog filter, these digital filters work with zero phase shift. It also takes a series of distance pulses as input and converts the time-based profile into the equal-distance-based profile. This feature removes the requirement of constant vehicle velocity of the profilometer during operation.

A large amount of data needs to be processed to apply this method. To yield one channel of profile data, three channels of signal--acceleration, relative displacement, and distance pulse--are needed for accurate results in the integration process. The sampling rate for this method must be higher than that for profile data. The raw data of a simulated profilometer are 30 times greater in volume than that of direct profile data if the sample rate is 10 times the profile sample rate. At the present time small on-board computers have difficulty in sustaining this kind of data collection rate continuously. Thus, it is recommended that this method be used only for a short section of pavement, unless a large computer system is available.

PAVEMENT SIGNATURE COMPARISON

AFD is used with harmonic analysis to find slab or joint faulting. The harmonic analysis is used to find harmonic content in the same wavelength as the slab length. AFD analysis is then used to determine whether the pavement has joint faulting or slab curl.

SAMPLE INPUT-OUTPUT

The control program locates the large volume data sets, such as profile by International Business Machine's (IBM) job control language (JCL), and then recodes these data into standard format and block size on the disk. It follows another set of control input supplied by the user to perform the analysis task. An example of a set of control input is shown in Figure 6.

In this example the user specifies the PSI analysis first but prefers a quarter-car simulation model and a concrete pavement rather than the default paths. He or she also supplies two parameters of profile data, sample distance and vehicle speed, to the program. Next he or she asks for ride quality analysis by default; the ISO method is executed. Following that, he or she asks for ride quality analysis, this time by using the Virginia model, and he or she also puts in the rms value of the roll rate. Note that CONC is all that is read by the computer in the PSI request, but CONCRETE PAVEMENT was input by the user for his or her understanding. Similarly, RIDE is all that is required, but the first time RIDE QUALITY was used. This feature is useful.

Figure 7. Sample program output generated by input given in Figure 6.

```
                    ECHO USER INPUT
   PSIØ
                    QCAR                 CONCrete pavement
                                         END
   DATA
                    VARB    2
                    CVEL  65.0
                    PSAD  0.1016
   RIDE quality
                    LINEAR transfer function
   RIDE
                    UNAM                 ROLU
   DATA
                    VARB    1
                    RROL  0.8
   FINISH
          ****** PRESENT SERVICEABILITY INDEX ANALYSIS *****

OPTIONS AND PARAMETERS USED:
   ROUGHNESS EXPRESSED IN : ROUGHNESS INDEX(INCHES/MILE)
   PAVEMENT:  BITUMINUS
      PAVEMENT PARAMETERS:
         CRACK AND PATCHING=  0.0  (IN FT**2/1000FT**2 OR FT/1000FT**2)
         MEAN RUT DEPTH=  0.0  INCHES
   PSI FORMULA:THE ASSHO FORMULA
   ROUGHOMETER:MAYSMETER WITH MEASURED ROUGHNESS INDEX    130.700INCHES/MILE

THE RESULTS:
   THE ROUGHNESS INDEX =    130.7000INCHES/MILES
   THE PSI (PRESENT SERVICEABILITY INDEX) = 2.58

***MESSAGE:ALL PARAMETERS AND PATH SELECTIONS ARE SET TO DEFAULT VALUES.
   ALSO ALL DATA SETS ARE ZEROED

              ****** RIDE QUALITY ANALYSIS ******

OPTIONS AND PARAMETERS USED:
   ANALYSIS MODEL:  ISO STANDARD 2631
      LINEAR TRANSFER FUNCTION OF VEHICLE IS USED
         VEHICLE TYPE:  A STANDARD CAR OR MIDSIZE CAR
   ADDITIONAL DATA REQUESTED:  LINEAR FORM OF AMPLITUDE-FREQUENCE
         DISTRIBUTION FORMAT OF PROFILE
   ADDITIONAL DATA REQUESTED:  LINEAR FORM OF POWER SPECTRUM DENSITY
         OF PROFILE
      PROFILE SAMPLE DISTANCE    0.07620 METER
      VEHICLE VELOCITY    17.66660  METER/SECOND

THE RESULTS:
   AVAILABLE FREQUENCY DATA POINTS:  50
   THE AVERAGE TIME FOR A RIDE BECOMES UNCOMFORT IS   525.10 MINUTES
   THE MINIMUM TIME FOR UNCOMFORT IS    18.20 MINUTES

              ****** RIDE QUALITY ANALYSIS ******

OPTIONS AND PARAMETERS USED:
   ANALYSIS MODEL:  UNIVERSITY OF VIRGINIA MODEL
      USER PROVIDES THE RMS VALUE OF VEHICLE VERTICLE ACCELERATION
      USER PROVIDES THE RMS VALUE OF VEHICLE ROLL RATE
      PROFILE SAMPLE DISTANCE   0.07620 METER
      VEHICLE VELOCITY    17.66660  METER/SECOND

THE RESULTS:
   THE RMS VALUE OF SEAT ACCELERATION IS    2.0000000 METER/(SECOND**2)
   THE RMS VALUE OF ROLL RATE IS    0.8000000  DEGREE/SECOND
   THE UVA RIDE QUALITY INDEX IS    4.1743240
      ON A SCALE OF 1-- THE BEST TO 7--THE WORST

***MESSAGE:ALL PARAMETERS AND PATH SELECTIONS ARE SET TO DEFAULT VALUES.
   ALSO ALL DATA SETS ARE ZEROED
```

The program first echoes all user control input. After performing the task, it prints out the option taken and the results of the analysis. An example of the output is shown in Figure 7.

CONCLUSION

This package is a part of the computer program (MAPCON) developed for FHWA. Intermediate data sets are temporarily stored to increase the efficiency of the program. For example, once the half-car simulation is performed, the three output data sets can be used by different branches: relative displacement between vehicle body and axle used by the PSI branch; seat acceleration used by both ride quality branches; and roll rate used by the Virginia model. In this way, repeated computation is avoided. Thus, the package provides the highway engineers and management personnel with a useful and simple tool and removes most routine manual data processing.

Although many of the programs and analysis methods have been published in bits and pieces, some have not. They have never been integrated into a single versatile package. Thus, for the first time, a complete analysis program is available to pavement researchers and managers for use in analyzing pavement characteristics such as serviceability, ride quality, and safety.

ACKNOWLEDGMENT

The research described in this paper was conducted as part of the FHWA research project, Methodology for Analyzing Pavement Condition Data. Rudolph R. Hegmon served as contract monitor of this project, and his assistance is greatly appreciated.

REFERENCES

1. E.B. Spangler and W.J. Kelley. GMR Road Profilometer--A Method for Measuring Road Profile. HRB, Highway Research Record 121, 1966, pp. 27-54.
2. J.R. Darlington and P. Milliman. A Progress Report on the Evaluation and Application Study of the General Motors Rapid Travel Road Profilometer. HRB, Highway Research Record 214, 1968, pp. 50-67.
3. W.R. Hudson. High-Speed Road Profile Equipment Evaluation. Univ. of Texas, Austin, Res. Rept. 73-1, Jan. 1966.
4. J.C. Wambold and W.H. Park. A Data Processing Method Giving a Better Physical Description of Random Signals. Proc., 20th International Instrumentation Symposium, Albuquerque, NM, 1974.
5. A.D. Brickman, J.C. Wambold, and J.R. Zimmerman. An Amplitude-Frequency Description of Road Roughness. HRB, Spec. Rept. 116, 1971, pp. 53-67.
6. L.G. Richards, I.D. Jacobson, and R.D. Pepler. Ride-Quality Models for Diverse Transportation Systems. TRB, Transportation Research Record 774, 1980, pp. 39-45.
7. P.G. Smith, S. Macintyre, and T. Yang. Noncontract Road Profile System. Federal Highway Administration, Final Rept., Feb. 1980.
8. K.T. Cheng. Calculation of the Amplitude-Frequency Distribution Format of a Signal Using a Bump-by-Bump Analysis. Pennsylvania Transportation Institute, Pennsylvania State Univ., University Park, Rept. S91, Oct. 1980.

Publication of this paper sponsored by Committee on Pavement Condition Evaluation.

Suggested Improved Methodology for Relating Objective Profile Measurement with Subjective User Evaluation

LARY R. LENKE

Considerable effort has been directed at relating subjective user evaluation with pavement profile characteristics. Improvements in the methodology for conducting subjective evaluations have recently been made and are cited. Profile characteristics that describe subjective evaluation have previously included statistical properties of elevation and slope. This paper questions the theoretical validity of correlating profile elevation and slope with subjective evaluation. Profile curvature is suggested as a theoretically sound profile measurement that can be related to subjective evaluation. Recommendations are made for verifying a relation between profile curvature and subjective evaluation, and the potential is outlined for its application in highway practice.

Since the conclusion of the American Association of State Highway Officials (AASHO) road test, much effort has been directed at relating subjective human response with the physical properties of a pavement profile. The methodology used for obtaining this subjective evaluation of pavement section, known as the present serviceability index (PSI) and outlined by Carey and Irick (1), has been generally accepted by the pavement evaluation community as a state-of-the-art method for determining pavement serviceability.

This subjective measure is currently popular; however, this method has important shortcomings in terms of the development of the rating scale and its application. Shortly after completion of the AASHO road test, Hutchinson (2) suggested that the principles of psychophysics, widely used in experimental psychology and marketing research, would be more appropriate than PSI for establishing a subjective rating scale for pavement evaluation. When this method of scale construction is used these systematic errors are removed:

1. The error of leniency, which refers to the constant tendency of a rater to rate too high or too low for whatever reasons;
2. The halo effect, which refers to the tendency of raters to force the rating of a particular attribute in the direction of the overall impression of the object rated; and
3. The error of central tendency, which refers to the fact that raters hesitate to give extreme judgments of stimuli and tend to displace individual ratings toward the mean of the group.

Hutchinson showed that these errors are inherent in the AASHO road test development of PSI.

The development and verification of a rational subjective scale for pavement evaluation that incorporates the methods of psychophysics has only recently been accomplished. Weaver and Clark (3) and Weaver (4) showed that the principles of psychophysics yield a representative rating scale for subjective pavement evaluation. The serviceability scale values obtained are similar to those of the AASHO road test PSI but cannot be related directly because of the inadequacies of the PSI in terms of subjective scale construction and data-gathering techniques.

The subjective human evaluation of pavements depends on the magnitude of the various acceleration components that occur as a vehicle traverses a pavement section. Shahin and Darter (5) cite numerous references that indicate that subjective human tolerance levels, in addition to acceleration magnitude, depend on factors such as duration of exposure and frequency of acceleration. Goldman (6) found that subjective human response to vibration is relatively constant in terms of average peak acceleration in the frequency range of 0-50 Hz. This is well within the range of frequencies encountered in typical pavement and vehicle response functions. Also, the duration of exposure encountered in most subjective pavement evaluations is similar in length and is relatively short. Based on Goldman's work, the U.S. Air Force (7) currently uses a nominal 0.4-g level for determining rough areas by using a known input profile in a computer code (TAXI) that simulates the vertical acceleration response of a given aircraft.

Although it is generally accepted that subjective human response is related to acceleration (the vertical direction being the main component), there is no consensus on the physical pavement profile parameter directly related to, and responsible for, this acceleration and resultant human response. Profile roughness numerics currently in use and outlined by Gillespie and others (8) are (a) spectral densities of elevation or slope and (b) root mean square (RMS) statistics of elevation or slope. Other numerics outlined include those obtained directly from the various response-type road roughness measuring systems (RTRRMS) currently in use, particularly the accumulated displacement value of the axle-body motion of a particular RTRRMS described as an inches-per-mile (I/M) statistic. Gillespie (8) suggested that this I/M statistic does not account for the velocity of the RTRRMS and should be transformed to obtain an average rectified velocity (ARV) to account for various RTRRMS operating speeds.

The problem with the various statistics outlined above is their apparent inability to predict the subjective human response of the traveling public. Although much of this apparent lack of correlation may be attributed to the past use of the AASHO road test PSI as the subjective measurement, one might also suspect the profile statistics currently being used to predict serviceability. Shahin and Darter (5) cite previous work that indicates the shortcomings of spectral density methods; Holbrook and Darlington (9) indicate that conventional multiple regression techniques are not applicable because of the high intercorrelation between frequency bands of pavement profile spectra. Holbrook and Darlington put forth a correlation method that eliminates this interdependency of frequency bands.

There are limitations and constraints in conducting a statistical analysis of pavement profile parameters; however, the real issue may be that elevation or slope are not the true correlates of subjective user response.

PROFILE CURVATURE AS A THEORETICALLY SOUND CORRELATE

Seemann and Nielsen (10) related airfield pavement profile statistics with the computer-simulated response of aircraft. This computer simulation (TAXI) of an aircraft traversing a runway yields vertical acceleration information of the aircraft for the discrete profile data (usually 6 in or 2 ft). The acceleration data are then analyzed statistically to

Figure 1. Profiles of constant slope.

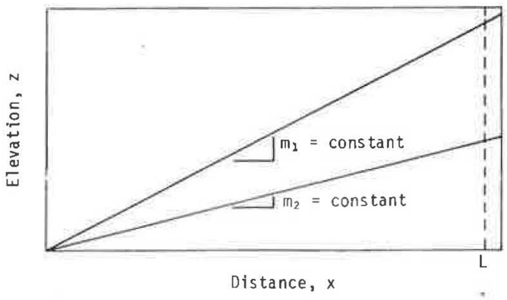

Figure 2. RMS acceleration versus RMS slope.

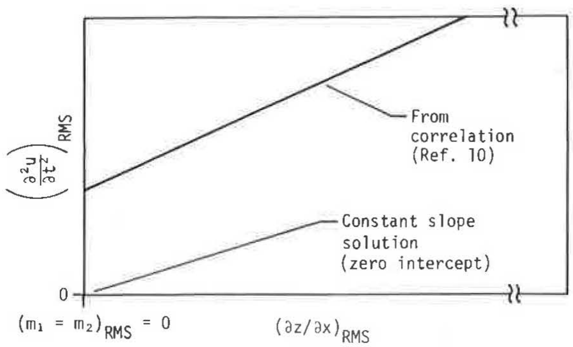

Figure 3. Curvilinear motion in vertical plane.

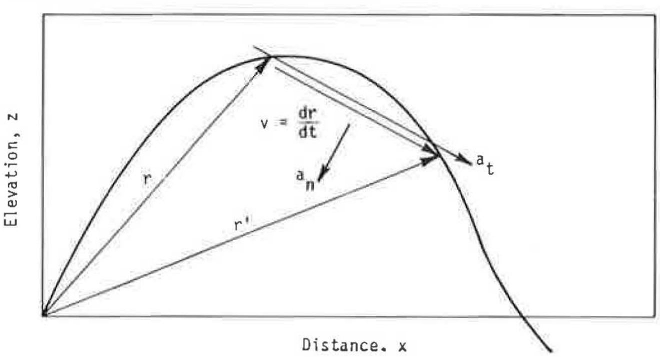

determine a RMS level of acceleration for an entire runway profile.

Their first attempt was to correlate RMS acceleration levels with elevation levels, or

$$(Z)_{RMS} \sim (\partial^2u/\partial t^2)_{RMS} \quad (1)$$

which states that the RMS elevation level is proportional to aircraft vertical RMS acceleration for the entire runway profile. The result of this correlation was very poor. A second attempt was to correlate RMS change in elevation (or slope since the profile sample spacing is constant) between discrete elevation points with RMS acceleration values, or

$$(\Delta Z)_{RMS} \sim (\partial^2u/\partial t^2)_{RMS} \quad (2)$$

This relation yielded an excellent correlation (r = 0.96) and further efforts to relate acceleration and profile data ceased because of the correlation obtained.

This correlation, although good, may not be theoretically sound or the best obtainable. Consider two different profiles of constant slope, $m_1 > m_2$, that otherwise are perfectly smooth (Figure 1). Because these two runway profiles are perfectly smooth the aircraft will not have a vertical component of acceleration because the aircraft velocity is constant. The RMS slope values for perfectly smooth profiles of differing slope are zero. The corresponding RMS acceleration level is also zero, so a plot of RMS slope versus RMS acceleration would have an intercept of zero. However, this is contradictory to the correlation obtained by Seemann and Nielsen (10) where a level of RMS acceleration exists for a RMS slope level of zero (Figure 2). This would suggest (excluding a nonlinear solution of RMS acceleration versus RMS slope) that the correlation of RMS acceleration with RMS slope is invalid.

It is now suggested that the second derivative of elevation with respect to distance be considered; i.e., the rate of change of slope $[\partial^2z/\partial x^2]$, or profile curvature. From an intuitive viewpoint this seems to make sense. Take for example a vertical curve. The response of a vehicle passing through a vertical curve can be reduced by reducing the difference in initial and final grades, by lengthening the vertical curve distance, or by a combination of both. These variables affect the rate of change of slope; i.e., for the above vertical curve the rate of change of slope is decreased.

The suggested numerical relation between vertical acceleration and profile curvature is

$$(\partial^2u/\partial t^2)_{RMS} \sim (\partial^2z/\partial x^2)_{RMS} \quad (3)$$

and if a constant of proportionality is included, then

$$(\partial^2u/\partial t^2)_{RMS} = k(\partial^2z/\partial x^2)_{RMS} \quad (4)$$

The above equation is similar to the classical wave equation

$$\partial^2z/\partial t^2 = c^2(\partial^2z/\partial x^2) \quad (5)$$

where c is the wave speed.

If aircraft elevation at pilot station (u) and profile elevation (z) can be related, Equation 4 can be put into a form similar to Equation 5. From the following relation between u and z,

$$u = z + z_{ps} \quad (6)$$

where z_{ps} is the distance from the profile to the pilot station (point at which vertical acceleration is of interest), it is evident that

$$\partial^2z/\partial t^2 = (\partial^2u/\partial t^2) - (\partial^2z_{ps}/\partial t^2) \quad (7)$$

If one assumes that z_{ps} is constant, then

$$\partial^2z/\partial t^2 = \partial^2u/\partial t^2 \quad (8)$$

and the wave equation is satisfied. This formulation assumes that the aircraft is a particle, with velocity (v), in continuous contact with the profile.

Furthermore, the theory of curvilinear particle dynamics (11, pp. 464-466) and elementary calculus (12, pp. 551-553) shows that the following relations exist. Take a typical profile (Figure 3) with position vectors r (time t) and r' (time t + Δt). The velocity of a particle that traverses this profile is shown to be

$$v = dr/dt \quad (9)$$

and for the case of an airplane (particle) that

Figure 4. RMS acceleration versus RMS curvature.

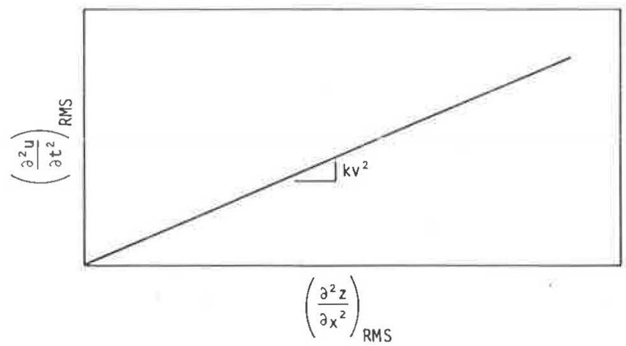

Figure 5. Idealized profile.

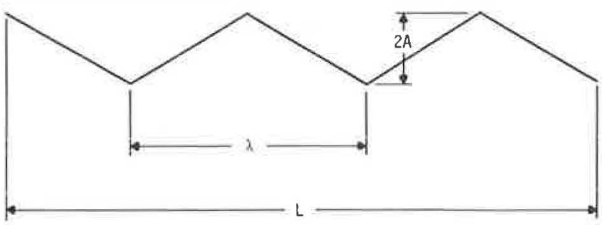

Figure 6. Vertical acceleration versus amplitude and wavelength.

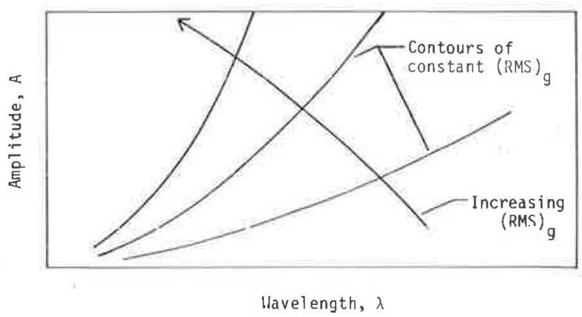

traverses the above profile, this velocity it taken to be constant. The acceleration for the above particle is the vectoral sum of tangential and normal components

$$a = a_t i_t + a_n i_n \tag{10}$$

where i_t and i_n are unit vectors in the tangential and normal directions, respectively. The acceleration components are

$$a_t = dv/dt \tag{11}$$

which is zero because v is constant, and

$$a_n = v^2/\rho \tag{12}$$

where ρ is the radius of curvature. The normal acceleration can be taken as

$$a_n = d^2z/dt^2 \tag{13}$$

and, from calculus, the curvature κ is

$$\kappa = 1/\rho = (d^2z/dx^2)/[1 + (dz/dx)^2]^{3/2} \tag{14}$$

but the $[dz/dx]^2$ term in the denominator can be assumed to be zero for virtually all pavement profiles (1.5 percent error for a 10 percent slope); therefore,

$$1/\rho = d^2z/dx^2 \tag{15}$$

and now substitution of Equations 13 and 15 into Equation 12 yields

$$d^2z/dt^2 = v^2\ (d^2z/dx^2) \tag{16}$$

which is identical to the wave equation (Equation 5).

The constant k in Equation 4 might be interpreted as a function of the aircraft type and its associated dynamic properties as well as the velocity of the aircraft. This would suggest that Equation 4 might take the form of

$$(\partial^2u/\partial t^2)_{RMS} = k\,v^2\ (\partial^2z/\partial x^2)_{RMS} \tag{17}$$

where v is the aircraft velocity and k is a constant that accounts for the dynamic response of the aircraft. Assuming that u and z from Equation 8 are interchangeable, Equation 17 is virtually identical to Equations 5 and 16.

For a given aircraft and velocity, Equation 17 can be assumed as shown in Figure 4. Notice that the intercept is zero; this accounts for the case of a constant slope, perfectly smooth profile.

Typical profiles exhibit a characteristic wavelength (λ) and corresponding amplitude (2A) that exist for the most part over the entire profile length (L). This wavelength and amplitude are functions of the soil type and structural stiffness of the profile pavement. This can be represented pictorially as in Figure 5. The curvature can be expressed in finite difference form as

$$\partial^2z/\partial x^2 = (z_i - 2z_{i-1} + z_{i-2})/(\Delta x)^2 \tag{18}$$

If one now looks at a characteristic wavelength and amplitude of a profile, Equation 18 can be expressed as

$$\partial^2z/\partial x^2 = -\,16A/\lambda^2 \tag{19}$$

Substitution of Equation 19 into Equation 4 yields

$$\partial^2u/\partial t^2 = -\,k\ (16A/\lambda^2) \tag{20}$$

and replacement of the partial derivative with the RMS acceleration yields

$$(RMS)_g = k'\ (A/\lambda^2) \tag{21}$$

where k' = 16 k, the negative sign being eliminated because of the use of RMS levels of acceleration and profile curvature. Equation 21 can be rearranged as

$$A = [(RMS)_g/k']\ \lambda^2 \tag{22}$$

McKeen (13) found from his work on expansive soils that A, λ, and $(RMS)_g$ are related graphically as in Figure 6. If A is plotted versus λ^2, one might expect a plot similar to that of Figure 6 [i.e., a family of straight lines with slope $(RMS)_g/k'$]. Mathematically this is identical to Equation 22. Thus, the theoretical basis of Equations 4 and 17 would seem substantiated based on this experimental work of McKeen.

PROFILE CURVATURE VERSUS SUBJECTIVE EVALUATION

Although the dynamic responses of aircraft and automobiles are quite different (the latter being less complicated), it should be evident that the above theoretical considerations are easily applicable to

Figure 7. Psychophysical rating versus RTRRMS output.

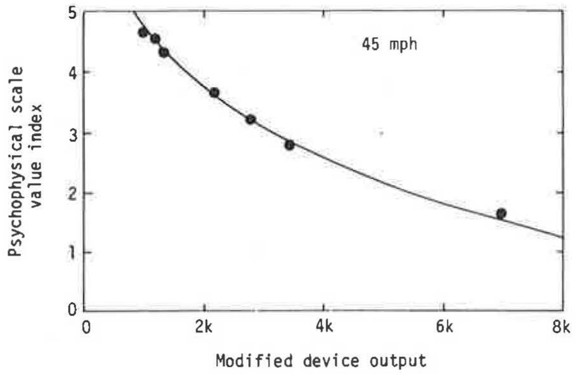

highway pavements and the associated problem of relating a pavement profile with subjective human response. The described wave equation applies to the curvilinear motion of particles and is not directly applicable to systems that have frequency response characteristics. Equation 17 is suggested as a modified wave equation that incorporates a factor (k) to account for the dynamic response of a system that traverses a pavement profile. This factor should be dependent on frequency and complex in nature.

The work of Weaver and Clark (3) would seem to support the above postulate. Their Figure 22 can be viewed as a semilogarithmic transform of the wave equation (reproduced in Figure 7). A psychophysical scale value of five (perfect pavement) corresponds to the threshold of perception of human response to vertical acceleration, which approaches zero, and a scale value of zero (impassable pavement) can be thought of as an acceleration that is very great and in theory approaches infinity. The modified device output is a measurement obtained from RTRRMS, which can be thought of as a relative measure of profile curvature.

According to the wave equation formulation, contours of increasing constant velocity would lie closer to the origin in Figure 7. Weaver has indicated that this is generally the case for most pavement systems. However, for rigid pavement systems the opposite condition has been known to occur. The presence of construction joints and expansion joints in rigid pavements permits the possibility of discontinuous slope and elevation of a pavement section, which will affect the dynamic response of a test vehicle. Characteristic wavelengths and amplitudes associated with these joints tend to be more pronounced in a rigid pavement system than in a flexible pavement system as well as being more uniform in nature. Because the factor k of Equation 17 is postulated to be dependent on frequency (and therefore on wavelength), the suggested wave equation would explain Weaver's observations.

Furthermore, McKeen (13) found from his work on expansive soil-pavement interaction that characteristic wavelengths and amplitudes depend on the type of clay and the pavement rigidity. It has been postulated that characteristic wavelengths and amplitudes may exist for all engineering pavements, these characteristics being dependent on soil and pavement type as well as structural rigidity.

The above discussion suggests that the wave equation formulation may be a feasible method for relating pavement profile and subjective human response. It is anticipated that a subjective evaluation can be related to a statistical property of the curvature. This statistical property might be a power spectral property or a RMS property of the curvature. The latter might be formulated in a fashion similar to Equation 17 as

$$S.E. = kv^2\,(d^2z/dx^2)_{RMS} \qquad (23)$$

where S.E. is the subjective evaluation.

The power spectral formulation is developed in Equations 24-34. Equation 17 can be cast as

$$\ddot{z}(t) = v^2 z''(x) \qquad (24)$$

where the double dot ($\ddot{o}$) and double prime (") denote second derivative operations of elevation with respect to t and x, respectively. The autocorrelation of the above is

$$R_{\ddot{z}\ddot{z}}(\tau) = v^4\, E\left\{z''[x(t)]\,z''[x(t+\tau)]\right\} \qquad (25)$$

where E{ } denotes the expected value of. The above reduces to

$$R_{\ddot{z}\ddot{z}}(\tau) = v^4\, E\left\{z''(vt)\,z''[v(t+\tau)]\right\} \qquad (26)$$

where v is the vehicle velocity. Further reduction yields the autocorrelation of acceleration in terms of the autocorrelation of curvature

$$R_{\ddot{z}\ddot{z}}(\tau) = v^4\, R_{z''z''}(v\tau) \qquad (27)$$

The spectral density of Equation 27 is

$$S_{\ddot{z}\ddot{z}}(\omega) = v^4\int_{-\infty}^{\infty} R_{z''z''}(v\tau)e^{-i\omega\tau}d\tau \qquad (28)$$

The change of variable $\theta = v\tau$ yields

$$S_{\ddot{z}\ddot{z}}(\omega) = v^4\int_{-\infty}^{\infty} (1/v)\,R_{z''z''}(\theta)e^{-i(\omega/v)\theta}\,d\theta \qquad (29)$$

$$= v^3\int_{-\infty}^{\infty} R_{z''z''}(\theta)e^{-i(\omega/v)\theta}d\theta \qquad (30)$$

or

$$S_{\ddot{z}\ddot{z}}(\omega) = v^3\, S_{z''z''}(\omega/v) \qquad (31)$$

The above states that the spectral density of acceleration at the pavement vehicle interface is related to the spectral density of the pavement curvature.

The spectral density of the vehicle response is

$$S_{\ddot{u}\ddot{u}}(\omega) = |H(\omega)|^2 S_{\ddot{z}\ddot{z}}(\omega) \qquad (32)$$

with substitution of Equation 31 to yield

$$S_{\ddot{u}\ddot{u}}(\omega) = v^3|H(\omega)|^2 S_{z''z''}(\omega/v) \qquad (33)$$

where $|H(\omega)|^2$ is the frequency response of the vehicle system (the unsprung and sprung mass) as well as the human support system (car seat).

The power spectral formulation for subjective human response can now be assumed to be

$$S.E. = v^3|H(\omega)|^2 S_{z''z''}(\omega/v) \qquad (34)$$

where $|H(\omega)|^2$ is as above but also includes the response of the human body.

Equations 23 and 34 both state that the output (S.E.) is proportional to the input (curvature), the coefficient of proportionality being a complex frequency-dependent transform.

The frequency response terms need not be known explicitly, but it may be determined by means of statistical regression between S.E. and the profile curvature. The curvature portion of the regression might consist of a linear or nonlinear combination of the area under the curvature power spectral function plus higher order statistical moments. The higher order statistical moments represent the mean and standard deviation and reflect quantitatively the distribution of the curvature spectral function. Note also that the frequency response term in Equation 34 is a statistical property that reflects the inability of performing a power spectra transformation on the S.E. term.

APPLICABILITY TO HIGHWAY PRACTICE

RTRRMS measurements can also be related to profile curvature. With a knowledge of the curvature properties of various test sections, RTRRMS should be easily calibrated to yield a relation between device output and curvature at various travel speeds and subsequently to yield a measure of S.E.

It was shown that Figure 7 is a transform of the wave equation for a given RTRRMS. Similar relations for various RTRRMS should be easily obtainable. Gillespie and others (8) suggested the use of an average rectified velocity (ARV) as a measure of a RTRRMS output. A similar statistic could be developed that would be compatible with the wave equation formulation; this statistic might be called an average rectified acceleration (ARA). This ARA value could then be related to curvature and in turn to subjective evaluation or serviceability.

CONCLUSIONS AND RECOMMENDATIONS

The previous discussion indicates that RMS elevation levels do not correlate with RMS vertical acceleration; however, RMS slope levels correlate with RMS vertical acceleration but do not yield a unique solution. A profile curvature statistic will more adequately relate to statistics of vertical vehicle response based on a wave equation formulation that is known to have a solid basis in theoretical mechanics. It is anticipated that a relation between profile curvature and vehicle response can be extended to describe subjective evaluation, as acceleration and human response are known to correlate.

Verification of the relation between curvature and vehicle-human response will require correlation and parametric studies of Equations 17, 23, and 34. Subsequently, calibration of the various RTRRMS could be accomplished based on the relations of Equations 23 and 34.

ACKNOWLEDGMENT

The above paper is a result of work conducted for the U.S. Air Force Engineering and Services Center by the New Mexico Engineering Research Institute (NMERI) at the University of New Mexico. Appreciation is extended to R. Gordon McKeen and John P. Nielsen of NMERI for their input and encouragement. Special thanks are extended to Thomas L. Paez of the University of New Mexico Civil Engineering Department for his input on random processes.

REFERENCES

1. W.N. Carey, Jr., and P.E. Irick. The Pavement Serviceability-Performance Concept. HRB, Bull. 250, 1960, pp. 40-58.
2. B.G. Hutchinson. Principles of Subjective Rating Scale Construction. HRB, Highway Research Record 46, 1964, pp. 60-70.
3. R.J. Weaver and R.O. Clark, Jr. Psychophysical Scaling of Pavement Serviceability. Soil Mechanics Bureau, New York State Department of Transportation, Albany, Manual SEM-9, May 1977.
4. R.J. Weaver. Quantifying Pavement Serviceability as It Is Judged by Highway Users. TRB, Transportation Research Record 715, 1979, pp. 37-44.
5. M.Y. Shahin and M.I. Darter. Pavement Functional Condition Indicators. Construction Engineering Research Laboratory, Champaign, IL, CERL-TR-C-15, Feb. 1975.
6. C.M. Harris and C.E. Crede, eds. Shock and Vibration Handbook, 2nd ed. McGraw-Hill, New York, 1976.
7. A.G. Gerardi and A.K. Lohwasser. Computer Program for the Prediction of Aircraft Response to Runway Roughness. Air Force Weapons Laboratory, Albuquerque, NM, AFWL-TR-73-109, Vol. 1, Sept. 1973.
8. T.D. Gillespie, M.W. Sayers, and L. Segel. Calibration of Response-Type Road Roughness Measuring Systems. NCHRP, Rept. 228, Dec. 1980, 81 pp.
9. L.F. Holbrook and J.R. Darlington. Analytical Problems Encountered in the Correlation of Subjective Response and Pavement Power Spectral Density Functions. HRB, Highway Research Record 471, 1973, pp. 83-90.
10. D.R. Seemann and J.P. Nielsen. Methodology for Determining, Isolating, and Correcting Runway Roughness. Eric H. Wang Civil Engineering Research Facility, Univ. of New Mexico, Albuquerque, CEEDO-TR-77-22, June 1977.
11. F.P. Beer and E.R. Johnston, Jr. Vector Mechanics for Engineers: Dynamics, 2nd ed. McGraw-Hill, New York, 1972.
12. G.B. Thomas, Jr., and R.L. Finney. Calculus and Analytical Geometry, 5th ed., Addison-Wesley, Reading, MA, 1979.
13. R.G. McKeen. Design of Airport Pavements for Expansive Soils. Federal Aviation Administration, FAA-RD-81-25, Jan. 1981.

Publication of this paper sponsored by Committee on Pavement Condition Evaluation.

Abridgment

Road Profile Evaluation for Compatible Pavement Evaluation

DAVID W. McKENZIE AND W. RONALD HUDSON

An important application of the Surface Dynamics profilometer is to provide a stable calibration reference for response-type road roughness measuring (RTRRM) instruments. The latter devices, of which the Mays meter is typical, are relatively inexpensive and are used by many agencies for routine pavement monitoring. A special class of profile statistics, termed root-mean-square vertical acceleration (RMSVA), has been shown to reveal many of the road surface properties normally associated with roughness, including those measured by Mays meters. An RMSVA-based roughness index, which was tailored to describe the behavior of eight Mays meters run on 29 pavement test sections, is now the basis of a large-scale calibration program by the Texas State Department of Highways and Public Transportation. Although the Mays meter calibration problem motivated the development of RMSVA roughness indices, careful monitoring of a set of calibration test sections and other pavements has revealed interesting surface properties that could never be detected by Mays meters or by other RTRRM devices that reduce roughness evaluations to a single number. The RMSVA indices computed from a road profile can provide a signature that reflects roughness over a broad range of profile wavelengths. Distinctive signatures that correspond to certain pavement classes, or types of deterioration, have been tentatively identified and are presented here. Their interpretation remains a promising subject for future research.

The availability of accurate road profiles makes it possible to isolate, or describe mathematically, certain features of road surfaces that a particular roughness measuring device responds to. The Mays meter, a primary means of evaluating roads in many states, detects profile irregularities in the 4- to 40-ft (1- to 12-m) wavelength range, depending on vehicle speed. However, it has been shown that human ratings of road roughness correlate significantly with wave components that are beyond this wavelength range (1,2). Walker and Hudson (3) have demonstrated that about 80 percent of the variance in ratings in one large rating session in Texas (1968) could be explained by a profile statistic that incorporates amplitude measures for wavelengths up to 83 ft.

Nevertheless, the basic requirement of a calibration standard is that it correlate highly with the actual measurements of the type of device being calibrated. A weak correlation would result in an unstable calibration method, the final effect being a loss of potentially useful information in measurement data.

DEVELOPMENT OF CALIBRATION STANDARD

For our work in attempting to simulate the Mays meter with road profile statistics we had available the results of a calibration session for eight devices. All measurements were obtained within a three-month period surrounding an October 1977 profilometer run on 29 asphalt concrete pavement (ACP) test sections near Austin. Each measurement was obtained by averaging the results of four runs on a 0.2-mile section. (A fifth run, which had deviated most from the overall mean, was excluded.) This redundancy provided a measure of the repeatability of the Mays meter for successive runs. The table below contains the average section mean, the standard deviation of the section means (SD), and the standard error of repeatability (SE) for each unit. The repeatability (although slightly optimistic because of the excluded run) is quite good when we consider that 100 ± 5 in/mile corresponds approximately to a serviceability index of 2.7 ± 0.1.

Mays Meter	Mean	SD	SE
M1	104.17	70.13	5.01
M2	93.73	56.02	3.88
M3	101.87	67.83	6.47
M4	90.46	60.05	3.94
M5	95.91	69.16	7.19
M6	128.67	54.17	6.33
M7	116.96	56.34	7.27
M8	174.02	125.27	16.05

Most relevant to the problem of calibration is the relations revealed to exist among the different units. The correlation matrix and plots for the calibration session data indicate that the Mays meter roughness readings are highly correlated and, in fact, plots show that the relations are linear. If we were to seek a simple linear calibration function, with one of the units selected as the reference device, then a good reference would be unit M3, whose measurements explain about 97 percent of the section-to-section variation in response in the other units.

The results convinced us that a linear calibration model would be adequate provided a profile statistic could be found that would be effective in assuming the role of Mays meter M3. Unlike M3, of course, it must also have long-term stability, depending only on the profilometer or other instruments to obtain a reasonably accurate profile. Moreover, since calibration requires that measurements from all units be transferable to a common scale, we cannot expect to find a single statistic that agrees much better with the units than they do between themselves; hence, we can be satisfied if our candidate index, when statistically compared with Mays meter measurements in a linear regression, achieves a coefficient of determination (R^2) of approximately 0.97. This means that standard errors of estimate (SE) should be on the order of 10 in/mile or 0.2 serviceability units.

Correlation of Mays Meter with Root-Mean-Square Vertical Acceleration

A computer program was written that reads sequences of profile elevations (two profilometer wheelpaths) and computes a set of special summary statistics for each road section. These statistics, which are termed root-mean-square vertical acceleration (RMSVA) indices at base lengths 1 ft, 2 ft, 4 ft, etc., are proportional to the RMS difference between adjacent profile slopes. Each slope is measured over a fixed horizontal distance--the base length that corresponds to that index--and the numbers are scaled to have units of feet per square second, which corresponds to RMSVA of a hypothetical point in contact with the road and travels horizontally at 50 mph.

Some RMSVA indices are highly correlated with Mays meter roughness readings. In fact, different components of the profile wavelength are revealed in the indices obtained at different base lengths to provide a more complete description of road rough-

Figure 1. Correlation of Texas Mays meter measurements with RMSVA.

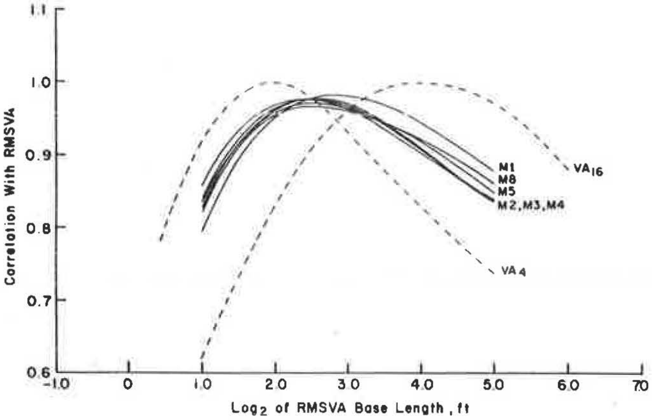

ness than could be obtained with a Mays meter. RMSVA is most sensitive to profile disturbances at wavelengths of approximately twice the base length. For example, if a pavement's RMSVA at base length 8 ft if unusually large, then the pavement is unusually rough in terms of its 16-ft-long waves.

For the purpose of analyzing the Mays meter data provided by the Texas State Department of Highways and Public Transportation (TSDHPT), the following indices were obtained from an October 1977 profilometer run of the 29 Austin test sections: $AV_{0.5}$, VA_1, VA_2, VA_4, VA_8, VA_{16}, VA_{32}, and VA_{65}.

The subscripts represent base length (b) in feet. VA_b was calibrated as the average RMSVA over both right and left wheelpaths and over two profilometer runs. In each case a sampling interval of 0.169 ft was used over a section length of 1050 ft. This particular sequence of base lengths was chosen in view of both the sampling interval and the correlation between indices. (For example, the correlation between VA_2 and VA_4 is about the same as that between VA_4 and VA_{16}.) The profilometer exhibited excellent repeatability with respect to these indices. The standard errors of duplication (SE), for example, can be compared with the standard deviation (SD) of the section means (see table below).

Base Length (ft)	Mean(VA_b)	SD(VA_b)	SE
0.51	82.52	29.71	2.60
1.01	28.48	10.56	0.83
2.03	9.13	3.73	0.28
4.06	3.43	1.77	0.07
8.11	1.38	0.86	0.13
16.22	0.64	0.43	0.008
32.45	0.23	0.19	0.017
64.85	0.13	0.075	0.005

When multiple regression procedures were applied to the Mays meter data, it was found that the two indices, VA_4 and VA_{16}, were sufficient to explain the response of each Mays meter on the 29 test sections. Furthermore, no significant improvement in the correlations came about by allowing different combinations, or functions, of RMSVA indices. Figure 1 shows that the correlations of the two indices, VA_4 and VA_{16}, with Mays meter roughness are large compared with their correlation with each other; hence, each statistic contains relevant information that is not contained in the opposing statistic. Such plots actually indicate that the peak response for most Mays meter units is at a base length smaller than 8 ft and that perhaps another pair, say VA_3 and VA_{12}, would have provided marginally better correlations. Comparison of the Mays meter data with VA_4 and VA_{16} produced regression equations that, with few exceptions, have markedly similar coefficients.

The method used for arriving at a single profile index was to fit each Mays meter Mi (run at the standard speed of 50 mph) to the nonlinear model

$$Mi \simeq \alpha_1 + \beta_1 (VA_4 + R\,VA_{16}) \quad (1)$$

where coefficient R is determined to provide an optimum calibration for the collection of Mays meter trailers as a whole. This nonlinear regression problem is easily solved by plotting the total regression sum of squares for Equation 1 at various values of R and interpolating the minimum. In this manner, R^2 = 2.5 was obtained.

Such considerations led us to the linear calibration model

$$Mi \simeq \alpha_1 + \beta_1\,MO \quad (2)$$

where

$$MO = 20 + 23\,VA_4 + 58\,VA_{16} \quad (3)$$

The coefficients in the RMSVA statistic MO were selected so that α_1 and β_1 are approximately 0 and 1, respectively, for the Mays meter trailers. Thus, MO will serve as our ideal Mays meter. The results of fitting this model to the Mays meter and RMSVA data are given in Table 1.

The regression results of Table 1, when plotted, reveal two distinct Mays roughness meter (MRM) groupings: trailers and cars. Although based on fewer data, the car-mounted Mays meters obviously differ from the trailers in their relation to MO. The five trailers, however, are so similar in their response that they would seem to be indistinguishable and thus be in no need of calibration. Yet, their correlation with MO is strong enough that units as similar to each other as M2 and M5 can be separated, as is shown in Figure 2. Ninety-five percent confidence intervals for their slope parameters (B and B) do not, in fact, overlap.

We summarize the Mays meter-RMSVA correlation study as follows: A profile statistic based on RMSVA at base lengths of 4 ft and 16 ft was successful in explaining approximately 97 percent of the response variation between five trailer-mounted Mays meters on 29 pavement test sections. This corresponds to a prediction standard error of about 10 percent of the Mays meter reading (in/mile), which compares favorably with what would be achieved if an actual Mays meter had been singled out as the reference device. Results for the three car-mounted Mays meters were not quite as favorable (R^2 = 0.91, 0.93, and 0.95); however, section data for the two units that deviated most were incomplete.

The correlation studies that produced the profile statistic MO (Equation 6) were carried out in early 1978 and since then the statistic has been used regularly by TSDHPT for the calibration of its Mays meters. Although MO was tailored to describe Mays meter data obtained around October 1977, subsequent Mays meter calibrations have continued to demonstrate the high correlations described above.

Rescaling of RMSVA Indices

The Mays meter simulation MO has proved to be an effective standard for Mays meter calibration; however, the individual RMSVA indices (base lengths 1, 2, 4, 8, 16, 32, 65, and 130 ft) are genuine roughness traits that have been useful for comparing pavements in other studies. Therefore, to make such

Table 1. Regression that results from fitting eight Mays meters to the linear model of Equation 5.

Item	M1	M2	M3	M4	M5	M6	M7	M8
α_i	-1.7	9.6	0.2	0.5	-7.9	28.6	8.9	-6.0
β_I	1.07	0.88	1.06	0.94	1.08	1.42	1.49	1.89
R^2	0.981	0.972	0.969	0.967	0.972	0.913	0.925	0.951
SE	9.7	9.5	12.2	11.1	11.9	16.4	15.8	27.9

Figure 2. Calibration results for two trailer-mounted Mays meters.

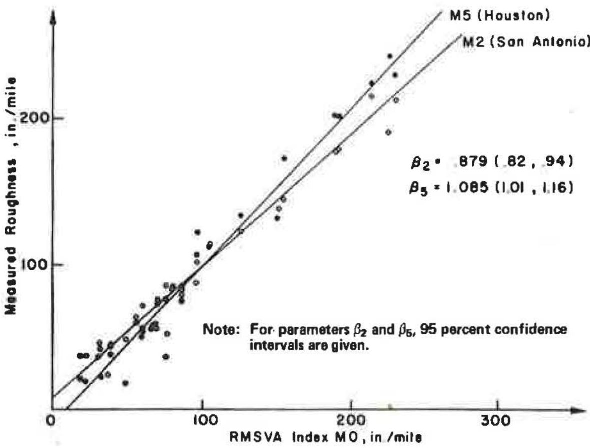

Figure 3. RMSVA signatures for untreated (top) and treated (bottom) ACP sections in a swelling clay environment—loop 410, San Antonio.

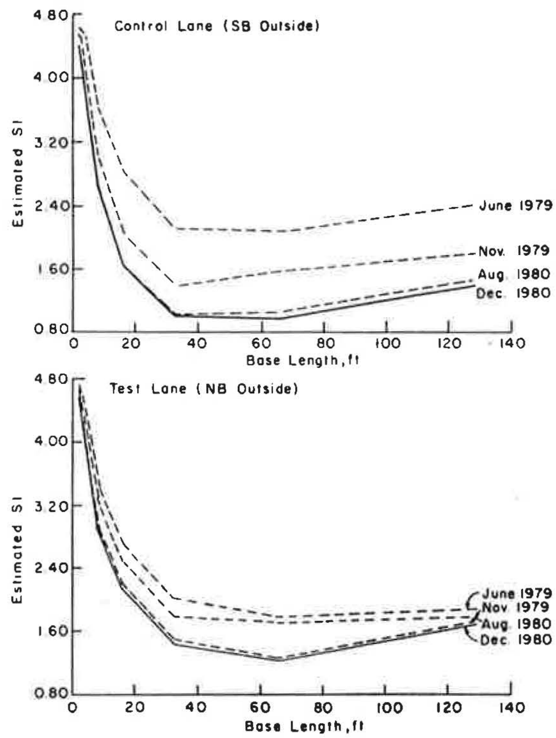

comparisons easier, rescaled versions of these indices are usually provided that resemble a sequence of serviceability ratings in the range 0-5.

The main advantage of such scalings is that their means, as determined on 31 ACP test sections near Austin (April 1981), are approximately the same, which makes it easier to judge their significance for other pavements. The test sections encompass a variety of roughness conditions, which exhibit a serviceability range of 0.63 to 4.83, with a mean of 3.12 and SD of 1.23.

The RMSVA data for two sections known to be subject to deterioration from expansive clays are shown in Figure 3 (SI versus base length), along with the corresponding values obtained periodically during the previous 18 months (dashed lines). Notice that the spectra of SI values form distinctive signatures that, in this case, changed very little during the last 4-month period. The test section (lower figure) shows the effect of treatment by a fabric moisture seal prior to the first profilometer run in June 1979. The differences, however, are confined to the longer RMSVA base lengths and would probably not be noticed in readings from a Mays meter. Data for these sections were provided by TSDHPT engineer Malcolm Steinberg.

CONCLUDING REMARKS

We must not confuse the problem of calibrating a group of instruments with the problem of interpreting their measurements. When the Texas Mays meter calibration method was first devised, the serviceability index (SI) was the best available estimate of present serviceability rating (PSR), a measure of roughness that is meaningful. Since serviceability estimates were desired from the Mays meters, SI was chosen as the standard against which different units were to be calibrated. This would have been a good approach, however, only if Mays meters were capable of measuring SI with as much accuracy as their precision would seem to indicate. Unfortunately, this is not the case. At best, Mays meters can be assigned scalings so that different units give comparable Mays meter roughness ratings. How the ratings should be used to predict other things, such as ride quality, is a problem to be considered apart from the calibration process itself.

Our study of the Texas Mays meters revealed that a simple profile statistic based on RMSVA could serve effectively as a calibration standard. When the statistic is rescaled by regression techniques to approximate a serviceability rating, we find that different Mays meters that are calibrated against it can measure roads and agree to within 0.1 or 0.2 serviceability unit. This precision, of course, says nothing about the accuracy of such measurements as predictors of subjective serviceability ratings because the Mays meter is necessarily limited in its response.

However, the Mays meter is capable of measuring a certain kind of roughness with good precision. The obvious benefit of this is in making comparisons; for example, in revealing differences between pavement sections and in showing trends in deterioration or the effects of rehabilitation on roughness. For this purpose, especially, a good calibration method based on a stable and valid reference is necessary.

ACKNOWLEDGMENT

We are pleased to acknowledge the work of Maitree Srinarawat, who assisted in much of the original data analyses in which the relevant RMSVA indices were derived. Also appreciated is the kind assistance of TSDHPT representative Brad Hubbard, who furnished the Mays meter data crucial to this study and who was first to point out certain deficiencies in the original calibration program. We are also pleased to acknowledge the combined efforts and support of the Center for Transportation Research at the University of Texas at Austin and the TSDHPT in cooperation with the Federal Highway Administration. The contents of this abridgment reflect our views, and we are responsible for the facts and the accuracy of the data presented herein. The contents do not necessarily reflect the official views or policies of the Federal Highway Administration or the TSDHPT. This paper does not constitute a standard, specification, or regulation.

REFERENCES

1. J.R. Darlington. Evaluation and Application Study of the General Motors Corporation Rapid Travel Profilometer. Michigan Department of State Highways, Lansing, Rept. R-731, April 1973.
2. J.P. Guilford. Psychometric Methods. McGraw-Hill, New York, 1954.
3. R.S. Walker and W.R. Hudson. Use of Profile Wave Amplitude Estimate for Pavement Serviceability Measures. HRB, Highway Research Record 471, 1973, pp. 110-117.

Publication of this paper sponsored by Committee on Pavement Condition Evaluation.

Inertial Profilometer Uses in the Pavement Management Process

ELSON B. SPANGLER

The inertial profilometer has the potential to become one of the most important tools in the pavement condition evaluation process. This paper discusses its continuing development, including a noncontact profile sensor, digital profile computation, and an array of computer software developments that will further enhance the inertial profilometer's contribution to the pavement management process. For historical purposes the paper also discusses the original development of the inertial profilometer at the General Motors Research Laboratories in the early 1960s and its introduction into the user community by K.J. Law Engineers, Inc.

The inertial profilometer was developed in the early 1960s at the General Motors Corporation Research Laboratories (GMR) (1). It was developed for the purpose of measuring, recording, and bringing a replica of a pavement surface profile into the laboratory for use in vehicle suspension computer simulations. The original development task was thought to be trivial but took four years and cost $0.5 million in 1960 dollars. This paper discusses that original development, its continued development as a commercial product under license from General Motors, and some future developments that will enhance the device as an important pavement management tool.

GMR PROFILOMETER

The development of the inertial profilometer at the General Motors Research Laboratories in the 1960s was made possible by the availability of high quality force balance accelerometers used in the Aerospace Industry for inertial guidance. Also important in the development was the availability of high quality analog computer components, including the integrators used in the profile computation. The GMR profilometer developed at that time (Figure 1) used a 6-in diameter wheel to follow the pavement surface (W), a high-quality potentiometer to measure the relative motion (W-Z) of the pavement-following wheel, and an accelerometer isolated from large pavement profile acceleration by being mounted on the vehicle's sprung mass. The accelerometer output ($\ddot{Z}$) and the potentiometer output (W-Z) were inputs to an analog computation that produced the measured pavement profile, W_m:

$$W_m = (W - Z) + \iint \ddot{Z}\,dt\,dt \tag{1}$$

The capability for measuring the spatial wavelength (Figure 2) was found to be more than adequate for vehicle ride studies. Measuring response remained flat for wavelengths up to 200 ft for even the low measuring velocities. The profilometer's short wavelength measuring capability was demonstrated by the ability of the pavement-following wheel to follow a wood shingle (Figure 3) placed on the pavement surface. The profilometer's overall measuring capability was demonstrated by its ability to measure (Figure 4) and isolate (Figure 5) pavement spatial wavelengths that caused ride quality problems in General Motors' cars on California highways.

Much of the work at the General Motors Research Laboratories was reported by Spangler and Kelly (1). Work that was not reported included the use of the GMR profilometer to measure airport runways and taxis strips, city streets traveled by General Motor's buses, and rail profiles (2) traveled by General Motor's locomotives. One of the more important results of this early effort was the ability to measure and record an accurate replica of many different pavement surfaces (Figure 6) for later examination, analysis, and processing by more-sophisticated engineering computer tools.

COMMERCIAL PROFILOMETER

After the 1965 TRB presentation on the GMR profilometer (1) the General Motors Corporation was requested by several transportation agencies to make the inertial profilometer technology available to the transportation community. K. J. Law Engineers, Inc., of Farmington Hills, Michigan, was granted a

Figure 1. GMR inertial profilometer.

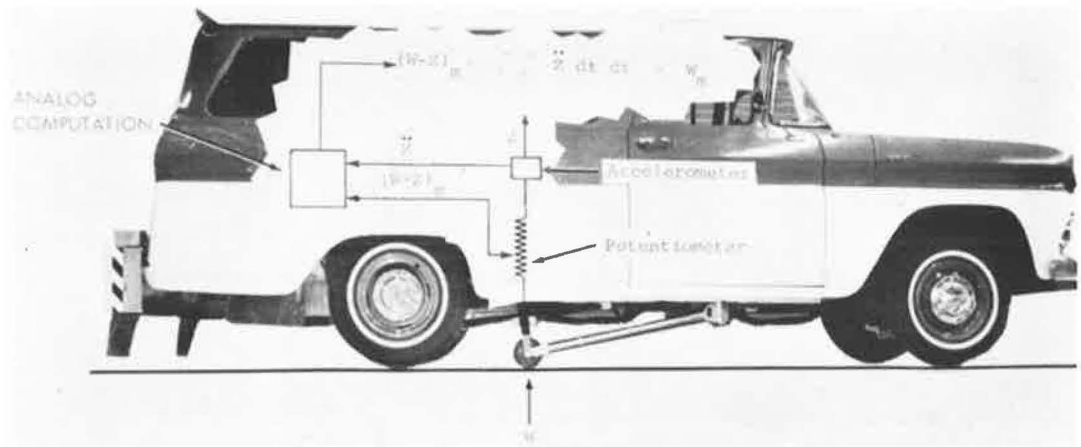

Figure 2. GMR profilometer wave-length measuring capability.

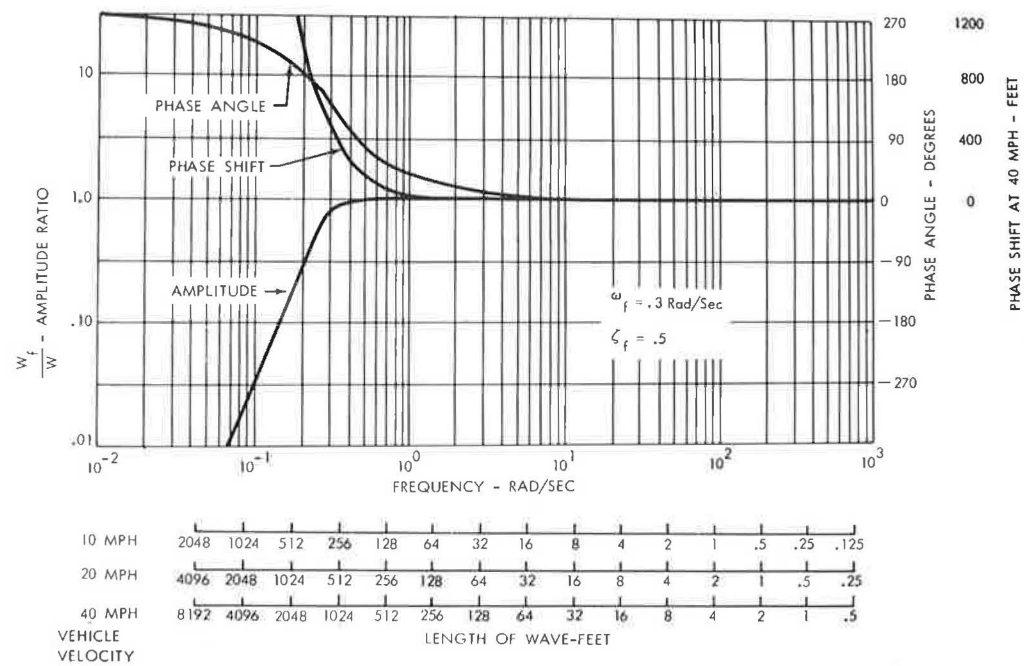

Figure 3. Pavement-following wheel response to wood shingle.

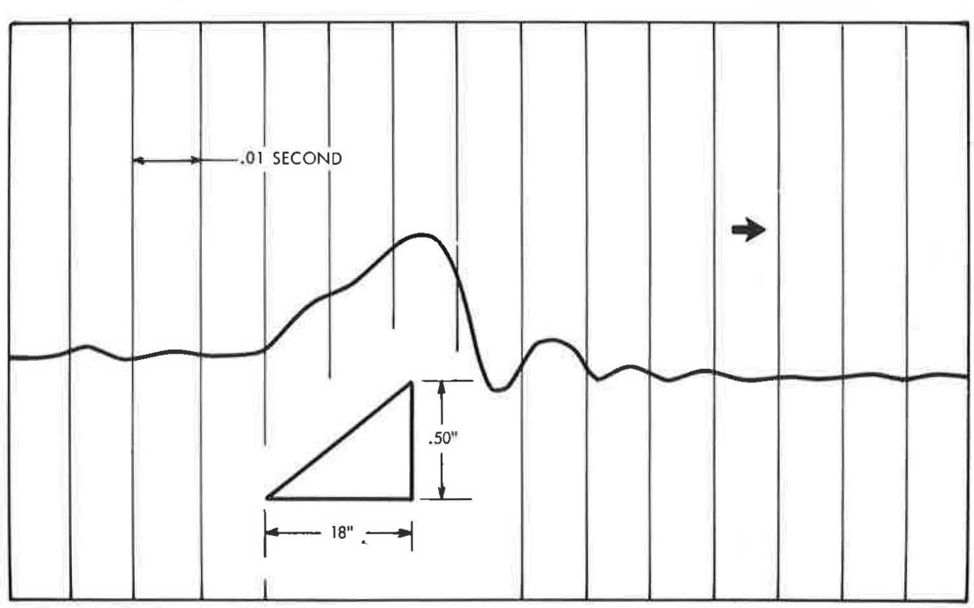

Figure 4. Pavement that induces automotive body shake.

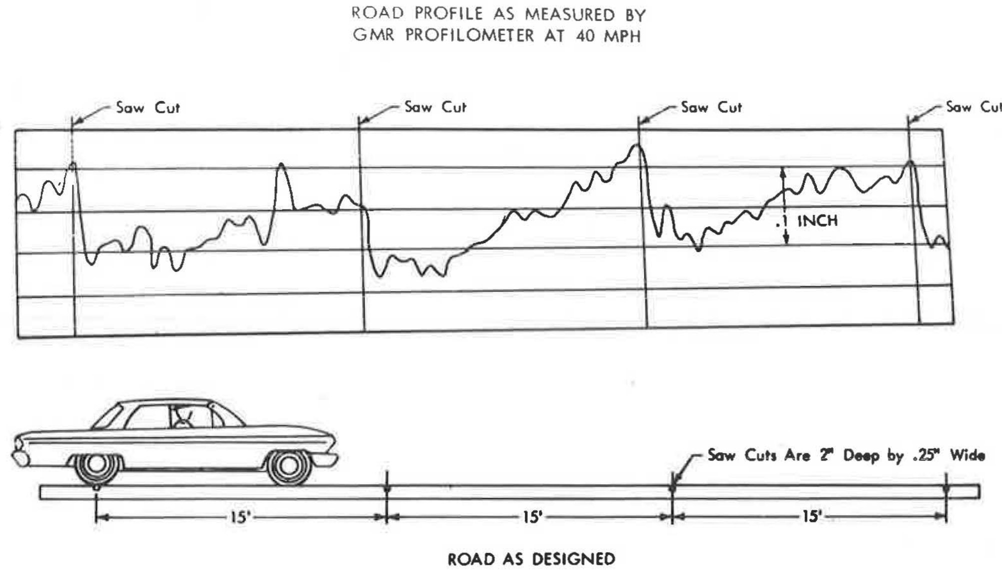

Figure 5. Harmonic analysis of measured pavement profile.

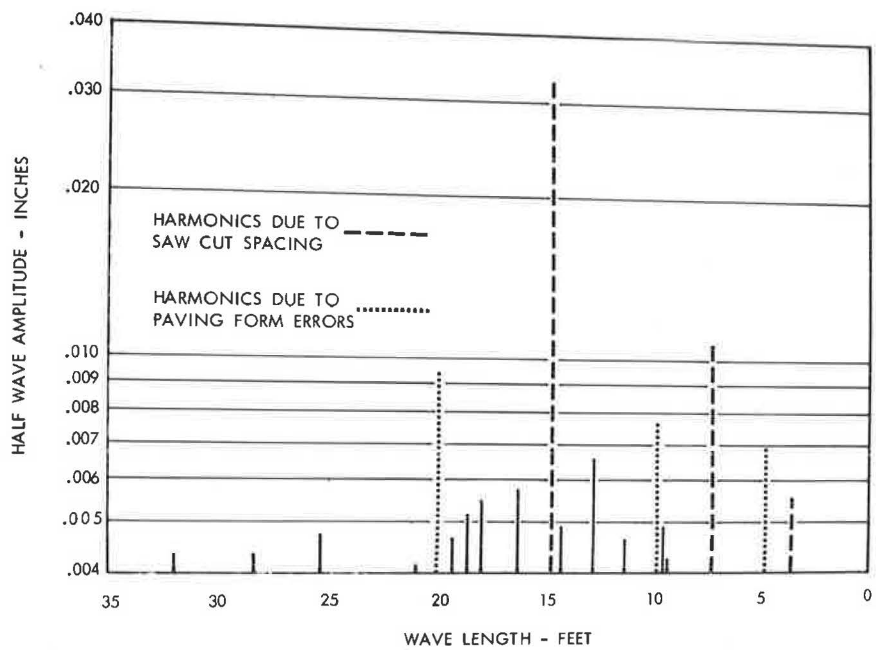

Figure 6. Characteristics of measured pavement surfaces.

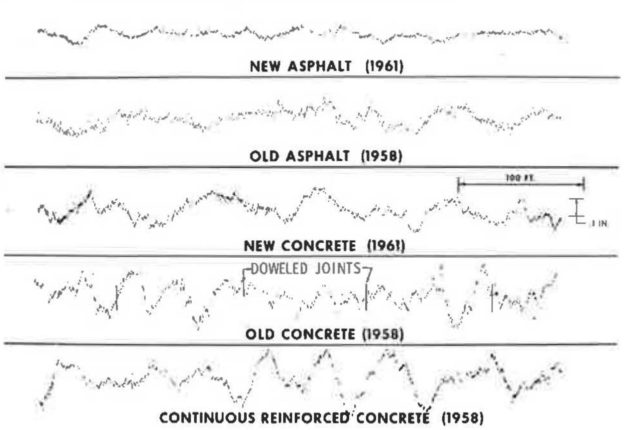

license to manufacture and sell inertial profilometer equipment under a General Motors Corporation patent. The requests also resulted in a cooperative effort between GMR and the Michigan Department of Transportation (3) in the evaluation of the GMR profilometer for application in typical highway department projects. Continued efforts by the Michigan Department of Transportation have produced an array of profile processing computer programs, including a bituminous fill paving program that will be discussed later in the paper.

Texas Profilometer

The first commercial profilometer built by K. J. Law Engineers, Inc., was manufactured in 1966 for the Texas Department of Transportation and operated by the Center for Highway Research at the University of Texas (4). Profilometers were then manufactured by

K. J. Law Engineers, Inc., for Pennsylvania and Kentucky (5) and later for Brazil under a World Bank project. The Pennsylvania, Kentucky, and Brazil profilometers were supplied with a quarter-car simulation device (5), which processed the measured pavement profile to produce summary ride quality data.

Restricted Use

The four profilometers manufactured by K. J. Law Engineers, Inc., between 1966 and 1976, were essentially the same state of the art as the GMR profilometer (1). Although, it was a significant advancement over prior pavement measuring technology, expanded use was restricted by many factors, including

1. Required pavement friction measurements,
2. Technical complexity,
3. Pavement following wheels, and
4. Pavement profile data processing.

Required Pavement Friction Measurements

About the time state transportation agencies were considering the pavement roughness problem, new federal requirements diverted their attention to the problem of pavement friction. Both problems are worthy of attention, but most states had insufficient engineering resources to address both effectively. As a result, a significant pavement roughness effort was delayed for a decade. This, however, might have been an advantage.

Technical Complexity

The inertial profilometer is a fairly complex measuring system. In the early systems it was almost necessary to know how the system worked to use it effectively. Although the new profilometer is more complex, the system requires limited knowledge to use it effectively.

Pavement Following Wheel

The pavement following wheel has been the most serious operational problem. This problem was recognized in the original design and development work at General Motors. The electronics technology at that time would not support a noncontact approach. A significant design effort was exerted on the pavement following wheel assembly to attain the level of performance and reliability that has been exhibited over the years. However, wheel damage, costly replacement, and unscheduled down time could not be avoided. Fortunately, noncontact relief is in sight.

Pavement Profile Data Processing

Pavement profile data processing is essential to the pavement management process. The output from the early profilometers was analog profile amplitude signals displayed on a strip chart, recorded as a function of distance, and stored on analog magnetic tape as a function of time. It was nice to see pavement profiles drawn out on the strip chart recorder, but what can you do with a hard copy profile drawing? Several users converted the analog magnetic tape data to a digital format for processing on a big, main-frame computer. However, this did not appear to be the solution for most transportation agencies. As a result, I and K. J. Law Engineers, Inc., developed the electronic quarter-car simulator, which gave the user immediate information on ride quality. In addition, it provided the simulated output of the Bureau of Public Roads (BPR) roughometer, which allowed several transportation agencies to retire their antiquated BPR roughometer devices. The quarter-car simulation has become a recognized data processing tool and has now been implemented as a computer software program.

NEW PROFILOMETER DESIGN

With time, many of the factors that restricted expanded use of the inertial profilometer have abated. The nationwide mandated measurement of pavement friction has been implemented with new sophisticated equipment and technically trained staff to support that equipment. These trained staff now have the same skills required to operate and maintain the new generation of inertial profilometer equipment.

The remaining factors were addressed in the design of the new digital model 690D Surface Dynamics inertial profilometer manufactured by K. J. Law Engineers, Inc. The first model 690D profilometer was delivered to the West Virginia Department of Transportation in the fall 1979. The most significant improvement was the introduction of the digital computer used to perform the digital computation of the measured pavement profile and to store the computed profile data in digital format on the computer's digital magnetic tape recorder. The user interface with the profilometer system is a computer terminal that interactively leads the user through an array of computer programs designed to assist in the effective use of the profilometer system. The computer programs available to the profilometer user fall into two categories: profilometer systems programs and pavement profile data processing programs.

Profilometer Systems Programs

The profilometer system programs are basic to the operation of the profilometer itself and include programs to perform the following procedures:

1. System calibration,
2. Set-up,
3. Pavement profile computation, and
4. Magnetic tape playback.

The programs are designed to perform these procedures with minimal user involvement. Where involvement is required, the user is led, interactively, through a sequence of nontechnical question and answer exchanges.

System Calibration Program

The system calibration program is designed to assist the user in the calibration of the entire profilometer system. The program leads the user, interactively, through the calibration procedure, collects the calibration data, and compares the results with acceptable values for that data. Where possible, the calibration procedure has been automated to reduce the need for user involvement.

Set-Up Program

One of the more important procedures is the set-up program, which allows the user to input pertinent historical descriptive information on the pavement whose profile is to be measured. The information collected in the set-up program includes (a) date, (b) time, (c) run number, (d) project number, (e) laboratory number, (f) direction measured, (g) distance measured, (h) beginning mile post, (i) beginning description, (j) ending description, (k) pavement surface, (l) material, (m) condition, (n) weather, (o) temperature, (p) measuring speed, (q) operator-driver, and (r) filter wavelength (ft).

Filter wavelength is the only technical question concerning the operation of the profilometer system itself. It could be easily omitted by making filter wavelength a constant. On completion of the set-up procedure, the set-up descriptive information is stored as text on the digital magnetic tape as a tape information header for the pavement profile measurements that will follow.

Profile Computation Program

The profile computation program performs the following important system functions: (a) reads transducer outputs, (b) computes pavement profiles, (c) stores pavement profiles on magnetic tape, and (d) outputs pavement profiles to strip chart recorder.

Pavement profile computations are made for the two wheel paths at least every inch longitudinally along the pavement surface. Pavement profile data point pairs are stored on magnetic tape at 6-in intervals. The pavement profile computation is independent of profile measuring velocity and changes in velocity that allow the driver to move at traffic speed during the pavement profile measuring process.

The pavement profile computation program, in addition to computing profile, can also compute a pavement profile summary statistic such as the simulated output of the BPR roughometer, Mays, PCA, or Cox ride meters, or root mean square (RMS) acceleration of a typical quarter-car vehicle. The summary statistic can be printed immediately on the users's computer terminal as it is computed.

Magnetic Tape Playback

After the profile measuring run has been completed, the magnetic tape playback program allows the user to play back and validate the pavement profile measurements just made.

Pavement Profile Data Processing Programs

In addition to the profilometer systems programs, an array of profile processing programs is available to the user for the analysis of the measured pavement profile stored on magnetic tape. Three profile processing programs will be discussed, including

1. Straightedge program,
2. Ride meter simulation and calibration program, and
3. Ski control bituminous fill program.

Straightedge Program

Most transportation agencies have, as part of their standard specification for roads, a surface tolerance specification that involves the use of a straightedge. For example, the West Virginia specification reads, "When tested with a 10-foot straightedge...the finished wearing course shall not show a deviation from the required surface greater than 3/16 inch."

The straightedge program is designed to automate the straightedge inspection of recorded pavement surfaces. The program gives the user the ability to enter the straightedge length (ft) and the maximum allowable straightedge deviation (in). The program then reads the desired pavement profile data from magnetic tape, simulates the movement of the straightedge down the pavement surface, and prints out, on the user's computer terminal, the straightedge deviations that exceed the allowable maximum for both wheel paths as a function of distance (ft). The typical output data format shown below would be preceded by the descriptive information entered by the user in the set-up program.

Distance From Beginning (ft)	Deviation (in) Left Track	Right Track
33.00	0.12	
33.50	0.11	
34.00	0.15	
34.50	0.18	0.10
35.00	0.14	
35.50	0.11	0.11
36.00		0.12
36.50		0.12
37.00		0.11
252.50	-0.10	-0.10
253.00	-0.14	
253.50	-0.13	
257.50	0.13	
259.00	0.16	

Negative straightedge deviation values indicate a hump in the pavement profile with the center point of the pavement surface being above the computed straightedge. With this information, the user can return to pavement locations that exceed the allowable specification tolerance for more detailed inspection if required.

Ride Meter Simulation and Calibration Program

The ride meter simulation and calibration program provides the user with the standard ride index (RI) for that pavement profile and assists the user in establishing a calibration for an actual ride meter when driven over an array of pavement surfaces. The vehicle simulation model used is based on the golden car parameters proposed by Gillespie (6). User inputs to the calibration part of the program are standard and measured RI data point pairs for an array of pavement surfaces that have a wide range of RIs. The output of the program yields a calibration equation and shows how well the calibration equation correlates with the data used, Figure 7.

Ski Control Bituminous Fill Program

The ski control bituminous fill program is based on the original work of the Michigan Department of Transportation. This program simulates the paving process of a bituminous paving machine (Figure 8) whose screed is controlled by the movement of the center point of a paving ski. A 30-ft ski, used in the Michigan and West Virginia bituminous fill programs, produces a good, predictable ride quality surface with a significant reduction in short wavelength content. By using a computer simulation of a straightedge or ride meter on these surfaces, improvement in ride quality can be evaluated. In the West Virginia bituminous fill program a reduction in the number of straightedge deviations is used as a measure of improved pavement surface quality.

Shown below is the interactive question-answer exchange that initiates the bituminous fill computation:

```
ENTER BITUMINOUS FILL PARAMETERS

ENTER BITUMINOUS FILL WIDTH:                    10.0
ENTER NUMBER BITUMINOUS FILL LAYERS:             2
ENTER THICKNESS OF FIRST LAYER:                  1.0
ENTER WEIGHT OF MATERIAL FOR FIRST LAYER:      146
ENTER THICKNESS OF SECOND LAYER:                 1.0
ENTER WEIGHT OF MATERIAL FOR SECOND LAYER:     146
```

Figure 7. Ride meter calibration data.

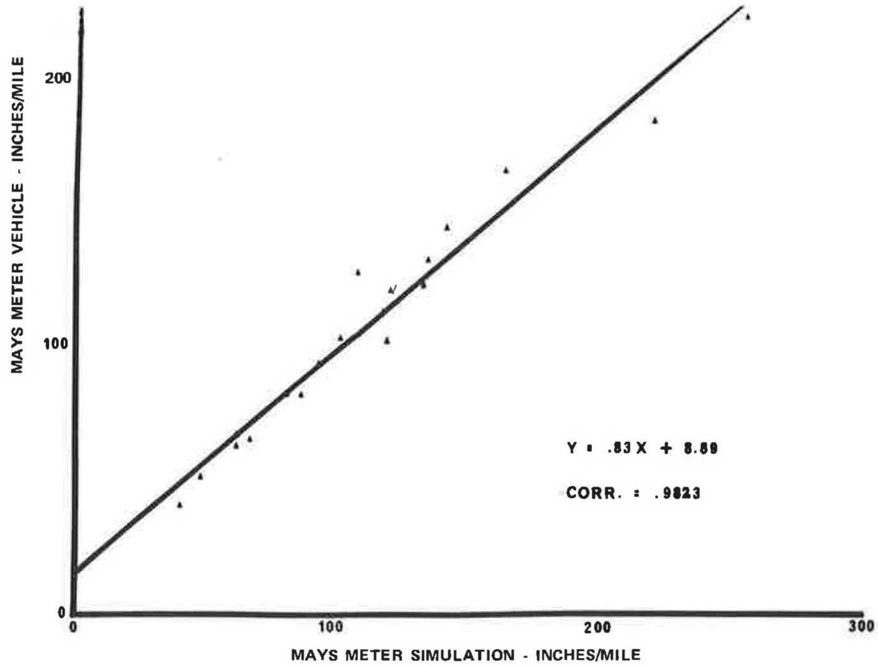

Figure 8. Ski-controlled bituminous paving machine.

Figure 9. Printed output of bituminous fill program.

```
LENGTH:     3168.00 FEET
 WIDTH:       10.00 FEET

STR. EDGE DEVIATIONS BEFORE 1ST FILL = 71.00
RIDE INDEX - RMS ACCELERATION        =   .093 G

FIRST LAYER:

            THICKNESS:       1.00 INCHES
      LEVELING VOLUME:       4.46 CU. YDS.
     THICKNESS VOLUME:      97.77 CU. YDS.
         TOTAL VOLUME:     102.23 CU. YDS.
      LEVELING WEIGHT:       8.80 TONS
     THICKNESS WEIGHT:     192.71 TONS
         TOTAL WEIGHT:     201.51 TONS

STR. EDGE DEVIATIONS AFTER 1ST FILL =    .00
RIDE INDEX - RMS ACCELERATION       =    .069 G

SECOND LAYER:

            THICKNESS:       1.00 INCHES
      LEVELING VOLUME:       2.24 CU. YDS.
     THICKNESS VOLUME:      97.77 CU. YDS.
         TOTAL VOLUME:     100.01 CU. YDS.
      LEVELING WEIGHT:       4.42 TONS
     THICKNESS WEIGHT:     192.71 TONS
         TOTAL WEIGHT:     197.13 TONS

STR. EDGE DEVIATIONS AFTER 2ND FILL =    .00
RIDE INDES - RMS ACCELERATION       =    .022 G
```

While the bituminous fill computation is in progress the resulting paved surface profiles are drawn on the strip chart recorder as a function of distance. After the computation, results of the bituminous fill program are output on the user's computer terminal. Printed results from the two computed bituminous fill passes, including the straightedge deviations and RI before paving and after each paving pass, are shown in Figure 9. The fill or leveling material thickness is computed for each location along the profile surface by the simulation of the ski-controlled paver. The overlay thickness is added to the leveling thickness to get total thickness at each location. Volume is computed by multiplying by lane width. Multiplying the total computed volume by the unit weight of the material produces total weight, in tons, of material required for each paving pass. The Michigan Department of Transportation, in the use of their bituminous fill program, has found that the computed weights are within 5 percent of actual project amounts.

Noncontact Profile Sensor

A noncontact profile sensor was not available for the model 690D digital profilometer delivered to the West Virginia Department of Transportation in 1979. However, a new light-beam noncontact sensor has been developed by K. J. Law Engineers, Inc., and will be retrofitted on the West Virginia Profilometer in time for the 1982 measuring season.

Second Texas Profilometer

One of the more aggressive user's of the inertial profilometer has been the Center for Highway Research, University of Texas at Austin. Funded by the Texas State Department of Highways and Public Transportation, the University of Texas Center for Highway Research has been a leader (7,8) in the evaluation of the inertial profilometer's capabilities and pavement profile data processing techniques. They are also well acquainted with the inadequacies of their early vintage profilometer and have purchased a new model 690D Surface Dynamics profilometer, which is essentially the same as the West Virginia profilometer discussed earlier. Although Texas would like to have the noncontact profile sensor, they chose to stay with the pavement following wheel until the noncontact sensor has proven successful on the West Virginia profilometer. The new Texas profilometer will be in operation in the 1982 measuring season.

Ohio Profilometer

The first model 690D profilometer to be built with a noncontact pavement profile sensor will be a unit purchased by the Ohio Department of Transportation for delivery early in 1982. An important part of the Ohio profilometer acquisition is their desire for ongoing systems support for the use of the inertial profilometer in their pavement management process. This support, which is available through Surface Dynamics, Inc., as an engineering consulting service, will allow the profilometer system and pavement profile data processing programs to be tailored to their own particular needs. It will also allow development of new programs, required by the agency, to assist in their pavement management process.

NEW PROFILOMETER DEVELOPMENT

Much progress has been made in recent years to make the inertial profilometer a more useful tool in the pavement management process. This development work is continuing and will produce profilometer features designed to assist the profilometer user community.

Pavement Profile Computation Program

Several optional software extensions are being developed for the pavement profile computation program. These extensions, which are designed to provide additional pavement management information, include

1. Reinitialization,
2. Cross-slope computation, and
3. Rut depth measurement.

Reinitialization

The reinitialization option gives the pavement profile computation program the ability to instantly reinitialize the computation of pavement profile, remove all past profile history, and provide accurate profile measurement from the moment of reinitialization. This option is valuable where long wavelength content from prior pavement profile measurement masks short wavelength content of interest and the prior pavement profile is not required. It also provides a method for rapid recovery from transient response that results from measuring vehicle acceleration at start up.

Cross-Slope Computation

In the pavement profile computation program, the pavement profiles of the two wheel paths are computed independently with no established cross-slope relation between the two profiles. The cross-slope computation option provides a valid cross-slope relation between the computed profiles of the two wheel paths. Valid cross-slope information is important in the simulation of paving equipment and the computation of material quantities involved in the pavement resurfacing process.

Rut Depth Measurement

Rut depth information is also important in the computation of material requirements in the pavement resurfacing process. Information on rut depth can be obtained by measuring the relative elevations of the two wheel paths and the quarter-point (half way between wheel paths). To make the rut depth computation three pavement profiles need to be measured and their elevation related by cross-slope information. The rut depth measurement option, therefore, requires hardware to measure a third (quarter-point) pavement profile and cross-slope computation. The third pavement profile is stored on magnetic tape along with the profiles for the two wheel paths.

Profile Processing Programs

Additional pavement profile data processing programs in development include

1. Computer-control grind program and
2. Pavement management data base program.

Computer-Control Grind Program

In the computer-control grind program a computer algorithm is used to remove short wavelength content from the recorded measured pavement profile to produce a pavement profile that meets the desired ride quality. User inputs to the program are desired ride quality, unit cost of grinding, and desired printout distance interval. Outputs of the program, printed on the user's terminal, are depth-of-cut data at the selected distance intervals along the pavement surface, and the estimated total cost of the resulting grinding process. Figure 10 illustrates how the program computes a new pavement profile to meet a desired RMS acceleration ride quality. Figure 11 shows the grind depth-of-cut for each location along the pavement surface. Grind area is the cross-sectional area between the original and ground profiles. The grind cost is for a lane width of pavement. The computer-control grind program is designed to give a grind contractor a list of pavement grind depths that will bring a pavement surface back to a specified ride quality. A computer-control bituminous paving program is also being developed based on the same computer algorithm.

Pavement Management Data Base Program

The pavement management data base program is designed to use the profilometer's computer capacity to process and store large amounts of pavement management field data when the system is not being used for measuring profiles. The digital magnetic tape system can store up to 10 million characters of pavement field data on a 7-in reel of digital magnetic tape. The program gives the user a method for entering, storing, and retrieving field data related to pavement inventory condition by project or sections of a project. Items stored on tape in the field data base include (a) pavement geometrics, (b) traffic volume, (c) traffic loads, (d) structural capacity, (e) ride quality, (f) surface condition, and (g) skid resistance.

The pavement management data base program is intended as a starter system that can be expanded by the addition of a larger bulk storage device, such as a disk, as the user's requirements expand. The profilometer computer system can communicate with a

Figure 10. Computed ground pavement profile.

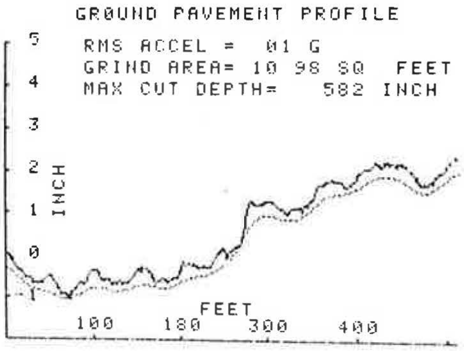

Figure 11. Pavement grind depth-of-cut.

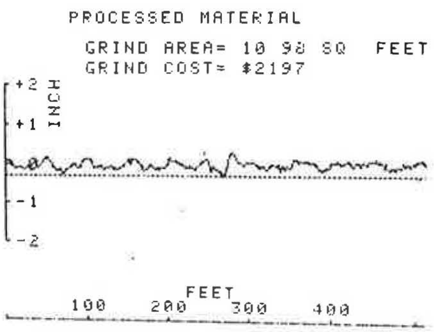

data processing center through a conventional phone line interface.

CONCLUSIONS

The capabilities of the inertial profilometer have continued to improve since its early development at GMR in the 1960s. Its continued development has resulted from advancements in instrumentation, digital signal processing, and the expanded demands of the user community. These advancements have led to a high-quality, cost-effective tool for the evaluation of pavement condition, which has capabilities far beyond its original pavement profile measuring task. The profilometer system's ability to collect, store, retrieve, and process pavement management field data gives it the potential to be an important element in the total pavement management process.

REFERENCES

1. E.B. Spangler and W.J. Kelly. GMR Road Profilometer--A Method for Measuring Road Profile. HRB, Highway Research Record 121, 1966, pp. 27-54.
2. E.B. Spangler and H.A. Marta. Dynamic Measurement of Rail Profile and Related Locomotive Truck Motions. ASME, Rept. 66-RR-1, 1966.
3. J.R. Darlington and P. Milliman. A Progress Report on the Evaluation and Application Study of the General Motors Rapid Travel Road Profilometer. HRB, Highway Research Record 214, 1968, pp. 50-67.
4. W.R. Hudson. High-Speed Road Profile Equipment Evaluation. HRB, Highway Research Record 189, 1967, pp. 150-163.
5. J.L. Burchett, R.L. Rizenbergs, and T.A. Moore. Surface Dynamics Profilometer and Quarter-Car Simulator: Description, Evaluation, and Adaptation. Kentucky Department of Transportation, Lexington, Res. Rept. 465, 1977.
6. T.D. Gillespie, M.W. Sayers, and L. Segel. Calibration of Response-Type Road Roughness Measuring Systems. NCHRP, Rept. 228, Dec. 1980, 81 pp.
7. R.S. Walker and W.R. Hudson. Practical Uses of Spectral Analysis With the Surface Dynamics Road Profilometer. HRB, Highway Research Record 362, 1971, pp. 104-119.
8. R.S. Walker and W.R. Hudson. Use of Profile Wave Amplitude Estimates for Pavement Serviceability Measures. HRB, Highway Research Record 471, 1973, pp. 110-117.

Publication of this paper sponsored by Committee on Pavement Condition Evaluation.

Prediction and Significance of Wet Skid Resistance of Pavement Marking Materials

D.A. ANDERSON, J.J. HENRY, AND G.F. HAYHOE

A data base of full-scale locked-wheel skid resistance is presented for typical marking materials, including traffic paints of various formulations, hot spray and extruded thermoplastics, cold preformed plastics, temporary tapes, and some two-part systems. A variety of pavement surface types, including dense- and open-graded asphalt and portland cement concrete, are used in the study. British pendulum numbers and macrotexture profile data are presented for field applications and for laboratory samples of marking materials. Equations are developed for predicting skid resistance from these data. The effects of glass beads, weathering, and polishing are examined in laboratory and field experiments. In all cases, the skid resistance of the marking materials is less than that of the pavement to which they are applied. From the results of a simulation study, a description is given of the effects of differential pavement friction on the handling and stability of four-wheeled vehicles and single-track vehicles. A tentative procedure for setting minimum acceptable levels of marking material skid resistance for four-wheeled vehicle operation is developed from the simulation results. A procedure for setting minimum levels of skid resistance for single-track vehicle operation could not be established. An alternative approach to the problem is suggested.

Little is known about the high-speed wet skid resistance of pavement marking materials. Michigan (1) measured the skid resistance of paints and plastics installed on concrete pavements. Skid resistance at 64 km/h (SN_{64}) ranged from 4 to 37 and British pendulum numbers (BPN) ranged from 14 to 31. These values are cause for concern, particularly during

Table 1. Materials included in research program.

Material[a]	Code	No. of Formulations Studied
Conventional Alkyd paint	AC	2
Conventional chlorinated rubber paint	CC	2
Alkyd quick-dry paint	AQ	2
Chlorinated rubber quick-dry paint	CQ	2
Alkyd paint with premixed glass beads	AP	2
Chlorinated rubber paint with premixed glass beads	CP	2
Hot extruded thermoplastic	HE	5
Hot sprayed thermoplastic	HS	3
Cold applied plastic	CA	10
Temporary tapes	TT	5
Two-part epoxy and polyesters	TP	4

[a] The materials were further coded according to the following scheme (e.g., AC1WU): AC = conventional alkyd; 1, . . . n = formulation number; W = white (Y = yellow); U = unbeaded (B = beaded).

lane changing maneuvers and for two-wheeled vehicles. Whereas these numbers are cause for concern, there is no analytical technique or field test procedure for determining whether or not they constitute a safety problem.

One approach for assessing the significance of the skid resistance of marking materials would be to study accident data, as has been attempted for pavements (2). Unfortunately, definitive accident data are not available and, in the absence of these data, it is necessary to use analytical and simulation techniques to evaluate the effect of marking material skid resistance on vehicle performance.

This paper summarizes an extensive research study that was conducted on the skid resistance of pavement-marking materials. Three main points are addressed: (a) development of a data base, (b) prediction of field skid numbers from laboratory tests, and (c) results of computer simulation analysis on the significance of differential skid resistance.

TESTING PROGRAM

The various marking materials used in this study are summarized in Table 1. Five substrates were selected for the laboratory testing: smooth metal, fine sand asphalt, open-graded friction course, dense-graded asphalt, and broomed portland cement concrete (PCC). Individual 100x150 mm panels were made for each of the surfaces and the marking materials were applied with field application equipment at the same time the material was applied to the field test surfaces.

The marking materials were also applied to a number of pavement surfaces in the field, including dense-graded asphalt, open-graded asphalt, PCC, and a fine sand asphalt. The field sites included public roads with traffic as well as sites at the skid test facility of the Pennsylvania transportation facility, where there was no traffic. In all cases, except for the two-part polyester and epoxy materials, conventional application equipment was used so that the materials would be representative of full-scale field applications. Full details of the application procedures and the test surfaces are given elsewhere (3).

Laboratory Testing

The laboratory test procedures that were selected were designed to condition the samples in order to simulate traffic wear and environmental exposure. Measurement techniques included microtexture and macrotexture measurements and BPN.

The Pennsylvania State reciprocating pavement polisher was used to simulate field polishing. A five-step polishing sequence that used five grit sizes (105-, 74-, 30-, 15-, and 5-μm grit) was required to obtain terminal polishing with unmarked pavement samples. For the marking materials, a single polishing sequence with 1000 cycles and 30 μm grit produced terminal polishing (3). The polishing mechanism was different for the beaded and the unbeaded surfaces. There was no appreciable wear of the beads, even after 1000 polishing cycles. The polishing sequence merely removed paint overspray from the surfaces of the beads, which accounted for the decrease in BPN values for the beaded surfaces after polishing. On the other hand, the behavior of the unbeaded surfaces was erratic--the BPN of some materials increased during polishing whereas others decreased. In general, the increases were associated with very smooth, glazed surfaces such as the epoxies of unfilled paints. Decreases were associated with rippled or rough surfaces or with premixed materials where the polishing removed surface asperities.

Based on the test results, mechanical conditioning of the panels is necessary before BPN tests are conducted. Wear in the traditional sense that occurs with aggregate does not occur with marking materials. For beaded surfaces it is necessary to remove overspray so that the beads are exposed to the foot of the BPN pendulum. If the overspray is not removed, the reported BPN values will be in error on the high side. For the smooth, glazed surfaces polishing tends to increase the BPN value.

The foot of the pendulum can also condition the surfaces. Approximately seven swings of the pendulum are required to stabilize the readings. If ASTM E303 is adopted for use with marking materials, it will be necessary to change the test procedures so that, for example, the last four of seven readings are reported rather than simply deleting the first reading as is now specified (3).

It is imperative that laboratory samples be prepared in the same manner and with the same equipment as used in the field. The sprayed-on beads produced BPN values 14 points higher than did the dropped-on beads. Similar comments apply to spraying techniques and to materials applied with a doctor bar. The method of application can have a greater effect on the BPN values than will differences in materials.

Beaded and unbeaded panels were exposed in an Atlas Twin Arc Weatherometer. Microtexture and macrotexture values were not significantly different before or after exposure. Decreases in BPN were associated with beaded surfaces and attributed to a loss in overspray on the bead surfaces similar to the losses during polishing. Increases were associated with the unbeaded glazed surfaces. A patina developed on these surfaces but it was removed during polishing, much as it would be lost in the field due to traffic.

Field Test Program

In order to develop a rationale for predicting skid resistance on the basis of laboratory measurements, it was necessary to conduct full-scale skid resistance measurements and conduct the laboratory measurements both in the laboratory and in the field. These data were then used to develop the relation between skid numbers and the parameters measured in the laboratory. Also, monitoring of the field installations over a period of time provided insight into the effect of exposure to traffic and weather conditions.

To obtain skid numbers by using the Pennsylvania Transportation Institute (PTI) Mark III pavement friction tester, which conforms to full-scale locked-wheel skid-tester specification in ASTM

Table 2. Field data.

Material[a]	BPN 10-31-78	RMS (mm) 11-9-78	SN_{64} 10-31-78	BPN 4-13-79	SN_{64} 5-14-79	PNG (h/km) 5-14-79
Open-graded asphalt concrete						
Pavement	93.8		48.4		54.3	0.23
AC1WB	74.6	0.691	32.0	66.0	34.0	
AC1WU	61.4	1.709	30.3	49.4	28.7	0.86
CC1WB	71.0	0.688	31.4	63.6	32.0	1.34
CC1WU	47.0	0.691	16.9	54.2	23.0	1.68
AQ1WB	72.2	1.326	36.1	68.8	40.0	
AQ1WU	70.6	0.770	30.0	72.0	35.5	1.46
CQ1WB	72.2	0.541	39.9	68.0	39.0	1.10
CQ1WU	64.0	0.630	24.7	59.6	30.0	1.14
AP1WB	71.8	0.605	37.8	63.6	37.0	
CP1WU	76.0	1.227	37.0	75.0	49.3	1.12
CA3WB	57.2	0.330	31.8	51.4	31.7	1.53
TT1YB	51.2		47.7	57.0	46.5	1.07
TT2YB	66.8	0.538	41.5	67.0	37.0	0.75
TP1WB	59.8	0.297	37.4	36.6	34.0	1.10
Portland Cement Concrete						
Pavement	58.8		75.8		81.7	
AC1WB	51.8	0.104	17.9	50.4	21.0	1.14
AC1WU	49.2	0.084	12.7	49.8	14.0	1.88
CC1WB	51.2	0.089	17.8	46.4	20.5	1.11
CC1WU	48.6	0.198	9.7	35.6	12.3	2.21
AQ1WB	51.8	0.127	31.5	49.6	31.0	0.98
AQ1WU	66.6	0.074	22.2	62.6	21.5	0.81
CQ1WB	61.0	0.112	25.6	55.2	28.7	1.68
CQ1WU	48.6	0.135	12.8	47.0	14.7	1.96
AP1WB	52.2	0.107	28.2	47.6	25.7	1.31
CP1WB	56.2	0.082	29.4	47.4	32.0	1.72

[a]See Table 1 for explanation of code.

Figure 1. Variations in SN_{64} on the dense-graded asphalt public road site.

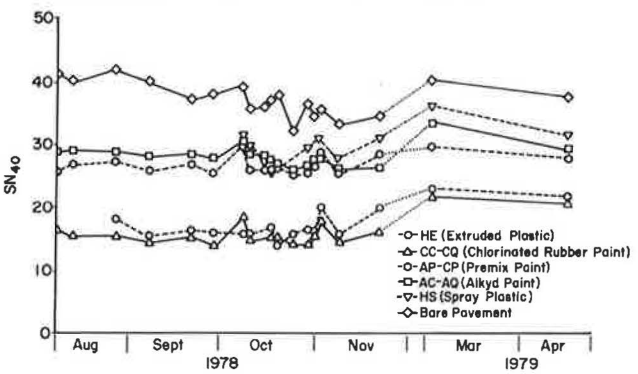

E274.79, it was necessary to apply the materials to the pavements in strips 0.3x6.5 m. Particular attention was given to apply the materials with equipment that would be representative of full-scale installations. Special equipment, developed by Prismo Universal Corporation for test line applications, that duplicates the performance of full-scale truck-mounted units was used.

Texture measurements, which can be made on laboratory samples, were performed at the field test sites as the materials aged in the presence of traffic and exposure to the elements. BPNs, which serve as a surrogate for microtexture measurements, and macrotexture profile traces reduced to their root mean square (RMS) values were found to be the most suitable methods for quantifying microtexture and macrotexture, respectively. Sandpatch measurements were unsuccessful on the marking materials because the sand did not show up well against the light background of the marking material and did not form distinct circles on the relatively smooth surfaces. Also, the sand became embedded in the softer plastic materials. Microtexture profile tracing equipment was found to be difficult to operate on many of the marking materials due to the high contact pressure developed under its extremely fine stylus. This pressure caused the stylus to dig into the softer marking material. The Pennsylvania State drag tester and the outflow meter were also considered but were rejected because they are designed for field testing and cannot be easily used with laboratory panels.

Table 2 summarizes typical measurements of skid resistance and texture for each material in fall 1978 and spring 1979 for dense-graded asphalt and PCC pavements. Data on other surfaces can be found elsewhere (3). The fall data include BPN, RMS (macrotexture), and SN_{64}, and the spring data include BPN, SN_{64}, and the percentage of normalized gradient of the skid resistance (PNG).

Examination of the data in Figure 1 reveals some general conclusions. The glass spheres (beads) increased the skid resistance of the paints. The paint surfaces retained their low skid resistance over the winter although they exhibited considerable wear and were expected to increase toward the levels of the unpainted pavement surfaces. This may be due to the combined effect of the loss of beads, which lowers the skid resistance, coupled with the loss of binder, which will eventually restore the original skid resistance of the pavement. The skid resistance of thermoplastics was also increased by beads. However, exposure to winter weather had a greater effect in reducing the advantage offered by the beads. In this case the formulations also contained beads so that when the surface beads were lost, both beaded and unbeaded applications benefited from the premixed beads.

It was not anticipated that pigment would have a significant effect on skid resistance. Three pairs of white and yellow paint formulations without beads were applied to the smooth tar-sand slurry surface. Initially there was no significant difference in skid resistance, but the white paints decreased in skid resistance to a greater extent over the winter,

Figure 2. Predictor equations for skid resistance of marking materials.

a. Traffic Paints

Unbeaded 22 applications $\overline{SN}_{64} = 20.7$ (s = 8.0)

$SN_{64} = .64\ BPN - 15.6$ $r^2 = .44$

$SN_{64} = .546\ BPN + 6.10\ RMS - 12.82$ $r^2 = .92$

Beaded 41 applications $\overline{SN}_{64} = 26.7$ (s = 6.8)

Chlorinated Rubber Base (20 applications) $\overline{SN}_{64} = 25$ (s = 8)

$SN_{64} = .725\ BPN - 15.4$ $r^2 = .61$

Alkyd Resin Base (21 applications) $\overline{SN}_{64} = 28.3$ (s = 5.1)

$SN_{64} = .356\ BPN + 7.10$ $r^2 = .36$

b. Thermoplastics

Unbeaded 12 applications $\overline{SN}_{64} = 18.7$ (s = 10.1)

Hot Extruded (7 applications)

$SN_{64} = .91\ BPN - 35.3$ $r^2 = .48$

$SN_{64} = .817\ BPN + 13.3\ RMS - 33.1$ $r^2 = .50$

Hot Spray (5 applications)

$SN_{64} = 64.4\ RMS + 3.9$ $r^2 = .45$

Beaded 26 applications $\overline{SN}_{64} = 24.7$ (s = 7.5)

Hot Extruded (16 applications)

$SN_{64} = .68\ BPN - 15.4$ $r^2 = .50$

$SN_{64} = .623\ BPN + 36.4\ RMS - 18.7$ $r^2 = .66$

Hot Spray (10 applications)

No acceptable correlation found

SN_{64} Hot Spray > SN_{64} Hot Extruded

c. Preformed Plastics 11 applications $\overline{SN}_{64} = 25.2$ (s = 8.7)

$SN_{64} = .158\ BPN + 58.4\ RMS + 5.95$ $r^2 = .76$

Note: The macrotexture profile root mean square (RMS) is expressed in mm in all the above expressions.

which indicates a lesser durability of the white paint when subjected to exposure, even in the absence of traffic.

As in the case of pavements, marking materials exhibit seasonal and short-term variations in skid resistance. These variations are shown in Figure 1. The average values of skid resistance (SN_{64}) are plotted for each formulation type on all days when measurements were made. Also evident in Figure 1 is that the chlorinated rubber base paints and the hot extruded thermoplastics have skid resistances about 10 units less than the other materials tested on this site. The relatively low skid resistance of the chlorinated paints persisted even after the coarse aggregate surface had worn through the paint.

Prediction of Skid Resistance from Texture Measurements

It was originally hypothesized that skid resistance of all types of marking materials could be predicted from texture measurements alone by using one set of prediction equations for all materials, including paints, thermoplastics, temporary tape, or preformed cold-applied plastics. However, a preliminary analysis showed that marking materials do not exhibit skid resistance behavior that is predictable solely from microtexture and macrotexture data. Apparently surface chemistry differences, which depend on formulation, play a significant role in skid resistance and therefore each type of material must be dealt with separately by using a prediction equation specific to that type or class of material.

Although a vast amount of data was available as a result of this study, in some cases, not enough data were available to develop meaningful prediction in the cases of the temporary tapes and the two component materials. Significant prediction equations that relate BPN or RMS (macrotexture) to SN_{64} were obtained for the various types of traffic paints, thermoplastics, and preformed plastics. The results are summarized in Figure 2. In some cases, BPN is sufficient to predict skid resistance for a given type of material, although in many cases the confidence of prediction can be improved by introducing a measure of macrotexture, such as RMS of macrotexture profiles. Since the latter may be difficult to obtain for some potential users, the poorer correlations that involve only BPN are included. In some cases little improvement was noted by including RMS and only the predictions by using BPN are listed.

Minimum Skid Resistance Levels

As shown above, pavement marking materials provide less skid resistance than the substrate on which they are deposited. This creates areas of differential friction across the surface of a pavement, which leads to potential hazards in vehicle operation. The degree of hazard present depends on the skid resistance of the substrate, the skid resistance of the marking material (relative to that of the substrate), and the area and geometry of the marking. The design of a roadway delineation scheme therefore requires recommendations, or guidelines, for setting minimum allowable skid resistance levels so that an appropriate marking material can be chosen.

Ideally, the recommendations would be expressed directly in terms of measurements obtained by using the test procedures described in previous sections. However, the performance of highway tires varies widely across the vehicle population, and the absolute value of measurements made from standard test procedures may not reflect the design requirements at a given site. In the subsequent discussion, the term coefficient of friction will be used to describe the frictional characteristics of the surface, instead of skid resistance, to emphasize that the highway design engineer may wish to provide his or her own interpretation and transformation of the standard test measurements.

The effect of differential pavement friction on the response of four-wheeled and two-wheeled vehicles was studied by means of a simulation analysis. The analysis of four-wheeled vehicle behavior is discussed in a paper by Hayhoe and Henry (4) and only the major results will be repeated here. Details of the simulation models and vehicle parameters may be found in the report by Henry and others (3).

Cars in Skidding Maneuvers

Locked wheel skidding maneuvers, in which the brakes of the vehicle are released at some point during the skid, were considered to be the maneuvers most likely to lead to a serious hazard in car operation on differential friction surfaces. Two different maneuvers were chosen as typical of vehicle trajectories and roadway delineation met with in practice.

In the first maneuver the vehicle slides obliquely across a stripe of marking material 150 mm in width. Simulation results showed that, for all combinations of pavement and marking material friction, this configuration does not provide a significant hazard.

Figure 3. Recommended maximum lengths of pavement marking for safe operation of cars in skidding maneuvers, vehicle speed at inception of the skid = 88 km/h.

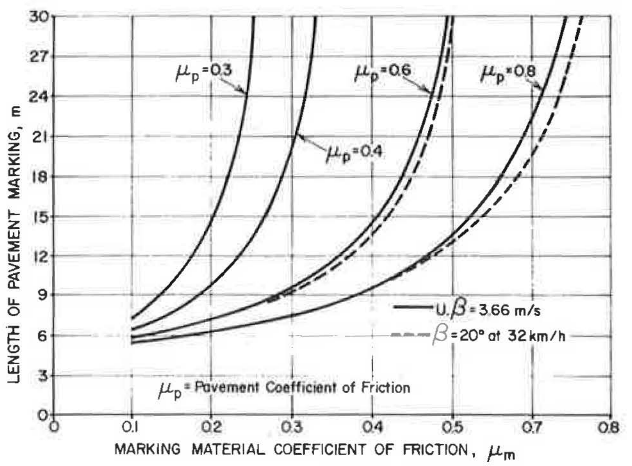

In the second maneuver the vehicle initially slides on bare pavement. The wheels on one side of the vehicle then slide onto a solid block of marking material while the wheels on the other side remain on the bare pavement. In this case, certain combinations of length of marked area, pavement friction, and marking material friction were found to create a definite hazard. Boundaries of safe operation are given in the design chart (Figure 3). Safe operation is indicated if a given combination of the two coefficients of friction and the length of differential friction surface falls to the right of the appropriate curve. Otherwise, unsafe operation is indicated.

The Figure 3 chart was constructed from the simulation results and illustrates the boundaries of safe operation for a specified set of operating conditions. A number of the assumptions made in constructing the simulation model and interpreting the results require validation. The chart should, therefore, be considered as giving a first approximation to the boundaries of safe operation.

Motorcycle Loss of Control on a Marking Stripe

An analysis of the motion of a motorcycle as it passes over an area of marking material is more difficult than an analysis for a car, because single-track vehicles are fundamentally unstable in roll. Without active control by the rider, the vehicle will simply fall over. Also, the locking of one or both of the wheels leads to rapid roll instability that cannot be corrected by the rider. Locked-wheel skidding maneuvers similar to those used in the four-wheel vehicle study were therefore not applicable. Rather, a maneuver in which the marking material caused a disturbance in the trajectory of the vehicle was required. An active steering controller, modeled in the simulation to stabilize the vehicle in roll, was a further departure from the methodology used in the four-wheeled vehicle study.

The maneuver chosen was as follows: set the vehicle in a steady state turn and then allow it to pass over a 150-mm-wide stripe of marking material at a given angle of attack. If the disturbance caused by the marking stripe was corrected by the steering controller, and the vehicle subsequently returned to the original steady state roll angle, the pavement-marking material configuration was acceptable. Otherwise, the configuration was not acceptable. The steady state roll angle in all simulation runs was set at 18.5°, which corresponded to a lateral acceleration of 0.3 g.

We concluded from the results of the simulation study that the risk of loss of control of a single-track vehicle as it passes over a pavement-marking stripe is increased by the following factors:

1. Decrease in the angle of attack,
2. Decrease in the marking material coefficient of friction,
3. Decrease in the pavement coefficient of friction,
4. Allowing of the vehicle to pass over the stripe more than once or to run over a number of stripes in succession, and
5. Decrease in forward speed.

Acceptance of these results depends on the confidence that can be placed in the procedure adopted for determining loss of control (i.e., whether or not the simulation steering controller was capable of generating a stable motion). Vehicle motion on a more extensive area of marking material than a single stripe was not investigated, but it seems reasonable to infer that a higher level of risk will prevail. Rider skill and experience clearly play a considerable role in the probability of an accident occurring on a given section of roadway, both as regards the rider's ability to anticipate road conditions and his or her ability to retain control once an emergency maneuver has been initiated. These considerations make it extremely difficult to formulate even the beginning of a general procedure for specifying acceptable levels of pavement marking material skid resistance for safe motorcycle operation.

However, it can be stated with a fair degree of certainty that a single-track vehicle operating on a pavement at a given level of acceleration (whether due to driving traction, braking, cornering, or any appropriate combination) is likely to become completely unstable if it passes across a marking material surface that has a coefficient of friction equal to or less than the vehicle acceleration measured in gravity units. There are two problems in trying to apply this statement: (a) How should the coefficient of friction of a typical motorcycle be defined and measured? and (b) Is a significant amount of differential friction allowable and, if so, how can safe levels be determined?

The first problem is a common one with four-wheeled vehicle operation, and a procedure developed for car tires would probably be equally applicable to motorcycle tires. The second problem is essentially concerned with human behavior relatively independently of vehicle behavior or vehicle-rider interaction. It depends mainly on whether a driver allows a consistent margin of safety against sliding when operating on various pavement surfaces. For example, when operating on a surface that has a coefficient of friction of 0.8, the driver might restrict vehicle accelerations to 0.6 g; on a surface that has a coefficient of friction of 0.6 he or she might restrict vehicle accelerations to 0.4 g. Other relations, such as the variation of safety margin with pavement friction, can also be postulated.

If such a relation could be established, the minimum allowable marking material coefficient of friction for safe motorcycle operation would be given by a function of pavement coefficient of friction (and, probably, by other highway design factors such as geometry), so that the vehicle would never operate on a surface whose coefficient of friction is lower than the maximum vehicle acceleration likely to be attained. On the other hand, if a consistent relation is found not to exist, or cannot be established, the minimum allowable marking material coefficient of friction could be given as the minimum allowable pavement friction for the sections of highway under consideration, irrespective of the existing or design pavement surface friction.

CONCLUSIONS

A data base for a large variety of pavement marking materials was established. A wide range of skid resistance levels was found, the lowest levels were for the hot extruded thermoplastic and the chlorinated rubber base paints that were used in the study. Glass beads and premixed beads and sand increased the skid resistance of the marking materials significantly. Spray thermoplastics provided higher skid resistance levels than hot extruded thermoplastics, due in part to the coarser texture produced by the spraying application. In the field both daily and seasonal variations in skid resistance were observed, and these variations should be accounted for in any field evaluation of marking materials.

The effect of accelerated laboratory polishing on marking material surfaces is much different from that on aggregate or unmarked pavement samples. Polishing tends to decrease the frictional resistance of beaded surfaces but tends to increase the frictional resistance of some unbeaded surfaces. Any laboratory evaluation of marking materials should include a light polishing to condition the samples. Accelerated weathering is not necessary as a conditioning step in a laboratory evaluation. Sample preparation is extremely important and should duplicate field application procedures as closely as possible. Preparation techniques can have a greater effect on BPN values than will differences in materials.

The marking materials studied in this project were grouped into six types: traffic paints, hot spray thermoplastics, hot extruded thermoplastics, preformed plastic, temporary tapes, and two-part systems. In analyzing the data and developing the predictor equations for skid resistance in terms of texture and BPN data it was necessary to treat each type separately. This resulted in six data sets, some of which were too small to provide significant correlations.

Predictor equations were developed by using linear regression techniques to predict SN_{64} from BPN values. Correlation coefficients for the more successful of these equations ranged up to 92. In some instances the prediction was improved by the inclusion of the macrotexture profile RMS.

When applied to pavements, marking materials cause a local reduction in skid resistance. The resulting differential frictions can create a hazard for drivers of automobiles and other four-wheel vehicles if the materials are applied to large areas such as gores, legends, and stop bars. Such applications should be avoided when possible, although a tentative design procedure has been developed for selection of materials that give safe levels of skid resistance. Current standards for such configurations should be reviewed in light of this finding. Lane delineation lines do not present a hazard for drivers of four-wheeled vehicles, even when the marking material skid resistance is extremely low. Almost any application of pavement marking materials will create a potential hazard for riders of single-track vehicles. Recommendations for minimum allowable levels of marking material skid resistance for safe operation of single-track vehicles could not be established. However, the skidding hazard presented by pavement markings to riders of single-track vehicles should be weighed against the safety benefit provided by the marking in the form of roadway delineation and warnings of safety hazards.

ACKNOWLEDGMENT

The research described in this paper was conducted as part of the Federal Highway Administration research project, Wet Friction of Pavement Marking Materials. Edward Harrigan served as technical monitor of this project and his assistance is greatly appreciated. We also express our appreciation to Prismo Universal Corporation for their assistance in applying the test materials.

REFERENCES

1. C.L. Richard. Skid Testing of Pavement Marking Materials. Michigan Department of State Highways and Transportation, Lansing, Final Rept., Project TSD-284-76, April 1976, 9 pp.
2. R.L. Rizenbergs and others. Accidents on Rural Interstate and Parkway Roads and Their Relation to Pavement Friction. TRB, Transportation Research Record 584, 1976, pp. 22-36.
3. J.J. Henry, D.A. Anderson, and G.F. Hayhoe. Skid Resistance of Pavement Marking Materials. Pennsylvania Transportation Institute, Pennsylvania State Univ., University Park, Final Rept. PTI 8005, July 1980.
4. G.F. Hayhoe and J.J. Henry. Effects of Differential Pavement Friction on the Response of Cars in Skidding Maneuvers. TRB, Transportation Research Record 836, 1981, pp. 61-67.

Publication of this paper sponsored by Committee on Surface Properties-Vehicle Interaction.

Tire Testing at Low Speed on an Ice Rink

GORDON F. HAYHOE AND JOHN J. HENRY

Procedures are described for measuring the performance of tire traction on an ice rink. Results are given from driving traction and locked wheel braking tests conducted at various speeds by using a modified road friction tester. Maximum test speed was restricted to 12 mph (19 km/h) by the small surface area of the ice rink, but the locked wheel braking results obtained are shown to be representative of higher speed tests if the test speed used is high enough that the tire force approaches its limiting (minimum) value. To enhance test repeatability, the sensing element of the transducer used to measure surface temperature should be completely frozen into the ice just below the surface. The ice surface should also be conditioned by running preliminary tests until the tire force measurements have reached a stable value. Contamination and damage to the ice surface from studded tire tests are described, and their effects on tire force generation and test repeatability are discussed.

Figure 1. Temperature response of ice surface with refrigeration equipment turned off.

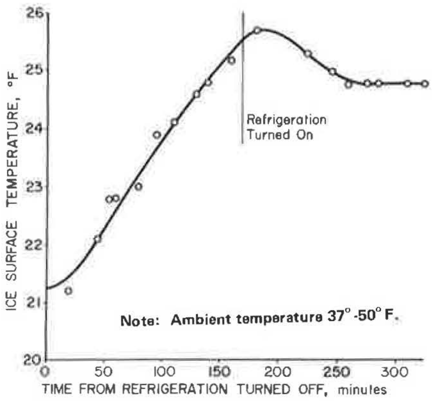

When measuring the performance of tires on an ice course constructed out-of-doors, problems of obtaining repeatable results often are encountered because of variable weather conditions. In addition, such test courses are difficult to construct and maintain in good condition, and, to a large extent, the prevailing weather conditions determine the scope and planning of the test program. The use of an enclosed ice rink largely overcomes these problems and provides a convenient means of measuring tire performance on ice. But, the use of an enclosed area and the testing on an artifically maintained surface introduced new problems, and old ones were made more acute. This paper discusses some of the problems encountered while conducting a test program in an ice rink as part of evaluation of winter driving traction aids for the National Cooperative Highway Research Program (NCHRP). The main problems that arose were in accurately measuring ice surface temperature, in ensuring that speed effects did not introduce bias into the results, and in dealing with contamination of the ice surface.

A major objective of the project was to specify and, if necessary, develop a set of test procedures for measuring the performance of highway vehicles under adverse winter conditions. Procedures for measuring tire performance on ice have been in use for many years [see, for example the National Safety Council and Sapp (1,2)], and most of the tests conducted during the NCHRP project were run according to established practice. The majority of the published results, however, deal with tests conducted on ice courses constructed out-of-doors, and the test results presented in this paper were selected from the final NCHRP report (4) to emphasize the problems that may be encountered when a test program is relocated to an indoor ice rink.

GENERAL TEST CONDITIONS

Testing was conducted in the Pennsylvania State University Ice Pavilion, which comprises an ice rink completely enclosed by a metal structure. Except that ambient temperature determines, to some extent, the surface temperature of the ice, environmental conditions had little effect on the characteristics of the ice surface. The ice area, which measured 200x100 ft (61x30.5 m), is surrounded by a guard fence, and a free run-on to the ice was not possible. All maneuvering, therefore, had to be done on the ice, which restricted speeds to an absolute maximum of 15 mph (24 km/h) and for normal testing to no more than 12 mph (19 km/h). Suitable entry and exit lanes would increase possible test speeds considerably.

The ice surface was prepared by using a Zamboni ice conditioning machine. This vehicle is designed to cut back and remove the top layer of the ice surface and then lay down a thin film of hot water. After the water has frozen, the resulting surface is smooth. About an hour is required for surface temperature to stabilize, and conditioning of the complete area requires about 20 min.

With the refrigeration equipment set to run normally, ice temperature varied between 21° and 16°F (-6° and -9°C), depending on the ambient temperature. If ambient temperature is sufficiently high, ice temperature can be varied by turning the refrigeration equipment on and off. Response time is long enough for tests to be carried out at essentially constant temperature while the temperature is changing. Figure 1 shows the results from an experiment where the refrigeration equipment was turned off for 3 h and then turned on at half power. The maximum rate of temperature change was approximately 1.7°F (1°C)/h.

ICE TEMPERATURE MEASUREMENT

Although an ice rink is generally more convenient to use than an ice course constructed out-of-doors, the measurement of ice temperature was found to be a critical factor in obtaining satisfactory test results. The first consideration is that minimum temperatures in a rink will not be as low as those attainable with an outdoor facility under similar climatic conditions. For example, the lowest ice temperature measured in the rink was 16°F (-9°C), which occurred when the ambient temperature in the rink was 10°F (-12°C) and the outside temperature was 0°F (-18°C). Test results cannot, therefore, be obtained at very low temperatures and, in order to determine the relation between tire performance and ice temperature with an accuracy equivalent to that obtainable in outdoor testing, either ice temperature must be measured more accurately or more tests must be run. Temperature can vary across the ice surface by as much as 4°F (2°C), which means that it is important to measure ice temperature as closely as possible to the area of ice used for testing, and preferably to make simultaneous measurements at points distributed over the test area.

During preliminary tests ice temperature was measured by pressing a thermistor probe against the ice. It became apparent, however, that the measurements were not consistent, even when standardized procedures were carefully followed. Various methods of holding the probe on the surface were also tried, including freezing the probe onto the ice, but to no satisfactory effect.

In an effort to determine the causes of the inconsistent measurements, the temperature gradient in the ice and in the air adjacent to the surface were measured by using seven thermocouple junctions fixed to a short length of circuit board. The assembly was frozen into the ice with the first junction 1/8 in (0.3 cm) above the concrete base of the ice rink. Figure 2 shows junction temperatures measured on two occasions. The fourth junction was located very close to the ice surface, and heat transfer along the circuit board and thermocouple leads undoubtedly affected the measurement, but the first three junctions show a linear temperature gradient that may be extrapolated to give surface temperature. Although the junction temperatures show, to a large extent, the temperature gradient in the thermocouple assembly, it is evident that a steep gradient exists in the air adjacent to the ice surface. This may account for some of the inconsistency noted during early tests because the gradient will vary with ambient temperature and thus vary

Figure 2. Temperature gradients at ice surface.

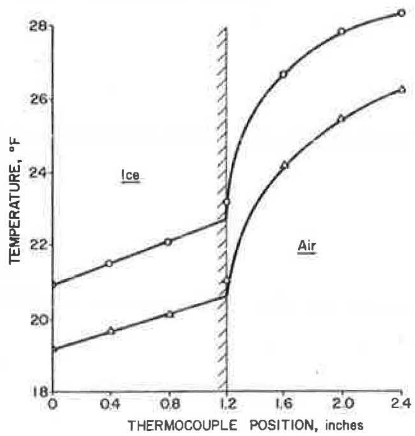

Figure 3. Oscillograph recording of increase in locked wheel friction as speed decreases.

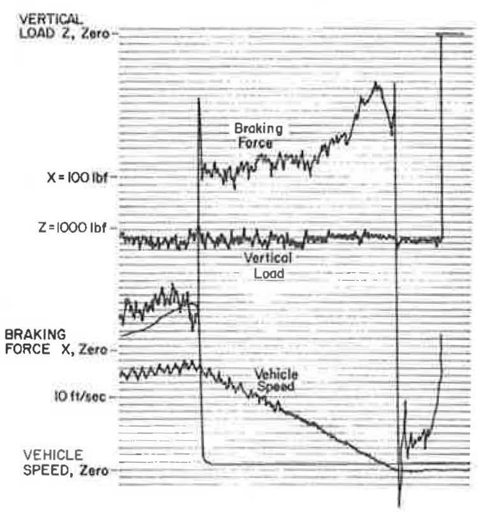

heat input to a probe pressed onto the surface. The effect will be exaggerated as the device that holds the probe onto the surface becomes longer. A further effect is that movement of a vehicle on the ice causes mixing of the air and consequent variations in probe temperature. For example, with the probe frozen onto the ice surface, an increase of 1°F (0.5°C) was induced by driving a car past the probe at a distance of 5 ft (1.5 m), although exhaust gas from the vehicle also may have influenced the rise in temperature.

Because of the shallow temperature gradient that exists in the ice, accurate and consistent results are obtained if the temperature probe is frozen into the ice just below the ice surface, and all temperatures quoted later were obtained by this method. In general, a thermistor probe with digital read-out equipment was used, but a mercury thermometer, used as a back-up, was found to be satisfactory.

LOCKED WHEEL BRAKING TESTS

The Pennsylvania State Mark III Road Friction Tester was used to measure locked wheel braking forces. This tester is of the single-wheel trailer type (3), with the test wheel mounted on a six-component strain-gauged hub. A test typically consisted of 10 skids repeated over a given section of ice, during

Figure 4. Braking performance of locked wheel against ice surface temperature.

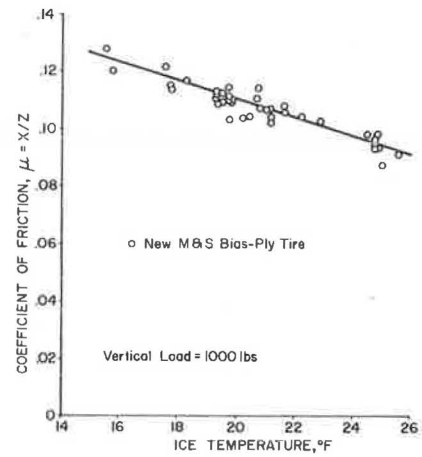

which braking and vertical forces were monitored. The forces were then measured and averaged and the coefficient of sliding friction was calculated. The standard deviation of braking-force measurements during a test was typically 2.5 lb (11 N) for unstudded tires. Vertical load was nominally 1000 lb (4.45 kN).

Succeeding tests were run over the same section of ice and, although a test session was always started on a smooth, newly conditioned surface, two or three tests were generally required to stabilize tire force at a reasonably constant value. The effect, however, was variable--on some occasions, the results of the second test of 10 skids were as much as 7 percent lower than the results of the first. On other occasions, both the first and second tests gave the same result.

While obtaining a satisfactory ice condition, the minimum speed for conducting a test was also determined. This was done by driving the tester over the ice as in a normal test, locking the test wheel, and then shifting into neutral. A typical output as the tester decelerated to zero is shown in Figure 3, where the characteristic increase in friction as speed decreases can be seen. Subsequent tests were run in excess of the speed at which the trace leveled out.

Test variability is an important consideration, and consequently a series of tests were run with a new mud and snow (M&S) bias-ply tire, broken in for 200 miles, to determine the precision that can be expected from ice rink tests. Two tests generally were run during a single session and results were obtained for ice temperatures in the range of 25° to 16°F (-4° to -9°C) and over a wide range of ambient temperature and relative humidity. The results, plotted against ice temperature, are shown in Figure 4, where it can be seen that dispersion of the data about a mean squared straight line is quite small, with 95 percent confidence intervals of the order of 5 percent. A systematic variation due to ambient temperature or relative humidity could not be found in the data and it was felt that the dominant causes of variation were day-to-day changes in the tester characteristics and inaccuracies in ice temperature measurement. [For a discussion of possible sources of data variation, see the final NCHRP report (4).]

Despite the day-to-day variation in test results, the braking test procedure itself was extemely sensitive, as is shown in Figure 5, which gives results from tests run with a M&S bias-ply tire and a M&S radial-ply tire, both of which have the same tread pattern. During the tests with each tire,

Figure 5. Variation of locked wheel braking performance with inflation pressure.

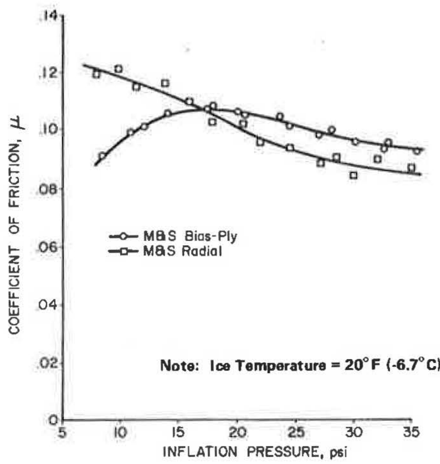

inflation pressure was varied from 8 to 35 psi (55 to 240 kPa). The two tires show similar behavior in the range of 18-35 psi (123-240 kPa), but below 18 psi (123 kPa) their behavior is markedly different. The figure illustrates how variations in tire pressure about a nominal test point can affect test results.

STUDDED TIRE TESTS AND ICE CONTAMINATION

Locked wheel braking tests were run with a tire nominally identical to the bias-ply tire used to obtain the results given in Figure 4, except that the tire was fitted with 96 controlled protrusion tungsten carbide studs. Test results from this tire showed wide variation compared with the results from the unstudded tire. From oscillograph traces of individual skid tests it was apparent that studded tire performance can vary by large amounts from skid to skid and during the same skid. There are at least two causes of this behavior: (a) the studs cut grooves in the ice (5), which can decrease performance in subsequent skids over the same section of ice by reducing stud cutting forces and reducing tire frictional forces; or (b) ice chips formed during a skid also can reduce tire frictional forces during subsequent skids.

The first effect was investigated by running a series of studded and unstudded tire tests in sequence. The unstudded tire was run first, followed by the studded tire. The ice was then swept clean of all ice chips and the unstudded tire rerun. The unstudded tire, in passing over a clean but stud-damaged section of ice, produced 12 percent less force than the same tire did in passing over a clean undamaged section of ice.

To investigate the second effect, a test was first run on clean ice with the unstudded tire, and then ice chips from the side of the rink were packed into the tire tread and a further test was run. This produced contamination of the ice surface when the ice chips were released from the tire tread during the initial skids. This contamination was similar to that produced by studded tire tests. Figure 6a shows an oscillograph trace from the first test where peaking of the brake force is apparent when the wheel locks or spins down. In contrast, a trace from the second test on contaminated ice (Figure 6c gives no indication of peaking) and a loss of performance is evident during the initial stages of the skid. The extent to which contamination produced during a skid affects performance for that particular skid is unclear, but the ice rink results show that subsequent skids can be seriously affected--and the results also explain the general absence of large peak forces in studded tire tests.

Figure 6. Oscillograph traces of locked wheel braking tests: (a) M&S tire, clean ice; (b) M&S studded tire, clean ice; and (c) M&S tire, contaminated ice.

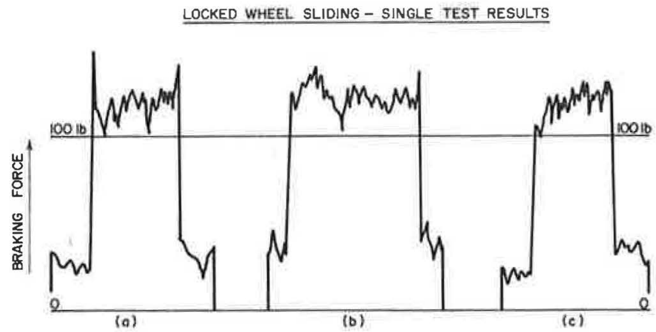

Table 1. Comparison between locked wheel braking tests conducted at Stevens Point and at ice rink.

Tires on Rear Wheels	Ice Temperature (°F)	Coefficient of Friction: Stevens Point	Ice Rink	Difference (%)
M&S	25	0.0789	0.0795	2.0
	26	0.0761	0.0764	0.4
Studded M&S	25	0.1159	0.0987	16
	26	0.1144	0.1317	14
M&S on road friction tester	20.4	0.0877	0.0843	3.4

The preceding discussion is based on contamination from studded tire tests, but exactly the same problems arise if the contamination is brought in from outside. For example, if the test vehicle is driven to the rink over snowy roads, it is almost impossible to clean the tires and the underneath of the vehicle sufficiently well to stop the problem from occurring.

STOPPING DISTANCE TESTS

The Winter Driving Hazards Program (WDHP) conducted by the National Safety Council (NSC) at Stevens Point in 1976 included a series of locked wheel stopping distance tests with studded and unstudded M&S tires. In cooperation with NSC and Kennametal Corporation, the same tires were later loaned to the NCHRP project. The tires were fitted to a car of the same model as used at Stevens Point, and locked wheel stopping distance tests were conducted on the ice rink. Initial speed for the WDHP tests was 20 mph (32.2 km/h), but 10 mph (16.1 km/h) was the highest safe speed that could be attained on the ice rink. The Stevens Point data were plotted as stopping distance against temperature, and a mean square straight line equation was computed. Stopping distance at the appropriate temperature was then calculated from the straight line equation. In the ice rink test series, one test consisted of 10 stops from a speed of 10 mph (16.1 km/h), all run over the same section of ice. To compare the two sets of results, stopping distances were converted to mean deceleration and are listed in Table 1.

Considering the small number of data points taken in the ice rink tests, the agreement with NSC data is remarkably good for the unstudded tires and is well within the scatter of the NSC results. A later

Figure 7. Traction drive assembly showing motor drive detail.

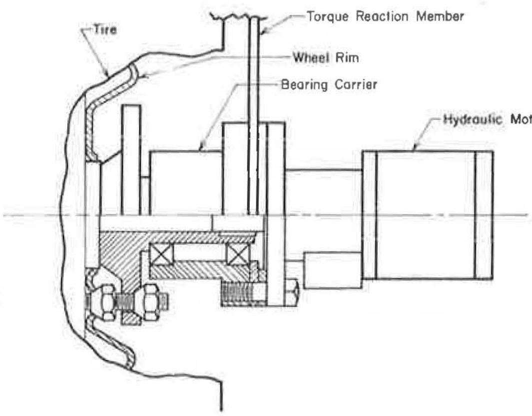

Figure 8. Traction drive showing torque reaction assembly.

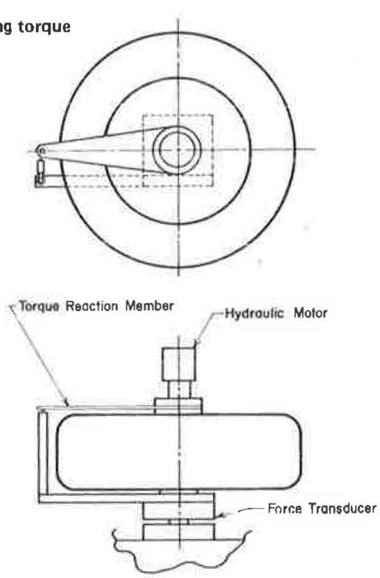

test in the ice rink that used a road friction tester did not give such good correlation (see Table 1), but the agreement is still close enough to indicate that tests at slow speeds on an ice rink do not introduce serious errors into the measurement of tire performance, at least for ice temperatures of 20°F (-6.7°C) and above.

On the other hand, the test results with studded tires show relatively poor agreement, but the difference is of the same order as the scatter in the Stevens Point data. There was no apparent difference between the test conditions in the two studded tire tests in the ice rink. The major part of the difference in measured performance was tentatively attributed to the effects of contamination of the ice surface.

DRIVING TRACTION TESTS

Driving traction tire forces were also measured by using the road friction tester. In order to do this, a torque drive was designed, built, and fitted to the test trailer. The drive consists of a high torque, low speed hydraulic motor driven by a variable speed hydraulic pump, with motive power supplied by a 5-hp (3.7-kW) gasoline engine. The hydraulic motor is mounted on extended wheel studs, as shown in Figure 7, and reaction torque is passed around the tire to the wheel hub side of the force transducer, as shown in Figure 8. By constructing the device in this way, it was not necessary to isolate the motor from the wheel in the longitudinal direction as normally is done with driven wheel transducer assemblies. When braking tests are carried out, the motor shaft is withdrawn from the intermediate drive shaft and a spacer placed between the motor and the bearing carrier.

The test procedure adopted to measure traction force was to drive the test wheel at a constant speed and vary vehicle speed in order to vary wheel slip ratio. Both traction and locked wheel braking tests were run over the same section of ice so that the two modes of operation could be compared. Vehicle speed was varied between tests but was held constant during each pass over the ice. The average coefficient of friction for each pass was measured and plotted against wheel slip speed (where slip speed is the speed at which the tire contact patch slides over the ice). Traction results were also plotted against wheel slip ratio.

Figure 9 gives results obtained with the M&S bias-ply tire and, in common with other published data, shows reduced performance in traction compared with braking. As the force of locked wheel braking is a function of slip speed, and reduces to a constant value with increased speed, it might seem reasonable that the same functional relation applies to traction. This, however, is clearly not the case, and a different functional relation is required to account for the difference between braking and traction. Rolling resistance losses and pressure distribution in the contact patch are both factors that can conceivably modify traction forces, and most likely do have an effect, but a more plausible explanation of the gross behavior shown in Figure 9 is provided if tire friction on ice is considered to be predominantly dependent on the thermodynamic processes that control the generation of a water film in the tire-ice interface. Bowden and Tabor (6) give experimental evidence that water formation is a factor in sliding friction on ice, and the NCHRP final report (4) discusses the possible mechanisms of tire force generation on ice. Further work has shown that a stable water film can be formed and maintained under a sliding tire by the energy generated in viscous shearing of the fluid film, and that the forces that arise from fluid shear stresses match experimental results over certain ranges of tire operating conditions.

For comparison with the bare M&S tire, a number of tests were run with the studded M&S tire. In this test series, the traction and braking tests were run over a fairly small area of ice in four alternating sets so that the results would not be unduly biased by surface contamination and stud damage. No attempt was made to clean the ice surface between tests, although care was taken not to pass over exactly the same track too many times. Comparison of Figures 9 and 10 for locked wheel braking at high speed shows a modest improvement in performance for the studded tire over the bare tire, but performance at low speed was reduced. In traction, the studded tire did not seem to be affected by surface contamination to the same extent as in braking, and a substantial improvement in performance is shown (Figure 11) over almost the whole slip range. At slip ratios of less than 0.5, average studded tire performance was slightly less than that of the bare tire, but as slip ratio increased, traction force decreased less abruptly than with the bare tire. The two tires showed approximately the same performance at a slip ratio of 9, with the studded tire then becoming less effective at zero vehicle speed.

Figure 9. Traction and locked wheel braking results, M&S bias-ply tire.

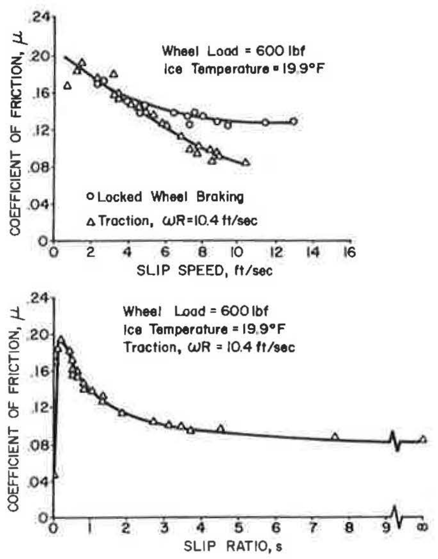

Figure 10. Traction and locked wheel braking results, M&S bias-ply studded tire.

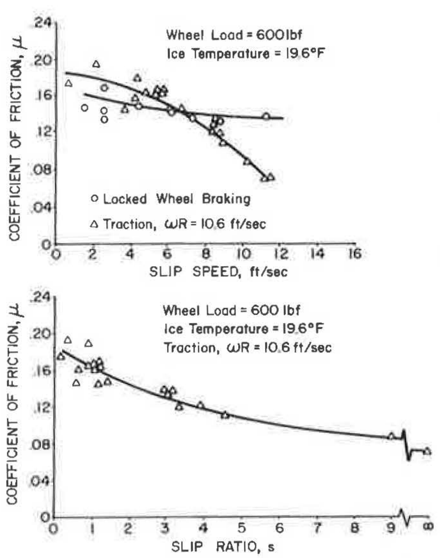

Immediately following the studded tire tests, a number of tests were run with the bare M&S tire over the contaminated section of ice. The results are given in Figure 12, which shows that performance was reduced compared with the tests on clean ice, particularly for traction at low slip ratios.

CONCLUSION--IMPLICATIONS OF THE TEST RESULTS

The results presented show that accurate and repeatable results can be obtained from tire tests conducted in an ice rink, providing a set procedure is followed carefully. Of primary importance is the accurate measurement of the temperature of the ice surface and the preliminary working of the ice surface to obtain limiting performance values.

The restrictions in speed imposed by testing in an ice rink are not particularly serious if they are recognized and accounted for in the test procedures. This can take the form of either running tests over a range of speeds to establish the speed relation or, in the case of locked wheel braking, ensuring

Figure 11. Relative driving traction performance of studded and nonstudded tires.

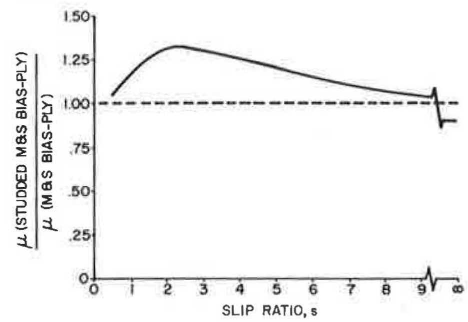

Figure 12. Traction and locked wheel braking results, M&S bias-ply tire, run after studded tire tests.

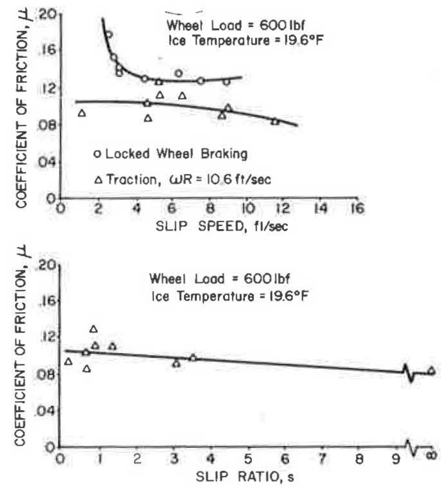

that the test speed is sufficiently high to give limiting tire performance. When conducting comparative tests, it is particularly important to establish the tire performance-velocity relation because wide variations of this characteristic can exist between different tires.

Contamination of the ice surface by either snow or ice chips significantly affects the peak traction attainable from a tire and can reduce limiting force values if present in sufficient quantities. Also associated with contamination of ice surfaces is the question of how the performance of studded tires should be measured. We found that the repeating of locked wheel braking tests with a studded tire over the same section of ice reduces tire performance. If studded tire use on the highway produces significant contamination, then not only will the performance of the studded tires be reduced, but the performance of bare tires also in use will be reduced. On the other hand, if locked wheel stops and rapidly spinning wheels occur only rarely, the performance measured in standard tests will probably underestimate the true effectiveness of studded tires.

From these considerations three test methods for measuring studded tire performance can be proposed:

1. Run two or three tests to damage and contaminate the ice surface and then run a number of tests from which the average performance will be calculated;
2. Run a number of tests, from which the average performance will be calculated, with each test run on a clean, undamaged section of ice; and
3. Run a number of tests over the same section of ice and average the results from all the tests.

The last procedure is the one usually adopted and it tends to produce variable results. The other two procedures will give significantly different results in locked wheel braking tests, although the results from traction tests should correspond fairly closely. Without knowing the highway conditions over which the studded tires will be used, it is not possible to state which of the three procedures will give the most representative result.

ACKNOWLEDGMENT

This study was conducted under National Cooperative Highway Research Program Project 1-16. The opinions and findings expressed or implied in this paper are ours. They are not necessarily those of the Transportation Research Board, the National Academy of Sciences, the Federal Highway Administration, the American Association of State Highway and Transportation Officials, or of the individual states who participate in the National Cooperative Highway Research Program. The cooperation and assistance of the National Safety Council are also gratefully acknowledged.

REFERENCES

1. Annual Winter Reports. Committee on Winter Driving Hazards, National Safety Council, Chicago, IL, 1939-1981.
2. T. Sapp. Ice and Snow Tire Traction. Automotive Engineering Congress, SAE, Paper 680139, Jan. 1968, 6 pp.
3. J.D. Decker. The Improved Penn State Road Friction Tester. Pennsylvania Transportation Institute, Pennsylvania State Univ., University Park, Automotive Res. Program Rept. S58, Dec. 1973, 24 pp.
4. G.F. Hayhoe and P.A. Kopac. Evaluation of Winter-Driving Traction Aids. NCHRP, Research Results Digest 133, June 1982, 6 pp.
5. P. Rosenthal and others. Evaluation of Studded Tires--Performance Data and Pavement Wear Measurement. NCHRP, Rept. 61, 1969, 66 pp.
6. F.P. Bowden and D. Tabor. The Friction and Lubrication of Solids. Oxford Univ. Press, New York, Vol. 2, Chapter 9, 1964.

Publication of this paper sponsored by Committee on Surface Properties-Vehicle Interaction.

Determination of Precrash Parameters from Skid Mark Analysis

W. RILEY GARROTT AND DENNIS A. GUENTHER

This paper presents the results of an experimental study to validate and improve the methods currently used in the reconstruction of accidents to determine precrash parameters from skid marks. This was accomplished by testing six vehicles, three cars and three trucks, that had a variety of tires and loadings on three differing types of pavements. Both severe (wheels locked) and moderate (no wheels locked) stops were made. Prebraking speed, the length of the skid marks produced, stopping distance, and a number of other variables of interest were measured for each stop. Analysis of the experimental data focused on repeatability of skid mark data, validity of the currently used skid mark length versus prebraking speed formula, accuracy of the various methods for measuring tire friction, and tire marks left by nonlocked wheels. The currently used skid mark length versus prebraking speed formula was found to be better for accident reconstruction when using test data from locked wheel stops than were either of two other formulas that were tried. Four methods for measuring tire friction were evaluated. Two of these methods, the American Society for Testing and Materials skid number and an estimate based on a standard table found in the literature, were shown to give incorrect results when used for heavy, air-braked trucks. For some conditions, stops for which none of the vehicle's wheels locked were found to produce tire marks that were longer than those produced during a locked wheel stop. The tire marks generated during non-locked wheel stops look like light shadowy (visible when viewed along their length but not from directly above) skid marks. Accident investigators must be careful when using light skid marks in the formulas to determine prebraking speed from skid mark length to ensure that the skid marks were made by locked wheels. Otherwise, too high an estimate of the vehicle's prebraking speed may be obtained.

Skid marks have an important role in the National Highway Traffic Safety Administration's (NHTSA) effort to increase vehicular safety on our nation's roads. The study of skid marks left on pavement after an accident has occurred helps experts in accident reconstruction determine the course of events that led to the accident and the precrash parameters of the vehicles involved. These, in turn, help NHTSA develop countermeasures to prevent accidents from occurring and to protect the occupants of vehicles involved in collisions.

Reconstructionists use the analysis of skid marks to help identify impact locations, vehicle trajectories, wheel lockup patterns, deceleration, and prebraking speed. The last three of these important quantities are calculated by means of relatively simple formulas based on a field investigator's report of the number and length of skid marks observed and the type and condition of the pavement on which the accident occurred.

The formulas used by accident reconstructionists are theoretical formulas and in their derivation a number of assumptions are made. If any of these assumptions are invalid, it could lead to errors between what actually occurred and the results of the accident reconstruction. Also, accident investigators frequently use standard tables (1,2) to estimate the coefficient of friction that was acting between a vehicle's tires and the road. These tables need to be checked for possible errors due to differing vehicle types, loading, tire types, and pavement composition.

The overall goal of this study was to increase knowledge of skid marks and to improve the accuracy of formulas and tables that involve them that are used in accident reconstruction. This was done by studying a large number of skid marks produced under controlled experimental conditions. Specifically, this study concentrated on (a) the repeatability of stops that produce skid marks, (b) the validity of the formulas and tables used to relate skid mark length to prebraking speed, (c) the best method of determining the coefficient of friction between the tire and the road for use in skid mark analysis, and

Table 1. Types of vehicles tested.

Vehicle	Class	Tires	Lightly Loaded Weight	Gross Vehicle Weight Rating
1980 Chevette	Subcompact car	P155/80R13 Armstrong radials	2 520	2 850
1980 Chevette	Subcompact car	A78/13 Armstrong bias ply	2 520	2 850
1980 Malibu station wagon	Intermediate car	P195/75R14 Uniroyal radials	3 910	
1976 Ford LTD	Full-sized car	P230/R15 Michelin radials	5 000	6 430
1976 Ford LTD	Full-sized car	H78/15 Cooper bias ply	5 000	6 430
1977 Ford F-250	Pickup truck	7.50-16 Remington bias ply	4 920	6 900
1977 Ford F-7000	Straight truck	Front, 10.0-20F Goodyear Super Hi Milers bias ply; Rear, 10.00-20F Goodyear Custom Cross Rib Hi Milers bias ply	9 430	27 500
1973 IH Transtar-Fontaine	Tractor-semitrailer	Front and trailer, 10.00-20F Goodyear Super Hi Milers bias ply; Rear, 10.00-20F Goodyear Custom Cross Rib Hi Milers bias ply	30 050	80 500

Table 2. Severe braking test matrix.

Vehicle Loading	Tire Type	Road Surface	1980 Chevette	1980 Malibu Station Wagon	1976 Ford LTD	1977 Ford F-250	1977 Ford F-7000	1973 IH Transtar-Fontaine
LLW, curb weight plus 300 lb	Bias ply	VDA asphalt	X		X	X	X[a]	X[a]
		Tar and gravel chip	X		X			
		Skid pad concrete	X		X			
	Radial	VDA asphalt	X	X[b]	X[b]			
		Tar and gravel chip	X		X			
		Skid pad concrete	X		X[b]			
Half-loaded	Bias ply	VDA asphalt				X		
GVW, fully loaded	Bias ply	VDA asphalt				X	X[a]	X[a]
	Radial	VDA asphalt	X		X[b]			

Note: Each test condition was run five times at 10, 20, 30, 40, and 60 mph for a total of 25 runs.
[a]All speeds were not used for safety reasons.
[b]Test condition was not run at 10 mph.

(d) the relation among the point of brake application, the onset of tire mark production, and the location of wheel lockup.

This paper summarizes the test program and procedures used. The principal results obtained from the testing are explained. The discussion of how to best measure the tire-road coefficient of friction outlined in this paper is presented in detail elsewhere (3). Details of the test program, test procedures, analytical methods used, and experimental results that were obtained are also contained elsewhere (4).

EXPERIMENTAL TESTING PROGRAM

During the summer of 1980, an experimental test program was conducted to supply the data needed to study the issues mentioned above. Three different types of tests were performed during the experimental program:

1. Severe braking tests in which the test driver applied the brakes of an instrumented test vehicle as rapidly and as hard as possible so as to cause rapid wheel lockup; this approximates panic braking such as might be done by a real driver when he or she becomes aware of an impending collision;
2. Moderate braking tests in which a servo-controlled brake actuator applied the brakes of an instrumented test vehicle at a predetermined constant level for which none of the wheels locked up to see if skid marks would be produced; and
3. Skid trailer tests, which measured peak and slide coefficients of friction for many of the tires used in this study, were performed on each of the different pavements used; the skid numbers of these pavements were also measured by using standard American Society for Testing and Materials (ASTM) test tires.

During the severe braking tests, the effect of changes in vehicle loading, tire type, and pavement type on the skid marks produced during a stop were studied for stops from five different initial speeds for each of six different types of vehicles. Table 1 gives the types of vehicles tested.

Tests were run with the vehicles (a) at lightly loaded weight (LLW), (b) fully loaded to gross vehicle weight rating (GVWR), and (c) half loaded (i.e., midway between the two other weights). Tests were conducted by using radial and bias ply tires on three test surfaces. The test surfaces used were the Transportation Research Center of Ohio (TRC) vehicle dynamics area (VDA), which is paved with asphalt, the TRC skid pad, which is paved with concrete, and a currently in-use public road, which is paved with a gravel chip and tar mixture laid over an asphalt road bed. Table 2 is a matrix of the severe braking tests.

Eight channels of data (only six for the F-7000) were strip-chart recorded for each stop. The data recorded were (a) distance traveled, (b) speed, (c) acceleration, (d) brake force or pressure applied, and (e) wheel rotational rate or lockup for each wheel. Also, the stopping distance (the distance from the beginning of the brake application until the vehicle reached a complete stop) and the prebraking speed were measured.

At the completion of each test stop, the skid marks produced during that stop were measured. This process begins by the measurer locating and marking the start and end of each skid mark. It is easy to

Table 3. Corrected stopping distances.

Vehicle	Loading	Surface	Tires	Nominal Speed (mph)	ASTM Skid No. at 40 mph	Slide Friction Coefficient at 40 mph for Nominal Load	Avg Corrected Stopping Distance (ft)	Long Corrected Stopping Distance (ft)	Short Corrected Stopping Distance (ft)	SE Corrected Stopping Distance (ft)	SE As Percentage of Avg Corrected Stopping Distance
Chevette	LLW	VDA	Bias ply	10			4.7	5.0	4.4	0.12	2.47
				20			17.4	18.1	16.7	0.27	1.54
				30			39.2	39.5	39.0	0.09	0.24
				40	81.1	0.848	69.4	70.3	68.3	0.34	0.48
				60			157.6	159.6	154.4	0.94	0.60
Chevette	LLW	Tar and gravel chip	Bias ply	10[a]			5.0	5.6	4.7	0.17	3.48
				20			20.1	22.5	17.7	0.81	4.00
				30			45.2	46.9	43.8	0.56	1.24
				40	60.8	0.714	80.2	86.6	75.2	2.12	2.64
				60			207.5	213.4	205.1	1.52	0.73
LTD	LLW	VDA	Radial	10			Not run				
				20			19.3	19.8	18.8	0.21	1.09
				30			45.6	46.9	45.0	0.36	0.78
				40	81.1	0.773	79.1	80.4	77.8	0.54	0.68
				60			167.7	170.2	165.0	0.85	0.51
Transtar-Fontaine	GVW	VDA	Bias ply	10			10.6	10.9	10.2	0.12	1.10
				20			33.0	34.2	30.4	0.69	2.08
				30			70.2	71.2	68.9	0.40	0.58
				40	81.1	0.566	119.3	121.7	116.1	0.93	0.78
				60			Not run				

Note: Five test runs were made at each nominal speed.
[a]Ten runs were made for this case.

locate the end of each skid mark because this is distinct and occurs where the test vehicle's wheels stopped. The start of the mark is harder to locate. The location of the start of the skid marks depends on the measurer's judgment. Therefore, to keep the results as consistent as possible, the same measurer was used throughout this study.

After the skid mark ends had been located, the length of each of the skid marks was measured with a tape measure, and the results were recorded. If the skid marks were curved, the path of the skid was followed as closely as possible to determine the true length of the mark.

During the moderate braking tests, the effect of changes in brake pedal force applied and road surface composition on the skid marks produced during a stop were studied. All test runs were made by stopping the subcompact passenger car from a single initial speed of 30 mph on several different pavements. All of these tests were run with the lightly loaded vehicle and radial tires.

The skid trailer tests used an ASTM skid trailer with ASTM tires to measure the skid numbers of each of the test surfaces used during this study. Peak and slide friction coefficients were also measured for each of the passenger car tires used on all of the test surfaces for which each particular tire was tested. Details of the skid trailer testing are given elsewhere (3).

Repeatability of Skid Mark Data

Two methods were used to check the consistency of the severe braking test data. First, the variability of the vehicle and the pavement was studied by looking at the distance the test vehicle took to stop for each test condition. Then, the consistency with which the measurer was able to mark the ends of the skid marks was analyzed. Before the stopping distances of test stops that were made from the same nominal prebraking speed but from slightly differing actual prebraking speeds could be compared, it was necessary to correct the stopping distances to account for the differing speeds. Corrected stopping distances were calculated for each run by means of Equation 1:

$$CSD = SD \cdot V_N^2 / V_A^2 \quad (1)$$

where

CSD = corrected stopping distance,
SD = actual stopping distance,
V_A = actual prebraking speed, and
V_N = nominal prebraking speed.

This formula was taken from the Society of Automotive Engineers recommended practice J-299, stopping distance test procedure. After they had been corrected, stopping distances for the same nominal speed could be compared directly.

Equation 1 was used to develop a table to summarize the corrected stopping distances of all of the more than 500 test stops that were made. This allowed comparison of the corrected stopping distances for varying loadings, pavements, and tires. Table 3 is a typical portion of this table. The last two columns of Table 3 give the amount of variability that was present in the testing. The next to last column contains the standard error in the corrected stopping distance (equal to the standard deviation divided by the square root of the number of trials), and the last column contains the standard error as a percentage of the average corrected stopping distance. To obtain some idea as to what the numbers in the last column mean for the five trials that were run for each test case, a standard error percentage of 1.14 percent means that 95 percent of the test values will be within 5 percent of the average value.

Analysis of the corrected stopping distances showed that the severe braking stops were repeatable. The average standard error as a percentage of the average corrected stopping distance was 1.75 percent. This indicates that 95 percent of all of the test stops had corrected stopping distances that were within 10 percent of the average value.

Significantly greater variability in stopping performance was observable for two sets of test conditions. For stops made from a nominal prebraking speed of 10 mph, the average standard error percentage was 3.14 percent. However, the maximum standard error for any of the 10-mph cases was 0.29

ft. Since the fifth wheel measures stopping distance with approximately this accuracy, this level of error is not significant. Testing on the tar and gravel chip pavement was also less consistent and repeatable. The average standard error percentage, for stops from all test speeds, was 3.10 percent on the tar and gravel chip pavement versus the 1.42 percent obtained for the other pavements. Corrected stopping distances were less consistent on the tar and gravel chip pavement due to variations in the composition and slickness of the surface. During the testing we noticed that the vehicle took longer to stop when a higher proportion of tar was present in the road.

Next, the consistency with which the measurer was able to measure the length of the skid marks produced during testing was checked. To determine the length of the skid marks on one side of the vehicle, the measurer must mark three points: the viewed from above (VFA) point, the viewed from ground level (VFGL) point, and the start of front marks (SFM) point. Determination of the precise location of the three points marked by the measurer was a difficult and somewhat subjective process because the skid marks tended to fade into the pavement. Although the same person was used as measurer throughout this program, there was clearly some run-to-run variability in the locations of the points chosen.

To determine the amount of variability inherent in the measurement process, the length of several sets of skid marks was measured every day for several days. By measuring the skid marks on a daily basis, enough time passed between each remeasurement so that the measurer could not remember the location of the marks from the previous day and had to relocate them. Data collected by measuring the length of eight skid marks produced during three stops on seven consecutive days was analyzed.

Skid marks decay with time. For the lightly traveled test surfaces that were used, this decay is very slow. To prevent this decay from biasing the analysis, linear regression was performed for each of the skid marks analyzed by using, as the model form,

$$S = C + Dn \tag{2}$$

where S is the skid mark length, n is the number of the measurement, and C and D are determined by regression. Only skid marks for which the 90 percent confidence interval on D included zero were then retained for analysis since these marks showed no significant decay with time.

The standard error, the standard error as a percentage of the average skid mark length, and the 95 percent confidence limits were calculated for each of the eight skid marks. The mark with the greatest variability had a 95 percent confidence limit of ±11.1 percent of its average length. On the average, the skid marks had a tight 95 percent confidence limit of ±3.8 percent of the average length. This indicates that the skid mark measurement process was repeatable.

Validity of the Skid Mark Length Versus Prebraking Speed Formula

A detailed analysis of the skid mark length data collected during the severe braking testing was conducted to either confirm the validity or else improve the existing prebraking speed versus skid mark length formulas. This was done by using the severe braking test data for performing regression analyses that determined values of coefficients in three model equations. The model equations have as their specific form,

$$S = A_1 V^2 \tag{3}$$

$$S = A_2 V^2 + C_2 \tag{4}$$

$$S = A_3 V^2 + B_3 V + C_3 \tag{5}$$

where

S = skid mark length,
V = prebraking speed, and
A_1, A_2, A_3, B_3, C_2, and C_3 = unknown coefficients, which were determined by regression.

Model 1 (Equation 3) has the same form as the standard skid mark length versus prebraking speed formulas. Model 2 (Equation 4) has the same form as the standard formulas would have if they were modified by assuming a constant distance between the start of braking and the onset of skid mark production. Model 3 (Equation 5) has the same form as the standard formulas would have if they were modified to account for a ramp brake application plus the traveling of a constant distance prior to the onset of skid mark production.

Separate regression analyses were performed for each of the 22 different combinations of vehicle type, tire type, pavement type, and loading that were tested. Regressions were performed for the skid marks left by each of the vehicle's individual wheels as well as for the average length from combinations of wheels. The numbers that follow were found by using the four-wheel average skid mark length. Similar results were obtained, however, for the regressions that were performed by using each of the individual wheel's skid marks.

Tables 4 and 5 give the results of the regressions by using the four-wheel average skid mark length for each of the three models. For the IH Transtar-Fontaine rig, for which the four-wheel average length was not used because this rig had more than four wheels, the regressions performed with the left front wheel and with the left leading tractor tandem data are given.

Table 4 contains the coefficient of determination (R^2) that was calculated for each model for the various test conditions. The lowest value of the coefficient of determination that was obtained for any of the models for any set of test conditions was 0.9784. For more than two-thirds of the cases shown, R^2 was above 0.9950 and 85 percent of the cases had it above 0.9900. These are extremely high values for the coefficient of determination and indicate that all three models could closely fit the experimental data. However, because R^2 was so large for all of the test cases, it was inadequate to determine which model was most accurate. This is because a model with more terms in it, such as model 3, normally accounts for more of the variation in the data. It may, however, be less useful for accident reconstruction than is a model with fewer terms in it such as model 1. To see how much more accurate the models that contained more terms actually were, the mean square error was studied.

The mean square error, which is the second measure of goodness of fit given in Table 4, is an estimate of the deviation of the regression curve from the actual data. It was analyzed by taking the average of the mean square errors for each model for all of the test cases given in Table 4. Also looked at was the influence of vehicle type, tire type, vehicle loading, and pavement composition on model accuracy. This was done by computing the average mean square error for selected subsets of the test conditions.

The average values of the mean square error that were found for all of the test cases were 28.01 for model 1, 20.08 for model 2, and 17.50 for model 3. This indicates that model 3 was the most accurate, followed by models 2 and 1, respectively. However, the improvement in accuracy between models was not great. The mean square error is the normalized sum of the squares of the residuals. The square root of the average values given shows that model 1 has a root mean square deviation between the model's predicted skid mark length and the actual skid mark length of slightly over 5.25 ft versus slightly under 4.25 ft for model 3. Given an average skid mark length of approximately 50 ft, this improvement of about 1 ft in accuracy is not significant.

A look at the individual test cases shows large case-to-case variations in the mean square error for the differing models. For some test conditions model 3 is significantly more accurate than model 1, with improvements in the deviation between the predicted and actual skid mark lengths of up to 5.25 ft occurring. There does not, however, seem to be any way of predicting in advance when this improvement will occur.

Table 4. Goodness of regression fits.

				Model 1		Model 2		Model 3	
Vehicle	Loading	Surface	Tires	R^2	Mean Square Error	R^2	Mean Square Error	R^2	Mean Square Error
Chevette	LLW	VDA	Bias ply	0.9993	3.95	0.9995	1.55	0.9997	1.01
	LLW	VDA	Radial	0.9990	5.05	0.9985	4.11	0.9986	4.07
	LLW	Skid pad	Bias ply	0.9989	6.06	0.9986	3.67	0.9986	3.82
	LLW	Skid pad	Radial	0.9990	4.63	0.9990	2.34	0.9991	2.23
	LLW	Tar and gravel chip	Bias ply	0.9889	111.99	0.9886	64.79	0.9946	32.22
	LLW	Tar and gravel chip	Radial	0.9859	151.39	0.9784	129.02	0.9845	96.88
	GVW	VDA	Radial	0.9971	16.99	0.9939	17.72	0.9939	18.50
Malibu	LLW	VDA	Radial	0.9988	8.04	0.9968	8.74	0.9986	8.65
LTD	LLW	VDA	Bias ply	0.9990	5.94	0.9978	6.19	0.9979	6.04
	LLW	VDA	Radial	0.9993	5.35	0.9983	5.25	0.9989	3.59
	LLW	Skid pad	Bias ply	0.9990	6.50	0.9979	6.77	0.9980	6.87
	LLW	Skid pad	Radial	0.9985	12.29	0.9960	12.48	0.9967	11.02
	LLW	Tar and gravel chip	Bias ply	0.9969	31.00	0.9937	30.95	0.9940	30.85
	LLW	Tar and gravel chip	Radial	0.9917	69.25	0.9844	67.79	0.9849	65.75
	GVW	VDA	Radial	0.9891	129.63	0.9902	55.23	0.9939	36.41
F-250	LLW	VDA	Bias ply	0.9983	8.91	0.9964	9.30	0.9965	9.47
	Half	VDA	Bias ply	0.9955	26.46	0.9968	10.29	0.9987	4.56
	GVW	VDA	Bias ply	0.9975	16.76	0.9977	8.52	0.9978	8.39
F-7000	LLW	VDA	Bias ply	0.9952	16.13	0.9899	14.15	0.9934	9.68
	GVW	VDA	Bias ply	0.9987	17.02	0.9988	6.62	0.9989	6.63
Transtar-Fontaine	LLW	VDA	Bias ply[a]	0.9973	3.14	0.9926	3.43	0.9928	3.69
	LLW	VDA	Bias ply[b]	0.9953	3.23	0.9877	3.39	0.9911	2.72
	GVW	VDA	Bias ply[a]	0.9984	7.97	0.9971	5.02	0.9971	5.31
	GVW	VDA	Bias ply[b]	0.9988	4.54	0.9967	4.57	0.9967	4.84

[a]Results for left front wheel. [b]Results for left leading tractor tandem wheel.

Table 5. Coefficients determined by regression.

				Model 1,	Model 2		Model 3		
Vehicle	Loading	Surface	Tires	A_1	A_2	C_2	A_3	B_3	C_3
Chevette	LLW	VDA	Bias ply	0.0413	0.0422	-2.237	0.0448	-0.199	0.626
	LLW	VDA	Radial	0.0390	0.0396	-1.500	0.0412	-0.121	0.258
	LLW	Skid pad	Bias ply	0.0392	0.0401	-2.333	0.0406	-0.040	-1.742
	LLW	Skid pad	Radial	0.0380	0.0389	-2.232	0.0406	-0.121	-0.485
	LLW	Tar and gravel chip	Bias ply	0.0523	0.0563	-10.068	0.0763	-1.508	11.722
	LLW	Tar and gravel chip	Radial	0.0537	0.0565	-7.491	0.0766	-1.521	14.640
	GVW	VDA	Radial	0.0415	0.0414	0.121	0.0415	-0.003	0.159
Malibu	LLW	VDA	Radial	0.0410	0.0424	-3.474	0.0429	-0.044	-2.694
LTD	LLW	VDA	Bias ply	0.0409	0.0408	0.117	0.0386	0.168	-2.316
	LLW	VDA	Radial	0.0437	0.0433	0.925	0.0362	0.594	-9.584
	LLW	Skid pad	Bias ply	0.0427	0.0428	-0.194	0.0412	0.118	-1.896
	LLW	Skid pad	Radial	0.0435	0.0430	1.320	0.0361	0.571	-8.815
	LLW	Tar and gravel chip	Bias ply	0.0494	0.0500	-1.641	0.0461	0.304	-6.086
	LLW	Tar and gravel chip	Radial	0.0478	0.0489	-2.952	0.0440	0.368	-8.278
	GVW	VDA	Radial	0.0512	0.0567	-14.151	0.0818	-2.111	23.979
F-250	LLW	VDA	Bias ply	0.0389	0.0389	-0.016	0.0373	0.125	-1.807
	Half	VDA	Bias ply	0.0414	0.0438	-5.830	0.0525	-0.650	3.555
	GVW	VDA	Bias ply	0.0420	0.0435	-4.125	0.0459	-0.178	-1.524
F-7000	LLW	VDA	Bias ply	0.0573	0.0595	-2.683	0.0790	-1.026	8.145
	GVW	VDA	Bias ply	0.0773	0.0802	-5.214	0.0831	-0.188	-2.773
Transtar-Fontaine	LLW	VDA	Bias ply[a]	0.0621	0.0621	0.058	0.0671	-0.210	1.946
	LLW	VDA	Bias ply[b]	0.0469	0.0478	-0.567	0.0300	0.746	-7.270
	GVW	VDA	Bias ply[a]	0.0707	0.0683	2.950	0.0689	-0.033	3.306
	GVW	VDA	Bias ply[b]	0.0613	0.0605	2.633	0.0603	0.013	4.598

[a]Results for left front wheel. [b]Results for left leading tractor tandem wheel.

To show the effects of pavement composition and variability on model accuracy, the average mean square error was calculated for each test surface. The results are given in the first three lines of Table 6. All of the models most accurately fit the experimental data for the testing on the skid pad; the VDA data ran a close second. Much poorer accuracy was obtained on the tar and gravel chip road. Note that this result is consistent with the greater variability in stopping performance on this surface that was pointed out earlier. Even on this surface, despite the relatively large improvements in mean square error from model 1 to model 3, the improvement in average root mean square skid mark length error was only about 2 ft, which is not significant.

Table 6 also gives the results of average mean square error calculations, which were made to determine the effect on model accuracy of tire type, vehicle loading, and vehicle type. The fourth and fifth lines of the table show that higher accuracy, and hence more consistent experimental data, was obtained with bias-ply tires than with radial tires. Since vehicles at GVW were only tested on the VDA, it was decided that this result should not be compared with the average mean square error from all of the LLW tests because these include the data from the highly variable tar and gravel chip surface. Comparison of the average mean square error from the GVW stops with that from the LLW stops, which were made on the skid pad or VDA, shows that the models less accurately fit the GVW data. Most of this increase in mean square error is attributable to the peculiar stopping behavior of the loaded Ford LTD.

Comparisons of model accuracy among passenger cars, pickup trucks, and the air-braked trucks was also made by using only the skid pad and VDA data. This revealed that the highest accuracy was obtained for the air-braked vehicles followed by the pickup truck, with the passenger cars third. This order was something of a surprise because the time delays that are inherent in air brakes were expected to result in less-consistent data. Also, it was anticipated that, due to these delays, model 3 would be by far the best for the air-braked vehicles. Instead, only a small improvement, which amounted to 0.5 ft in the average root mean square skid mark length error, was obtained.

For all three models, theoretical analysis of the assumed deceleration versus time curves and integration to determine stopping distance shows that the coefficient of sliding friction (U_s) is related to the coefficient of the velocity squared term (A_1, A_2, or A_3) by the equation

$$U_s = 1/2g A_i \qquad (6)$$

where g is the acceleration due to gravity. The complete theoretical analysis is contained elsewhere (4). From Equation 6, along with the values of A_1, A_2, and A_3 in Table 5, values of the slide friction coefficient have been calculated for each of the test conditions. These values are given in Table 7 along with results from two of the methods

Table 6. Average value of mean square error of selected test conditions.

Test Condition	Model 1	Model 2	Model 3
Tar and gravel chip road	90.91	73.14	56.43
Skid pad	7.37	6.32	5.99
VDA	17.44	10.26	10.64
Bias ply tires	17.97	11.95	11.52
Radial tires	44.74	33.63	27.46
Vehicle at LLW	26.64	22.00	17.57
Vehicle at LLW and on skid pad or VDA	6.86	6.25	5.61
Vehicle at GVW	32.15	16.28	13.35
Passenger car tests	37.87	27.77	21.86
Passenger car tests on skid pad or VDA	18.58	11.28	9.29
Pickup truck tests	17.38	9.37	7.47
Air-braked truck tests	8.67	6.20	5.49

Note: Values are the average of the mean square error for all tests run with the specified test conditions.

Table 7. Calculated and measured slide friction coefficients.

				Calculated Slide Friction Coefficients			Measured Slide Friction Coefficients		
							ASTM Skid No.	95 Percent Confidence Limits of Measured	
Vehicle	Loading	Surface	Tires	Model 1	Model 2	Model 3		Low	High
Chevette	LLW	VDA	Bias ply	0.809	0.792	0.746	81.1	0.819	0.877
	LLW	VDA	Radial	0.856	0.843	0.811	81.1	0.841	0.869
	LLW	Skid pad	Bias ply	0.852	0.833	0.823	79.1	0.793	0.843
	LLW	Skid pad	Radial	0.879	0.859	0.823	79.1	0.777	0.827
	LLW	Tar and gravel chip	Bias ply	0.639	0.593	0.438	60.8	0.653	0.775
	LLW	Tar and gravel chip	Radial	0.622	0.591	0.436	60.8	0.616	0.768
	GVW	VDA	Radial	0.805	0.807	0.805	81.1	0.841	0.869
Malibu	LLW	VDA	Radial	0.815	0.788	0.779	81.1	0.779	0.833
LTD	LLW	VDA	Bias ply	0.817	0.819	0.865	81.1	0.782	0.798
	LLW	VDA	Radial	0.764	0.771	0.923	81.1	0.746	0.800
	LLW	Skid pad	Bias ply	0.782	0.780	0.811	79.1	0.771	0.815
	LLW	Skid pad	Radial	0.768	0.777	0.925	79.1	0.720	0.756
	LLW	Tar and gravel chip	Bias ply	0.676	0.668	0.725	60.8	0.494	0.686
	LLW	Tar and gravel chip	Radial	0.699	0.683	0.759	60.8	0.486	0.608
	GVW	VDA	Radial	0.652	0.589	0.408	81.1	0.779	0.833
F-250	LLW	VDA	Bias ply	0.859	0.859	0.896	81.1		
	Half	VDA	Bias ply	0.807	0.763	0.636	81.1		
	GVW	VDA	Bias ply	0.795	0.768	0.728	81.1		
F-7000	LLW	VDA	Bias ply	0.583	0.561	0.423	81.1	0.554	
	GVW	VDA	Bias ply	0.432	0.416	0.402	81.1	0.539	
Transtar-Fontaine	LLW	VDA	Bias ply[a]	0.538	0.538	0.498	81.1	0.588	
	LLW	VDA	Bias ply[b]	0.712	0.699	1.113	81.1	0.588	
	GVW	VDA	Bias ply[a]	0.472	0.489	0.485	81.1	0.566	
	GVW	VDA	Bias ply[b]	0.545	0.552	0.554	81.1	0.566	

[a]Results for left front wheel. [b]Results for left leading tractor tandem wheel.

that were used to measure the slide friction coefficient.

The last three columns of Table 7 give measured slide friction values. Of these, the third from last column shows the ASTM skid number at 40 mph of the test pavement. For the passenger cars, the last two columns contain the lower and upper bounds, respectively, of the 95 percent confidence interval of the skid-trailer-measured tire-road slide friction coefficient. This friction coefficient was measured by mounting the tire of interest on the skid trailer, loading the trailer so as to approximate the normal load on the tire when it is mounted on the vehicle, and determining the slide friction coefficient at 40 mph. For large trucks, the next to last column contains the measured slide friction coefficient for the combination of tires mounted on each vehicle and the last column is blank because no information was available on the spread of these values.

Generally good agreement was obtained for the passenger car tests between the calculated and measured values of the friction coefficient. More than one-third of the values were inside the 95 percent confidence interval and three-fourths of the values were within 10 percent of these limits. The calculated values agreed best for model 1, followed by model 2, and model 3; however, the improvement between models was small. Similarly, for the pickup truck data, for which the friction coefficients of the actual pickup truck tires were not measured, model 1 provides the values that best agree with the measured ASTM 40-mph skid number. For the air-braked trucks, the skid number is generally well above the calculated friction coefficients. Reasonable agreement (half of values within 10 percent, all values within 20 percent), however, was obtained between the measured values and the values calculated by model 1. Values calculated from models 2 and 3 did not agree as closely.

The values of B_3 given in Table 5 vary from test case to test case, with a low value of -2.111 and a high value of 0.746. From theoretical analysis (4), B_3 is one-half the time it takes for the brakes to apply (i.e., one-half the time it takes the deceleration to rise from zero to the steady state value). Therefore, it should change only slightly from test case to test case for a given vehicle and it should always, for all vehicle speeds, be positive. However, as was just pointed out, the value of B_3 varies considerably for a given test vehicle. Furthermore, for more than one-half of the cases in Table 7, B_3 is negative. Calculation of the average value of B_3 for all 24 cases in the table yields -0.21, a negative value. Although tests for significance of B_3 showed that for some cases B_3 was probably significant and for others it was not, these facts lead one to suspect that B_3 is probably actually zero and show that the time needed for the brakes to apply does not significantly affect skid mark lengths. Even for the air-braked trucks, whose brakes come on relatively slowly due to pneumatic delays, four of the six B_3 values are negative, which indicates that brake apply times did not influence the results.

The constant terms in the model equation also show considerable variation--C_2 ranged between -14.151 and 2.950 and C_3 ranged between -9.584 and 23.979. Because these terms are due to the tire having to travel some distance after the onset of braking before producing skid marks, it is expected that C_2 and C_3 should always, for all vehicle speeds, be negative. The large positive values of C_3 that were determined for some sets of test conditions are thought to be mathematical artifacts that indicate that model 3 is not valid. Excluding the cases with large positive values, C_2 and C_3 are generally quite small, with occasional sets of test conditions for which large negative values were found. There does not seem to be any consistent pattern to allow one to predict when the large negative values will occur.

To summarize the above discussion, model 3 provides, in general, a slightly more accurate fit to the experimental data than does either model 1 or 2. For some cases, it is significantly more accurate, but these cases cannot be predicted in advance. However, study of the slide friction coefficients that are calculated from each model shows that model 1's are in slightly better agreement with the measured values than are either of the other models'. Furthermore, study of B_3, C_2, and C_3 reveals that it was impossible to predict their values and that there are discrepancies between their experimentally measured values and skid mark theory.

Overall, model 1, which is the currently in-use skid mark length versus prebraking speed formula, was confirmed by the data. The attempt to find a usable, better formula failed because, although models 2 and 3 more accurately fit the experimental data, the problems of predicting B_3, C_2, and C_3 make them unsuitable for practical, real-world use. Therefore, model 1 is the best formula that can be developed for use in accident reconstruction.

The above analysis also points out the inadvisability of using the ASTM 40-mph skid number for prebraking speed versus skid mark length calculations that involve heavy trucks. Considerable additional analysis was performed with the severe braking test data to evaluate several methods of measuring the tire-road slide friction coefficient. The methods evaluated were as follows:

1. Estimation of the friction coefficient based on the pavement type and condition; Baker has a table that can be used to make this estimate (1);
2. Measurement of the ASTM skid number of the pavement at 40 mph (omitting water) and use of that as an estimate of the friction coefficient;
3. Measurement of the tire-road slide friction coefficient with a skid trailer by the same type of test that is used to measure skid number, except that the actual tire is used instead of a standard ASTM one and the loading is changed to approximate the actual load on the tire when on the vehicle; a larger skid trailer is used for heavy truck tires; and
4. A severe braking stop from a specified prebraking speed by using the actual vehicle and tires, measurement of the length of the skid marks produced, and calculation of the friction coefficient from the theoretical skid mark length-prebraking speed formula; as is pointed out by Hutchinson and others (5), due to financial constraints, this method can be used only rarely in an actual field investigation.

A complete description of the evaluation of these friction measuring methods is contained elsewhere (3). To summarize the major result of these evaluations, all four methods for measuring tire friction provide acceptable estimates for passenger cars and pickup trucks. However, for heavy trucks, only methods 3 and 4 provide acceptable estimates of the tire-road friction. Methods 1 and 2 yield friction coefficients that are too high.

TIRE MARKS WITH UNLOCKED WHEELS

The testing found that a wheel frequently begins to produce skid marks before it locks up. (Technically, these are scuff marks but, since their appearance was similar to that of skid marks, the term skid mark is used in this paper.) In fact, for some runs, a wheel produced skid marks during most of the stop despite failure to lock up at any time during the stop.

The experimental observations mentioned above raised the possibility that the moderate braking of a vehicle (i.e., braking with none of the wheels locked at any time during a stop) could still cause skid marks to be left. Depending on the amount of brake pedal force that had to be applied to leave marks and on the corresponding magnitude of the resulting vehicle deceleration, these skid marks could be longer than those left by severe (panic type) braking. This would create problems when using the standard skid mark length versus prebraking speed formulas. These equations assume severe braking and would, for a moderate braking stop, predict that the vehicle was going faster than it actually was. Therefore, it is important to know whether or not longer skid marks can be produced during a moderate braking stop from a given speed than during a severe braking stop from the same speed. Furthermore, if this should prove to be the case, then it is important to know if there is some distinguishing feature of the scuff marks that allow one to know when the severe braking formulas are valid.

To study this question, a number of moderate braking tests were run by using the lightly loaded 1980 Chevette with radial tires. All test stops were made from a nominal prebraking speed of 30 mph by applying a constant, predetermined force to the brake pedal with a servo-controlled brake actuator. Most of the testing was performed on the three surfaces used previously. A few tests were run on a number of other surfaces to see if they would yield similar results.

The skid marks produced were generally much lighter than the ones produced during severe braking. As a result, it was normally impossible to distinguish between the front and rear wheel skid marks. Therefore, the entire length of the skid mark on the right and left sides was measured and recorded. It was then necessary to subtract the wheelbase of the vehicle (8.0 ft) from the measured length to determine the rear-wheel skid mark lengths.

The first set of moderate braking tests was run on the VDA asphalt. For this set, the Chevette was braked from 30 mph by pedal forces ranging from 30 to 100 lbs (it takes about 150 lbs to lock wheels). Even at the low pedal force of 40 lbs, noticeable skid marks were left.

The table below gives the corrected average skid mark lengths obtained from these tests versus the brake pedal force used to generate them. The test vehicle was a Chevette, LLW, run on VDA asphalt at a nominal speed of 30 mph and equipped with radial tires.

Pedal Force (lb)	Corrected Avg Skid Mark Length (ft)
40	88.1
50	71.7
60	62.5
70	55.8
80	55.2
90	51.7
100	40.8
∿300	31.6

The corrected average skid mark length is the average of the left and right skid mark lengths after they have had the wheelbase of the vehicle subtracted from them and are corrected for speed differences by means of Equation 1, with skid mark length substituted for stopping distance. This length increased as the applied brake pedal force decreased from the low of 31.6 ft that was obtained for the severe braking stops in an average of five stops to a high of 88.1 ft for an applied force of 40 lbs. This indicates a possible problem in using skid marks to determine prebraking vehicle speed. Specifically, if an accident investigator were to interpret the skid marks that were produced during the stop with 40-lb pedal force as having been produced during a severe braking stop, subsequent reconstruction would predict a prebraking vehicle speed of approximately 50 mph compared with the 30 mph that the vehicle actually was going.

There was a difference in darkness and intensity of the unlocked wheel, moderate braking skid marks as compared with the locked wheel, severe braking ones in that the moderate braking left only light, shadow-type marks. Normally, during severe braking, a light area occurs at the very beginning of the skid mark that is hard to see when looking directly down at the mark. To see this shadow properly, you have to look along the length of the skid mark from some distance away.

The moderate braking skid marks on the VDA asphalt are like these shadows in that they were just barely visible from directly above, but they are very clear from far away. The entire length of these marks is the shadow, with no dark portion such as normally appears in a locked wheel stop. To demonstrate this difference in appearance, Figures 1 and 2 show moderate braking skid marks, generated during a stop with 80-lb pedal force, next to severe braking skid marks. The moderate braking skid marks are to the right of the picture in Figure 1, and the light set are in the foreground in Figure 2. As Figure 1 shows, when viewed along their length, the moderate and severe braking skid marks are both dark. However, when viewed from above and to the side (as in Figure 2), the moderate braking marks are much lighter.

Unlocked wheel, relatively low deceleration stops produced long visible skid marks on two of the five other pavements tested on. On the basis of this testing, it is impossible to say just how much of a problem nonlocked wheel skid marks may cause for skid mark theory. At least for some pavements, it is possible to create longer skid marks with wheels that are braked so as to merely retard their motion than with locked wheels. It is not clear how prevalent this phenomenon is.

Since all of the nonlocked wheel skid marks were visible only as shadows (i.e., visible only when viewed along their length), the standard skid mark formulas are valid as long as the investigator only uses them for nonshadow skid marks. Any skid mark that is visible only as a shadow may be due to a nonlocked wheel for which the standard formulas are incorrect.

CONCLUSIONS

A number of results of interest to accident investigators and reconstructionists were developed during this study. First, the variability of stopping performance during severe braking stops of the type that leave dark skid marks was considered. This variability was found to be small for tests that were conducted on TRC's test pavements but increased to approximately 15 percent for tests on the tar and gravel chip public road. Testing during this project, with the hard and fast brake applications that were used, gave the minimum speed for producing a skid mark of a given length. Greater stopping vari-

Figure 1. Skid marks from moderate (left) and severe (right) braking viewed lengthwise.

Figure 2. Side view of skid marks from moderate (bottom) and severe (top) braking.

ability will be present in an actual accident situation. This is why a maximum value for the prebraking speed cannot be predicted from skid marks.

The process of measuring skid marks was found to be repeatable provided the measurements were made carefully. Less than a 5-percent error was typically made. Regression analyses were performed to see how well the currently used skid mark length versus prebraking speed formulas and two modified forms of the currently used formulas fit the experimental data. These analyses showed that the currently used formulas provided an excellent fit to the test data. Furthermore, neither of the modified formulas were able to explain the test data better.

Four methods of measuring the tire-road slide friction coefficient for use in skid mark analysis were evaluated. All four methods provided acceptable results for passenger cars and pickup trucks. However, for heavy trucks, only two of the four methods gave acceptable results--calculation of the friction from a stop and the skid-trailer-measured tire-road friction. The other two methods produced friction coefficients that were too high for trucks, which resulted in predicted speeds well above the actual ones.

Early in this study we found that wheels that did not lock during a stop could still produce long scuff marks, similar in appearance to skid marks. In fact, for some pavements stops for which none of the vehicle's wheels locked were found to produce tire marks that were longer than those produced during a locked wheel stop. The tire marks generated during nonlocked wheel stops look like light shadowy (visible when viewed along their length but not from directly above) skid marks. Accident investigators must be extremely careful when using light skid marks in the formulas to determine prebraking speed from skid mark length to ensure that the skid marks were made by locked wheels. Otherwise, too high an estimate of the vehicle's prebraking speed may be obtained.

ACKNOWLEDGMENT

We would like to thank all of the people who assisted in this project. We are especially grateful to Vern Roberts of the National Highway Traffic Safety Administration for sponsoring this study and to Richard Radlinski, Ron Houk, James Lin, and Mike Martin for their assistance in performing the testing and analysis.

REFERENCES

1. J.S. Baker. Traffic Accident Investigation Manual. Traffic Institute, Northwestern Univ., Evanston, IL, 1975.
2. J.C. Collins and J.L. Morris. Highway Collision Analysis. Charles C. Thomas Publisher, Springfield, IL, 1967.
3. W.R. Garrott and D.A. Guenther. Determination of Tire-Road Friction Coefficients for Skid Mark Analysis. National Highway Traffic Safety Administration, 1982.
4. W.R. Garrott, D. Guenther, R. Houk, J. Lin, and M. Martin. Improvement of Methods for Determining Pre-Crash Parameters from Skid Marks. National Highway Traffic Safety Administration, May 1981.
5. J.W. Hutchinson, N.G. Tsongos, R.C. Bennett, and W.J. Fogarty. Pavement Surface Information Needs in Accident Investigation. American Society for Testing and Materials, Chicago, IL, 1975.

Publication of this paper sponsored by Committee on Surface Properties-Vehicle Interaction.

Methodology for Analyzing Texture and Skid Resistance Data for Use in Pavement Management Systems

E.C. YEH, J.J. HENRY, AND J.C. WAMBOLD

Results of recent research in skid resistance have been incorporated into a methodology for use in pavement maintenance management programs by transportation agencies. The methodology, which is part of a computer program developed for the Federal Highway Administration (MAPCON), can perform the data processing to reduce and analyze the raw measurement data from various types of texture and skid resistance measurements. This paper discusses the capability and structure of the methodology. It covers aspects of skid resistance, adjustments for seasonal and weather-related variations, side force coefficients, and the hydroplaning potential. The use of the computer program is also discussed.

Skid resistance is a measure of the friction between the tires of a moving vehicle and the wet pavement. Pavement friction determines the amount of control available to the driver of the vehicle and is important for safety. In recent years research has improved the understanding and prediction of the skid resistance of pavements. Incorporation of recent research findings (1-5) to form a methodology for analysis of skid resistance will provide a compact tool for pavement management by transportation agencies. Similar methodologies can be applied to other pavement management inputs such as road roughness, pavement distress, and ride quality. An overall methodology, which uses the computer program methodology for analyzing pavement condition (MAPCON), has been developed by the Pennsylvania Transportation Institute to provide inputs by reducing and analyzing the raw measurement data into some significant quantities for use in management systems. This paper discusses the aspects of the program related to the skid resistance of the pavement.

METHODOLOGY

The methodology for the analysis of skid resistance has been developed from in-depth investigations of all the measurement methods, analyses, and research findings currently available. The structure of the analysis is illustrated in the block diagram in Figure 1, where the computation is performed by using inputs shown on the left side of the diagram to produce the outputs shown on the right side. The program can operate on such data as British pendulum numbers (BPNs), sand-patch data, or texture profiles to perform specified analyses and provide meaningful results.

The skid-resistance analysis describes the friction between vehicles and wet pavements currently quantified as skid number (SN), the friction force divided by the vertical load on a skidding tire. SN depends not only on pavement properties but also on the relative sliding velocity of the tire in the form (1):

$$SN = SN_0\, e^{-(PNG/100)V} \tag{1}$$

where

SN_0 = skid number intercept,
PNG = percentage of normalized gradient = $-(100/SN)(d/dV)(SN)$, and
V = sliding velocity.

Usually, SN at 64 km/h (SN_{64}) is used as a common index in evaluating pavement performance. The side force coefficient (SFC), the side force times 100 divided by the normal force on a cornering tire, is sometimes used for evaluating pavement safety because it is a measure of steering capability. In fact, Henry (1) shows that SFC is also a function of SN_0 and PNG, as follows:

$$SFC = SN_0[3(\rho^2 - \rho^3) + e^{-(PNG/100)(V/2)\tan\alpha}(1 - 3\rho^2 + 2\rho^3)] \tag{2}$$

where

$\rho = 1 - [\tan\alpha/3(SN_0)][d(SFC)/d\alpha] \quad \alpha \to 0$,
α = yaw angle, and
$d(SFC)/d\alpha$ = 1980 rad^{-1} for ASTM E 501 tire (6) and 1500 rad^{-1} for ASTM E 524 tire (6).

SN_0 and PNG are important parameters for skid-resistance analysis. They are used to predict and evaluate the pavement friction performance (SN and SFC) as a function of speed. However, SN_0 and PNG are parameters closely related to the pavement texture, with SN_0 related to the microtexture of the pavement and PNG related to its macrotexture. Thus, they can be estimated from texture measurements or computed directly from pavement friction tester data. There are four ways to provide estimates of SN_0 and PNG, which are described below as Pennsylvania State University (PSU) models I, II, III, and IV.

PSU Model I

PSU model I uses skid-trailer tester results and performs a log-linear regression from skid number-sliding velocity pairs (SN_i, V_i) to estimate the best values for SN_0 and PNG in Equation 1. The regression in this form provides excellent correlation with the experimental data (1).

PSU Model II

PSU model II uses one skid number at a known sliding velocity and one texture descriptor. The texture descriptor can be either a macrotexture or a microtexture parameter. Depending on whether the texture data are macro or micro, SN_0 or PNG is determined. Then Equation 3,

$$SN_0 = SN_V\, e^{(PNG/100)V} \tag{3}$$

is used with known PNG, or Equation 4,

$$PNG = (100/V)\ln(SN_0/SN) \tag{4}$$

is used with known SN_0.

PSU Model III

PSU model III uses texture data to estimate SN_0 and PNG.

Macrotexture Data for Estimating PNG

The macrotexture profile can be measured by using a texture profile tracer, either a mechanical instrument with a contacting stylus or a noncontact opti-

Figure 1. Functional block diagram for methodology in skid-resistance analysis.

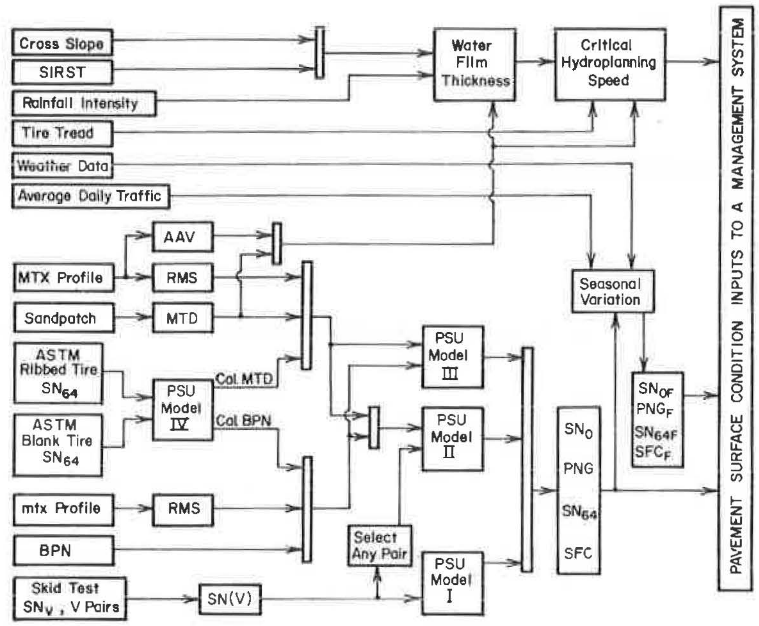

cal instrument. The macrotexture profile contains wavelengths in excess of 0.5 mm [the choice of 0.5 mm for dividing macrotexture and microtexture is based on the study by Henry (1)] and is reduced to its root mean square height ($RMSH_{MA}$). PNG can be estimated by the relation (1)

$$PNG = b_1 \, RMSH_{MA}^{b_2} \tag{5}$$

Typical values for b_1 and b_2 and coefficients for subsequent equations are listed in Table 1. These are typical values that have been developed by using the data collected in Pennsylvania. As additional data that describe a wider range of pavement designs become available, these values may be refined.

Sand-patch mean texture depth (MTD) measured from the sand-patch method is related to PNG (1),

$$PNG = c_1 \cdot MTD^{c_2} \tag{6}$$

Microtexture Data for Estimating SN_0

Microtexture profile data can be measured by using a microtexture profile tracer. The microtexture profile, which contains wavelengths below 0.5 mm, can be obtained and reduced to its root mean square height ($RMSH_{MI}$). This quantity is used to estimate SN_0 by (1),

$$SN_0 = d_1 + d_2 \cdot RMSH_{MI} \tag{7}$$

BPN can be measured by using ASTM E 303 (6) and can be related to SN_0 by (1)

$$SN_0 = e_1 + e_2 \cdot BPN \tag{8}$$

PSU Model IV

It has been found (4) that skid numbers measured by using ASTM E 524 smooth tire (Equation 9) (SN_{64}^B) and the ASTM E 501 ribbed tire (SN_{64}^R) correlate very well with BPN and MTD numbers in the forms of

$$SN_{64}^B = f_{1B} + f_{2B} \cdot (BPN) + f_{3B} \cdot (MTD) \tag{9a}$$

$$SN_{64}^R = f_{1R} + f_{2R} \cdot (BPN) + f_{3R} \cdot (MTD) \tag{9b}$$

by solving these two equations simultaneously, equivalent data for BPN and MTD can be computed from SN_{64}^B and SN_{64}^R. Then, PGN and SN_0 can be estimated by using the formula of Equations 6 and 8.

SEASONAL VARIATIONS

SN_0 and PNG can be estimated from PSU models I, II, or III. However, skid-resistance measurements on two hypothetically identical pavements will produce different skid numbers if the measurements are made at different times in the season or under different weather conditions. We must correct for these effects in order to compare pavements on a common basis. The object of this analysis is to determine a seasonally adjusted value for SN from measurements taken at any time during the season and also to account for the weather conditions that prevailed when the measurement was made. The seasonally adjusted value (SN_{64F}) is known when corresponding values of SN_{0F} and PNG_F are determined.

From a measurement of SN_0, the value of SN_{0F} can be determined:

$$SN_{0F} = SN_0 - SN_{0R} - SN_{0L} \tag{10}$$

where SN_{0R} is the short-term variation residual and SN_{0L} is the long-term variation residual. Equation 10 describes the changes that SN_{0F} undergoes as a result of long-term (annual) and short-term (weather-related) variations.

The short-term and long-term variations of SN_0 (SN_{0R} and SN_{0L}) can be estimated by using (3)

$$SN_{0R} = g_1 - g_2 DSF - g_3 TP \tag{11a}$$

$$SN_{0L} = SN_{0F} + \Delta SN_0 e^{(-t_1/h_4 - h_5 ADT)} \tag{11b}$$

and

$$\Delta SN_0 = h_1 - h_2 ADT - h_3 BPN \tag{11c}$$

where

ADT = average daily traffic,
DSF = dry spell factor,
TP = pavement temperature, and

Table 1. Typical values for coefficients.

Coefficient	Value	Equation	Remarks	Reference
b_1 b_2	0.35 -0.52	$PNG = b_1 \cdot RMSH_{MA}^{b2}$	$RMSH_{MA}$ in mm PNG in h/km	1
c_1 c_2	0.45 -0.47	$PNG = C_1 \cdot MTD^{C2}$	MTD in mm PNG in h/km	1
d_1 d_2	-44.4 9.44	$SN_0 = d_1 + d_2 \cdot RMSH_{MI}$	$RMSH_{MI}$ in mm	1
e_1 e_2	-34.9 1.32	$SN_0 = e_1 + e_2 \cdot BPN$		1
f_{1B} f_{2B} f_{3B}	-16.87 0.54 0.50	$SN_{64}^B = f_{1B} + f_{2B}(BPN) + f_{3B}(MTD)$	MTD in mm	5
f_{1R} f_{2R} f_{3R}	-9.19 0.74 0.15	$SN_{64}^R = f_{1R} + f_{2R}(BPN) + f_{3R}(MTD)$	Spring 1979 test	5
g_1 g_2 g_3	3.8 1.15 0.10	$SN_{0R} = g_1 - g_2 \cdot DSF - g_3 \cdot TP$	TP in °C	3
h_1 h_2 h_3	28.5 0.002 3 0.09	$\Delta SN_0 = h_1 - h_2 \cdot ADT - h_3 \cdot BPN$		2
h_4 h_5	67.67 0.003 7	$SN_{0L} = \Delta SN_0 \cdot e^{[-T_1/(h_4 - h_5 \cdot ADT)]}$	T_1 in days	2
j_1 j_2 j_3 j_4	0.005 979 0.11 0.59 -0.42	$WT = j_1(MTD^{j2}\ RAIN^{j3}\ CSLP^{j4}) - MTD$	MTD in mm RAIN in mm/h CSLP in m/m WT in mm For runoff length 11 m	6
k_1 k_2 k_3 k_4 k_5	8.454 8 0.05 0.01 1.879 8 0.01	$V_c = k_1[(TD/25.4) + 1]^{k2}\ MTD^{k3}[WT^{(k4/k5)} + 1]$	V_c in km/h TD in mm Based on 10 percent spin down 165 kPa tire pressure	6

t_1 = number of days between the day for which ΔSN_0 is estimated and the date when the measurement was made.

$$DSF = \log(1 + TR) \tag{12}$$

where TR is the number of days since the last rainfall of 2.5 mm or more with an upper limit of seven days.

PNG is also subject to seasonal variation. Research is under way to determine the dependence of PNG and time. The proposed relation is

$$PNG_F = PNG - i_1 t_2 - i_2 ADT \tag{13}$$

where t_2 is the number of days since PNG was measured. For the current methodology, i_1 and i_2 are set at zero, and the variation of PNG is thus ignored.

By using Equations 11a and 11b, SN_{0F} can be obtained. The seasonally adjusted value can thus be given as:

$$SN_{64F} = SN_{0F}\, e^{-0.64 PNG_F} \tag{14}$$

Also, SFC_F can be estimated by substituting SN_{0F} and PNG_F for SN_0 and PNG in Equation 2.

HYDROPLANING POTENTIAL

SN and SFC are the quantities that describe the longitudinal and lateral friction available for controlling vehicle motion under ASTM E274 conditions with an effective water film thickness of 0.5 mm. However, if the rainfall is heavy, the vehicle may hydroplane. This is the condition when the tires are separated from the pavement by the water wedge, and the friction becomes so low that loss of vehicle control may occur. The hydroplaning potential is best described by a critical vehicle speed for specified rainfall. The critical speed, above which hydroplaning may occur, can be calculated from the following equation (5) if sufficient data are available:

$$WT = j_1(MTD^{j2} RAIN^{j3} CSLP^{j4}) - MTD \tag{15}$$

$$V_c = K_1[(TD/25.4) + 1]^{k2} MTD^{k3}[(k_4/WT^{k5}) + 1] \tag{15a}$$

where

WT = estimated water film thickness;
RAIN = rainfall intensity;
MTD = mean texture depth, which is obtained by using the sand-patch method or arithmetic average of the macrotexture profile;
CSLP = cross slope;
TD = tire tread depth; and
V_c = critical hydroplaning speed.

USE OF THE PROGRAM

MAPCON, which can perform the computation discussed previously, is written for batch processing computers. The user must prepare the input card deck or its equivalent to run the program. Among the several choices in the analysis, the user can specify which model (PSU model I, II, or III) is to be used for estimating SN_0 and PNG and can indicate whether the seasonal adjustment is to be made. A common choice is set as the default. The typical values of the coefficients of the regression equation can be changed by the user as better data become available. The user has only to specify keywords to the desired choice, the variable names, and values for the input quantities. The output will echo these choices and selected options and print the computed results in an organized fashion in both SI and U.S. conventional units. The results of the data processing will estimate the skid number-

Figure 2. Examples of skid-resistance analysis.

Example 1

Input

skid numbers	sliding velocities (km/hr)
60	20
56	30
50	40
46	50

model: PSU model I

seasonal adjustment: none

Output

SN_0 = 72.5   PNG = 0.91 hr/km

SFC = 50.3 at 7° yaw angle

SN_{64} = 71.59

for given velocity 27 km/hr SN = 56.70

for SN = 65. the corresponding velocity = 12 km/hr

Example 2

Input

model: PSU model II

one (SN,V) pair: SN = 35, and velocity = 30 km/hr

texture data: MTD = 15 mm

seasonal adjustment: none

Output

SN_0 = 36.3   PNG = 0.126 hr/km

SFC = 34.56 at 7° yaw angle

SN_{64} = 33.48

Example 3

Input

model: PSU model III

texture data: MTD = 15 mm   BPN = 65.

seasonal adjustment: none

Output

SN_0 = 50.9   PNG = 0.126 hr/km

SFC = 48.39 at 7° yaw angle

for given velocity 60 km/hr SN = 47.19

for SN = 35. the corresponding velocity = 297.2 km/hr

for SN = 45. the corresponding velocity = [illegible]7.7 km/hr

sliding velocity relation, side force coefficients, and critical hydroplaning speed by using several possible combinations of inputs through various analyses. Figure 2 shows the output for three example runs.

CONCLUSION

A methodology is presented for skid-resistance analysis. It has been developed as part of the MAPCON computer program for the Federal Highway Administration for use by transportation agencies in the management of highway pavements. The program brings together recent research results. The equations and their coefficients are integrated into the computer program in such a manner that they may be modified to suit the user's needs or to accommodate improvements from future research.

ACKNOWLEDGMENT

The research described in this paper was conducted as part of the Federal Highway Administration research project, Methodology for Analyzing Pavement Condition Data. Rudolph R. Hegmon served as contract monitor of this project, and his assistance is greatly appreciated.

REFERENCES

1. J.J. Henry and W.E. Meyer. The Simulation of Tire Traction on Wet Pavements. 18th International Congress, Fédération Internationale des Societiés d'Ingénieurs des Techniques de l'Automobile, Hamburg, West Germany, May 1980.
2. B.J. Hill and J.J. Henry. Surface Material and Properties Related to the Seasonal Variations in Skid Resistance. ASTM, Washington, DC, STP763, Jan. 1982, pp. 45-60.
3. B.J. Hill and J.J. Henry. Short-Term Weather-Related Skid Resistance Variations. TRB, Transportation Research Record 836, 1981, pp. 76-81.
4. J.J. Henry. Use of Blank and Ribbed Test Tires for Evaluating Wet-Pavement Friction. TRB, Transportation Research Record 788, 1981, pp. 1-6.
5. B.M. Gallaway and others. Tentative Pavement and Geometric Design Criteria for Minimizing Hydroplaning. Federal Highway Administration, Rept. FHWA-RD-75-11, Feb. 1975.
6. 1980 Annual Book of ASTM Standards. ASTM, Washington, DC, Part 15, 1980.

Publication of this paper sponsored by Committee on Surface Properties-Vehicle Interaction.

Ontario Flexible Pavement Distress Assessment for Use in Pavement Management

W.A. PHANG AND G.J. CHONG

The method used in Ontario to assess the condition of the pavement at any time is described. The condition rating assigned is based on subjective judgment of riding quality and the appearance of rutting and distortion, surface defects, and cracks. The guidelines used for assisting the rater in the assessment process include typical descriptions of eight different stages in the life of a pavement and a catalog of photographs and descriptions. A more objective method is also described for calculating the pavement condition rating from measured roughness values and from the standard terms used to describe the visual observations of distress. The weighting for distresses used in these calculations was established from iterative correlations with subjective condition ratings. The condition rating and the description of distresses are used in determining suitable alternative maintenance and rehabilitation treatments, in setting their priority order, and in formulating rehabilitation programs.

The aim of pavement management is to make optimum use of the available funds to maintain a highway network that provides safe and comfortable passage to vehicles that carry persons and goods. Periodic assessments of pavement condition are essential ingredients of this management process. Ontario's method for assessing pavement condition relies on an examination of two principal features of the pavement to arrive at a pavement condition rating (PCR) for a stretch of road--riding quality and distress manifestations.

The riding quality of the pavement is rated subjectively on a riding comfort rating (RCR) scale from 0 to 10, where 10 represents a perfectly smooth surface, and 0 is a very rough, almost impassable, road. To assess RCR the rater travels in a passenger car at a standard speed of 80 km/h. The rater is usually the driver, and the vehicle is normally one with which he or she is familiar (1).

The distress manifestations (DMs) of the pavement surface are assessed after inspection of the length of road that is to be rated and in light of the descriptions of what is observed. Uniform word sets are used to represent scales for density of occurrence and severity of various distresses. DM is the sum of all types of distresses, weighted for density of occurrence and severity.

This paper describes the assessment method and how PCRs are used in Ontario for rehabilitation and

Figure 1. Alligator cracking.

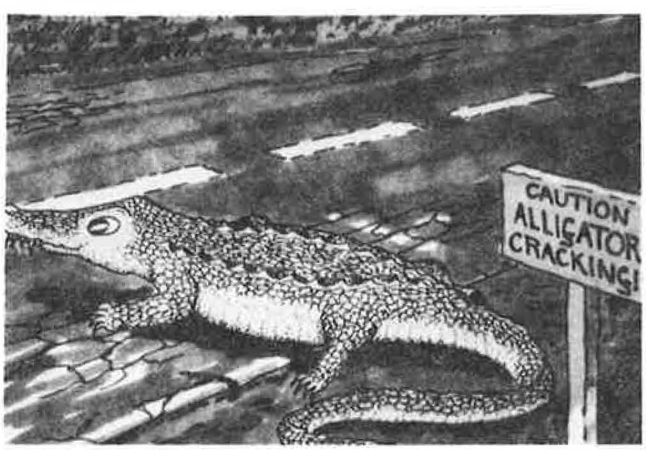

maintenance and in setting project priority order and programming.

ASSESSMENT METHOD

The assessment method (1) answers four simple questions:

1. What is the problem?
2. What causes the problem?
3. How bad is the problem? and
4. How big is the problem?

Consider the distressing situation of alligator cracking (Figure 1). First, the distress type is identified by comparison with catalog photographs of various distresses, which are accompanied by word descriptions of physical appearances and brief summaries of why it happens (see Figure 2). Next, the question of how bad is answered by describing the distress severity in one of these simple terms--Very Slight, Slight, Moderate, Severe, and Very Severe. The correct answer may be chosen by comparing the problem with the catalog photographs and descriptions (see Table 1). A catalog of photographs that shows the different stages of distress is contained in a manual describing their use in the assessment of PCR (1).

The question, "How big is the problem?", is answered by describing the density of occurrence of the distress by using the words few, intermittent, frequent, extensive, or throughout. These words refer to percentages of length or area of the road section that is being rated.

Class	Uniform Description	Guide (%)
1	Few	<10
2	Intermittent	10-20
3	Frequent	20-50
4	Extensive	50-80
5	Throughout	80-100

An example of a word description of a distress may be, "Severe alligator cracking occurs intermittently over the section."

The DMs are classified into four broad categories:

1. Surface defects such as coarse aggregate loss, raveling, and flushing;
2. Surface deformation such as rippling, shoving, rutt~~ing,~~ and distortion;
3. Cracking such as longitudinal, transverse, random, edge, alligator, and so on; and
4. Patching of distressed areas that indicates past problems; the type and extent of patching may give clues as to the underlying problems that need to be considered when rehabilitation is being planned and designed.

PCR is the final result of the combined assessment of RCR and DM. PCR is on a scale from 0 to 100. To aid in the assessment, eight stages in the life of a typical flexible pavement have been identified by word descriptions of riding quality, distortion, and distress, and a range of rating numbers

Figure 2. Sample page from distress catalog.

Description: - Cracks which form a network of multisided (polygon) blocks resembling the skin of an alligator. The block size can range from a few inches across to about two feet. The block size is indicative of the level (depth) at which failure is taking place. The small block sizes, 4 to 6 inches, indicate that movement is occuring in the upper (granular base) layer; this type of alligatoring is mostly observed on "thin" (less than 3 inches) asphalt surfacings, accompanied at times by slight depressions (perhaps ½ inch). See Figures 51, 52 and 53. The large block sizes, 12 inches and more, indicate that movement is occuring in the deeper layers and subgrade; this type of alligatoring is accompanied by large depressions (perhaps as much as 2 inches) together with a lateral movement outwards (and upwards) of the pavement edge; forms a "bird-bath" during rains. See Figures 54 and 55.

- Alligatoring is a consequence of the inability of a part of the structure to support the repeated loads due to a "softening" of the material. "Softening" is normally associated with an increase in moisture content.

- Alligator failures which are deep-seated in the subbase or base, are progressive, i.e. under traffic, and rains, they tend to spread rapidly, and traffic causes blocks of surfacing to be displaced and broken up. The only successful remedial treatment is the removal of all softened material in the affected area and replacement with sound granular material. Alligator failures which are in the upper layers, normally appear in the very early spring. They do not generally progress after warmer weather first appears, probably because drainage of the wet granular bases has increased its' strength.

Possible Causes: (1) Insufficient bearing support.
(2) Poor base drainage and stiff or brittle asphalt mixes at cold temperatures.

Example: *-Moderate Alligator cracking occurs frequently in outer wheel track.*

Figure 51, Alligator Crack

Figure 52, Alligator Crack

[Result of movement occuring in the upper (granular base) layer.]

Table 1. Guide for describing severity of pavement alligator cracking.

Class	Description	Guide[a]	Figure
1	Very slight	Alligator pattern just formed; distortion less than 1/2 in	
2	Slight	Alligator pattern established with corners of polygon blocks fracturing; distortion 1/2 in plus	56
3	Moderate	Alligator pattern established with spalling of polygon blocks; distortion 1/2 in plus	57
4	Severe	Polygon blocks begin to lift; distortion 1 in plus patching required	58
5	Very severe	Complete disintegration of affected area, potholes from missing blocks; more than 2 in distortion; immediate repair required	59

[a]Based on surface appearance. In describing the severity of alligator cracking, the characteristics of the alligator crack must also be described in terms of block size. Actual dimensions estimated to the nearest inch should be used (e.g., "Moderate alligator cracking with block size approximately 6 in overall").

Table 2. Guide for estimating PCR and priority for flexible pavements.

Treatment	Rating	Description
Reconstruct within 2 years	0-20	Pavement is in poor to very poor condition with extensive severe cracking, alligator cracking, and dishing; rideability is poor and surface is very rough and uneven
Reconstruct in 2-3 years	20-30	Pavement is in poor condition with moderate alligator cracking and extensive severe cracking and dishing; rideability is poor and surface is very rough and uneven
Reconstruct in 3-4 years	30-40	Pavement is in poor to fair condition with frequent moderate alligator cracking and extensive moderate cracking and dishing; rideability is poor to fair and surface is moderately rough and uneven
Reconstruct in 4-5 years or resurface within 2 years with extensive padding	40-50	Pavement is in poor to fair condition with frequent moderate cracking and dishing and intermittent moderate alligator cracking; rideability is poor to fair and surface is moderately rough and uneven
Resurface within 3 years	50-65	Pavement is in fair condition with intermittent moderate and frequent slight cracking, and with intermittent slight or moderate alligator cracking and dishing; rideability is fair and surface is slightly rough and uneven
Resurface in 3-5 years	65-75	Pavement is in fairly good condition with frequent slight cracking, slight or very slight dishing, and a few areas of slight alligator cracking; rideability is fairly good with intermittent rough and uneven sections
Normal maintenance only	75-90	Pavement is in good condition with frequent very slight or slight cracking; rideability is good with a few slightly rough and uneven sections
No maintenance required	90-100	Pavement is in excellent condition with few cracks; rideability is excellent with few areas of slight distortion.

appropriate to each stage has been assigned (see Table 2).

How Is Assessment Performed?

To make an assessment the rater first drives at the standard 80 km/h over the pavement and determines the riding quality. He or she then drives along the shoulders at slow speed (not to exceed 40 km/h) to observe the cracks and other distresses. Frequent stops are made to examine and measure particular distresses. At the end, he or she summarizes his or her impressions by placing check marks in the appropriate boxes of a condition rating checklist (Figure 3).

The rater then compares a summary description compiled from the checklist against the standard descriptions of the eight condition stages (column 3, Table 2) and decides which stage most closely fits the pavement being rated and whether it is closer to the top or bottom of the range. The rater then assigns, on a scale of 0 to 100, a PCR value to the rated pavement.

The rater also has to consider what and when rehabilitation may be needed (column 1, Table 2). For example, resurfacing within 2 years. He or she is thus alerted, at the time of inspection, to the need for closer examination where necessary, in order to make recommendations for remedial measures (2). For example, padding and leveling course plus one lift overlay may be the recommended treatment.

The PCR assessment is made by one, two, or more people, as are available for the task. PCR is the average value from these raters. The assessments are made in each of the five regions of the province by the engineering staff of the geotechnical office.

Assessments are generally made in late spring and early summer. Training circuits are established in the regions to maintain the standard assessment procedures through periodic calibration of staff members (Figure 4). The circuits are also used for training of new and inexperienced staff members.

Distress Index As an Alternative to PCR

A more objective method of assessing the PCR value of a pavement section, which can use measured ride roughness and the word descriptions of pavement distress to calculate a numerical value known as the distress index (DI), is under development. This alternative method of assessment is intended to minimize personal bias by raters. DI is determined by combining the RCR component with the DM component in accordance with this equation:

$$DI = 100(0.1RCR)^{1/2} \times [(320 - DM)/320] \quad (1)$$

Development of this methodology is reported elsewhere (2).

Essentially, RCR is the riding quality, which might be a measured quantity, converted to a scale of 0 to 10, through a correlation equation; e.g., RCR = a + b log 'Q' (3). DM, on the other hand, is the sum of defects obtained by summing the products of the sum of the density and severity weights, multiplied by the weight for the distress type. The equation shows that

$$DM = \sum_{i=1}^{27} C_i(S_i + D_i) \quad (2)$$

where

C_i = weighting value for a particular type of crack or other form of pavement distress (see Table 3),

S_i = Weighting value for severity of crack or other form of distress (see Table 4), and

D_i = weighting value for density of occurrence of the particular crack type or other form of distress (see Table 4).

The probable maximum value of DM is 320.

Figure 3. Flexible pavement condition checklist form.

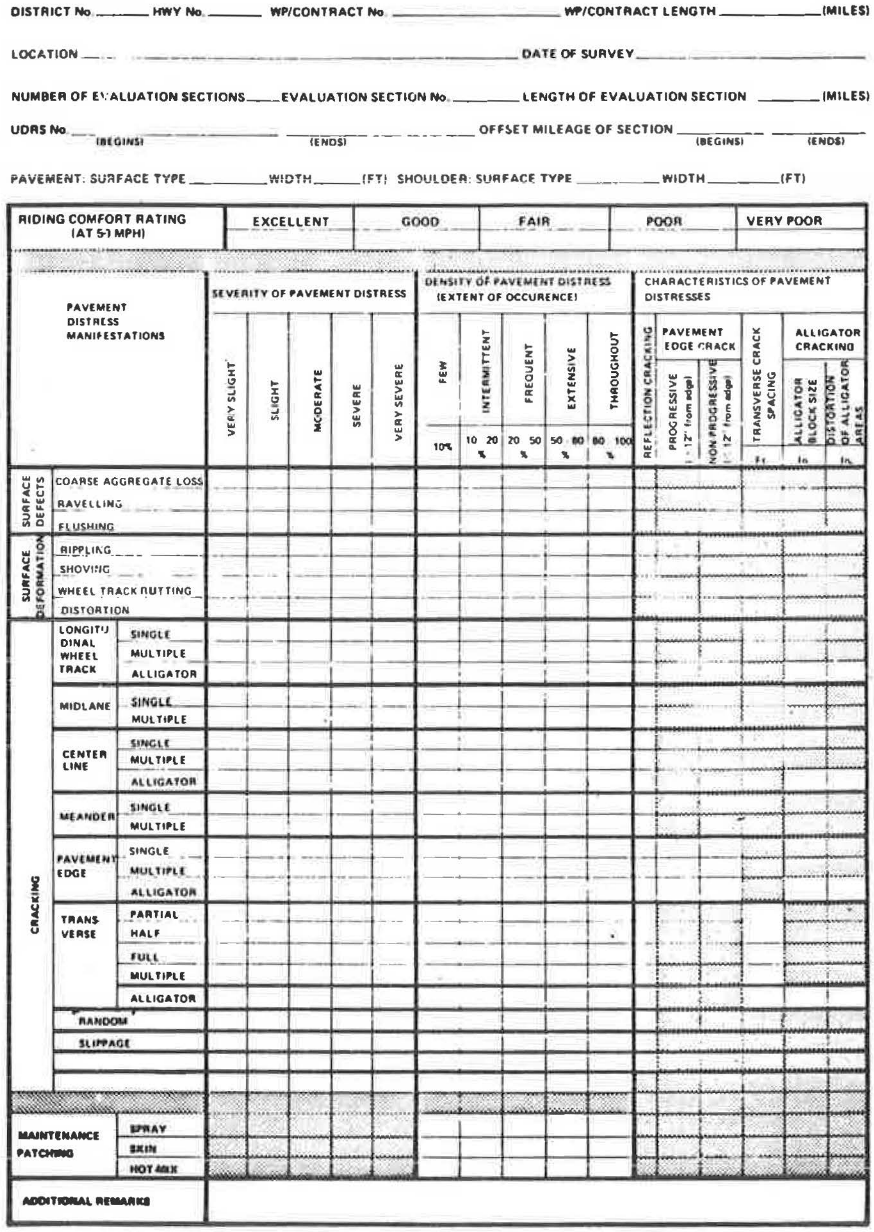

This new methodology is being developed so that a more-systematic way of combining riding quality and pavement distress may result in more consistent and unbiased ratings for use in priority planning and optimum effectiveness. The effect of DM on DI was investigated (4). The result indicates that, on a provincewide basis, DM values are generally less than 100 and the effect on DI does not exceed 30 percent (see table below).

DM	Effect on DI (%)
20	6
40	12
60	19
80	25
100	32

Since DI is a function of roughness as well as distress, we must conclude that roughness is much more important in the measurement of pavement serviceability (PCR) than is distress and that distresses that affect roughness are much more significant than distresses that do not.

Additional evidence to support the second conclusion are the high weighting values determined for surface distortion, rutting, and alligator cracking longitudinally in wheel tracks and at transverse cracks. These weightings were determined after iterative examination of a large number of PCR correlations with DI, RCR, and DM. Figure 5 shows an example plot of the correlation of calculated DI (represented by asterisks) with subjective PCRs.

PCR DATA BANK

PCR data that are collected by the regions are reported either as the work is completed or on an annual basis. These reports are entered in a computerized data bank and an updated summary report is produced that captures the salient features of individual reports. An example is shown in Figure 6. The computer printout of the summary report serves as a ready reference of pavement condition and as a basis for developing an overall picture of system

Figure 4. Typical sections included in training circuits.

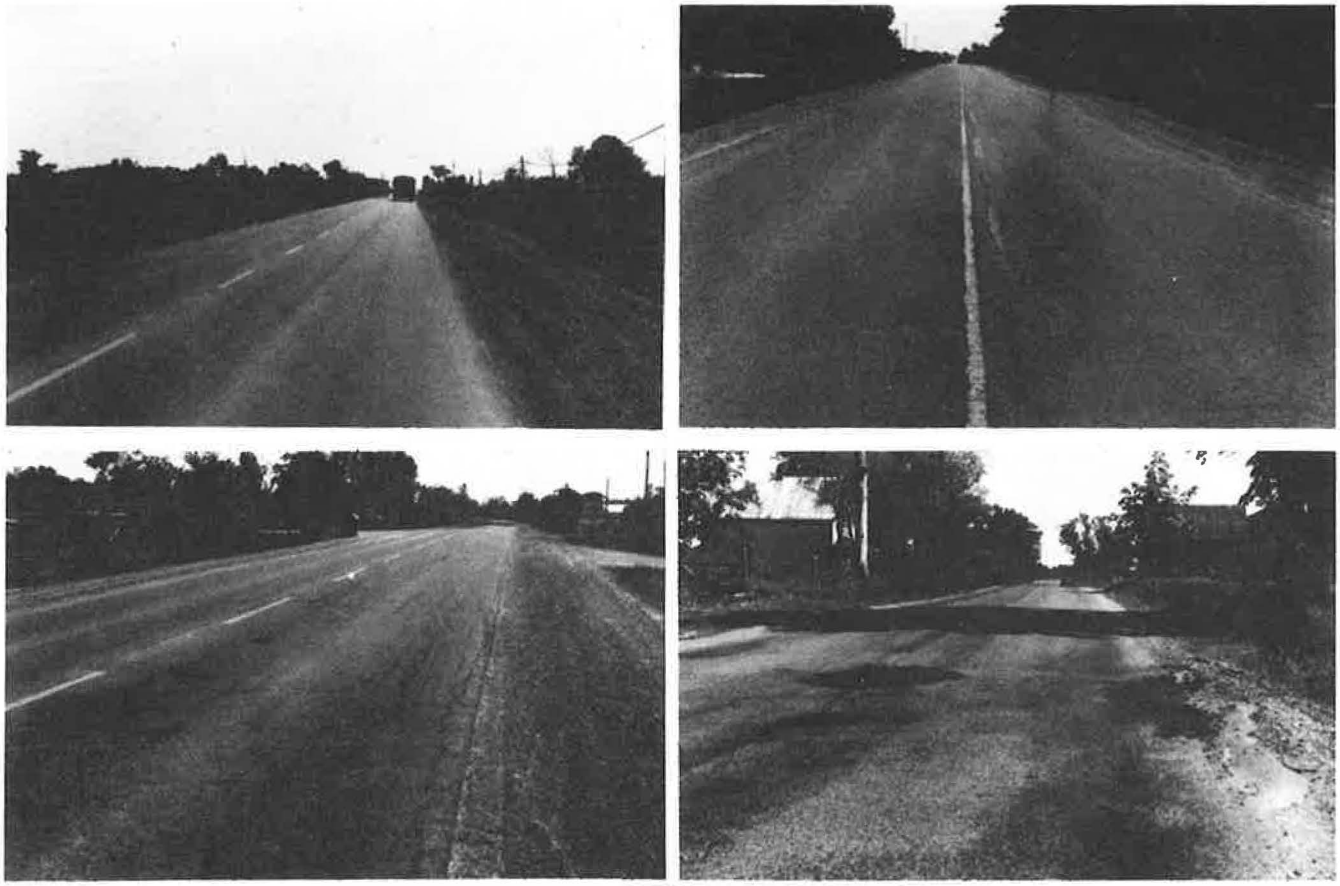

Table 3. Distress weighting factors and description codes.

Pavement Condition	Pavement Distress Manifestations: Description	Cracking	Code	Weighting Value (C_i)
Surface defects	1. Coarse aggregate loss		CA	3.0
	2. Raveling		RA	3.0
	3. Flushing		FL	0.5
Surface deformation	4. Rippling		RI	0.5
	5. Shoving		SH	0.5
	6. Wheel track rutting		WR	3.0
	7. Distortion		DT	3.0
Cracking	8. Longitudinal wheel track	Single	S/LWT	1.0
	9.	Multiple	M/LWT	1.5
	10.	Alligator	A/LWT	3.0
	11. Mid lane	Single	S/ML	0.5
	12.	Multiple	M/ML	1.0
	13. Center lane	Single	S/CL	0.5
	14.	Multiple	M/CL	1.0
	15.	Alligator	A/CL	2.0
	16. Meander	Single	S/ME	0.5
	17.	Multiple	M/ME	1.0
	18. Pavement edge	Single	S/PE	0.5
	19.	Multiple	M/PE	1.0
	20.	Alligator	A/PE	1.5
	21. Transverse	Partial	P/TRV	0.5
	22.	Half	H/TRV	0.5
	23.	Full	F/TRV	0.5
	24.	Multiple	M/TRV	2.0
	25.	Alligator	A/TRV	3.0
	26. Random		RD	0.5
	27. Slippage		SL	0.5

condition and system needs (e.g., color-coded maps).

PCR in Pavement Management

PCRs are used to develop priority lists for rehabilitation work (i.e., pavement management at a network level). These lists are accompanied by estimated cost figures that improve from ballpark figures through preliminary design cost estimates to estimated costs after design, depending on planning and programming needs, as shown in Figure 7.

Other factors beside the available budget and policy issues influence the composition of a construction program, such as those listed in Figure 8. A fully developed pavement management system would have examined all of the alternatives as well as their costs to obtain the optimum effectiveness of the program. Unfortunately, we do not have such a process in place; we do, however, have a process that uses optimum designs for individual projects in the program.

At a project level, when alternative rehabilitation designs must be considered, a knowledge of the presence (or absence) of the various types of DMs and their rates of change with respect to traffic and time is a valuable asset in the design process. Certain distresses denote drainage and frost heave problems that must be corrected. Other distresses indicate structural inadequacies, and yet others point to problems with materials.

Other Uses of PCR

PCR assessments and planning and programming job

Table 4. Severity and density weights and description codes.

Weight (D_i or S_i)	Severity: Description	Code	Rut Depth (cm)	Crack Width[a] (cm)	Density: Description	Code	Percentage of Area Length
0	Very slight	0	<0.5	<0.7	Few	5	<10
1	Slight	1	0.5-1	0.7-1	Intermittent	6	10-20
2	Moderate	2	1-2	1-2	Frequent	7	20-50
3	Severe	3	2-5	2-3	Extensive	8	50-80
4	Very severe	4	>5	>3	Throughout	9	>80

[a]For cement-treated base use 0.3 instead of 0.7.

Figure 5. PCR versus calculated DI.

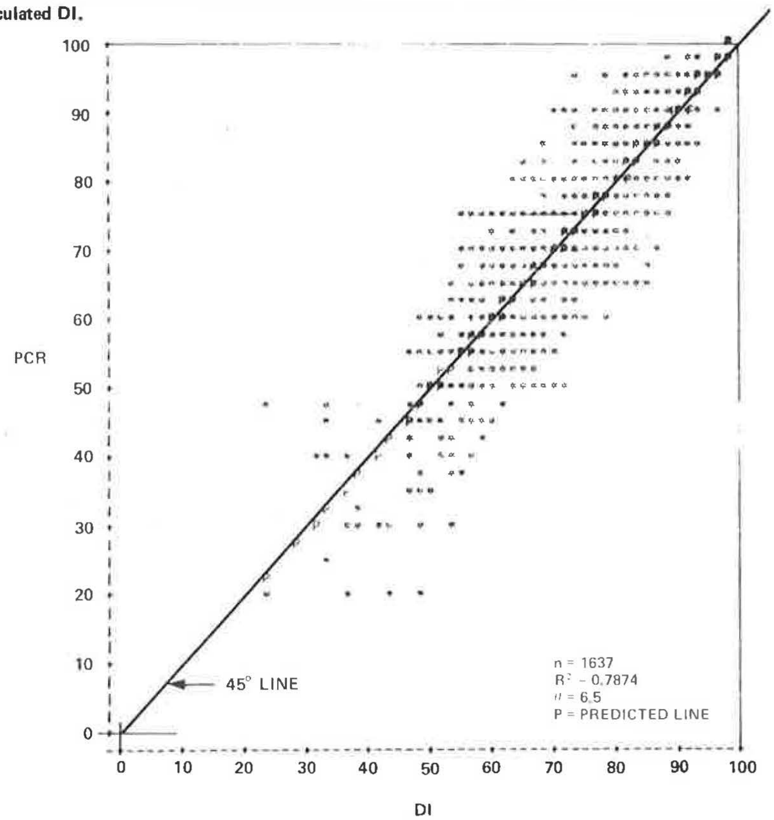

listings are used by maintenance staff on the development of overall corrective maintenance plans and preventive maintenance programs. For example, candidates for preventive maintenance can be identified from their expected performance or PCR history, as shown in Figure 9 (5). The distress assessment method, in a simplified category formulation, has been used to develop guidelines to enable the maintenance patrol to decide which of the various alternative corrective maintenance treatments available is the most cost effective (6,7).

FURTHER DEVELOPMENTS

Recent developments in the field of automation of data collection promise the availability of more timely pavement condition data than are currently available. One piece of equipment that was developed by a company in Ontario, working in conjunction with the provincial highway organization, is the automated road analyzer (ARAN) (8). ARAN measures and records on magnetic tape the following:

1. Road roughness (accelerometer),
2. Distress manifestations (visual) through keyboard entry,
3. Transverse profile (acoustic),
4. Surface texture (radar technology), and
5. Alignment (gyroscope).

These are complemented by a series of computer graphic output formats.

The company offers services to process, store, and manipulate the data and to provide optimized programs for corrective maintenance and rehabilitation. They will even estimate quantities of padding and leveling courses needed for rehabilitation. The services of the company have been used by several municipalities and regional and provincial roads authorities in Canada and recently in the United States, where the benefits of pavement management are beginning to be appreciated.

CONCLUDING REMARKS

Ontario chose a subjective route to assess its pavements because during the last two decades of considerable highway construction activity there was no lack of skilled and experienced personnel. But shrinking budgets and rising costs point toward more automation of data collection and processing as the way of the future. We have gone a long way toward development of the technology.

Figure 6. Example of PCR-DI data bank output.

```
DATE RUN : 81 09 03                              FLEXIBLE  PAVEMENT  CONDITION  REPORT                                        PAGE    77
                                          T E S T   D A T A    I N    S E P T E M B E R .     1 9 8 1

  OFF     LENG     PCR      RCR     DI       DM     AGE     SURVEY     AADT    SURFACE     SURFACE        CRACKING                       PATCH  URCY DIR
  SET                                                       DATE               DEFECTS     DEFORMATION                                          RATE
                                                            YR MO              CA RA FL    RI SH WR DT    LWT  ML  CL  MEA  PE  TRV   I   D

REGION    : SOUTHWESTERN-LONDON                   HIGHWAY NO. :  86

LHRS NO. : 38230          SECTION LENGTH : 12.9     DESCRIPTION : MACTON-WATERLOO RD 5
   5.5     7.6     50      4.0     51     52.0     14     81  5     3700    29 45 00    00 00 00 15    S16 S15 A26  00 A15 F29    1  7      0
   5.5     7.6     50      3.7     55     56.0     13     80 10     3350    29 25 05    00 00 19 15    S16 S05 S26  00 A15 F29    1  9      0
   5.5     7.6     58      4.2     55     46.0     11     78  3     3600    29 00 00    00 00 29 00     00  00 S15  00 S15 F29    1 10      0

LHRS NO. : 38240          SECTION LENGTH : 11.1     DESCRIPTION : TRALEE-HWY 19
   0.0    10.1     80      7.8     82     38.0      3     80  6     5000    19 00 00    00 00 09 00     00 S15 S17 S16 S06 F19    0  0      3

LHRS NO. : 38260          SECTION LENGTH : 20.1     DESCRIPTION : W JCT HWY 23
   0.0    10.0     55      6.0     61     69.0     18     79 11     3300    09 19 00    00 00 19 16    S28 S26 S29 S25 S26 F29    1  6      4
  10.0    10.1     50      5.0     56     65.0     18     79 11     3300    19 19 00    00 00 19 15    S27 S15 S28  00 M15 F29    1  6      4

LHRS NO. : 38270          SECTION LENGTH :  6.4     DESCRIPTION : HURON RD 12(TO WROXETER)
   0.0    13.0     95      9.0     88     20.0      5     78 11     3250    09 06 00    00 00 00 00    S05 S25 S15  00 M25 F15    0  0      0

LHRS NO. : 38300          SECTION LENGTH :  9.2     DESCRIPTION : WINGHAM-JOSEPHINE ST-HWY 4
   0.0    16.6     88      7.5     80     40.0      5     80  7     2600    19 16 00    00 00 07 15     00 S15 S26 S25 S16 F18    0  0      0
   0.0    16.7     95      9.0     88     20.0      3     78 11     2900    09 06 00    00 00 00 00    S05 S15 S25  00 S15 F16    0  0      0

LHRS NO. : 38320          SECTION LENGTH : 10.6     DESCRIPTION : LUCKNOW-HAVELOCK ST-BRUCE RD 1
   0.8    18.1     75      7.0     77     41.5      4     80  7     1300    19 00 25    17 00 07 17    S15 S15 S26 S25 S15 F17    0  0      0
   0.8    18.1     76      7.5     89     10.5      3     79  6     1250    05 00 00    00 00 00 00     00  00 S25  00 S15 F29    0  0      0
```

Note: 1 — LHRS - Linear Highway Reference System —

Numbers are given to node points i.e. intersections, political boundaries, etc.
A length of road is defined by an LHRS number and offset distance, and by the length of the section.

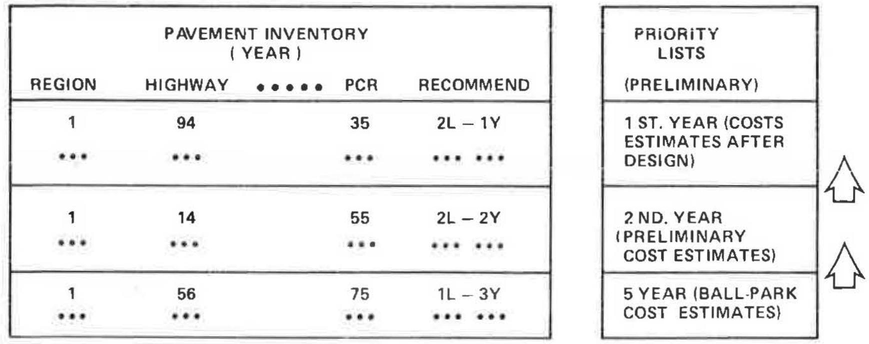

Figure 7. Stages in setting priority of rehabilitation projects.

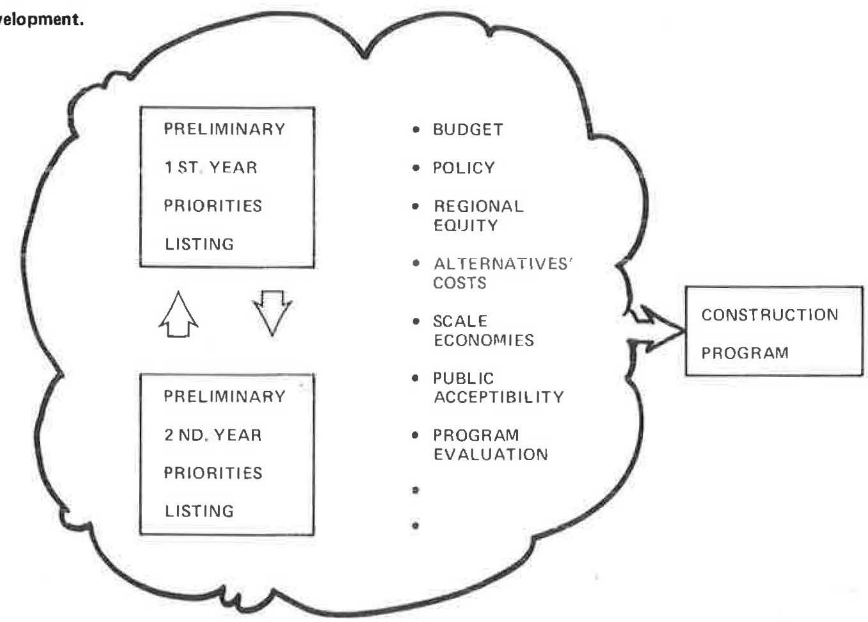

Figure 8. Other factors that influence program development.

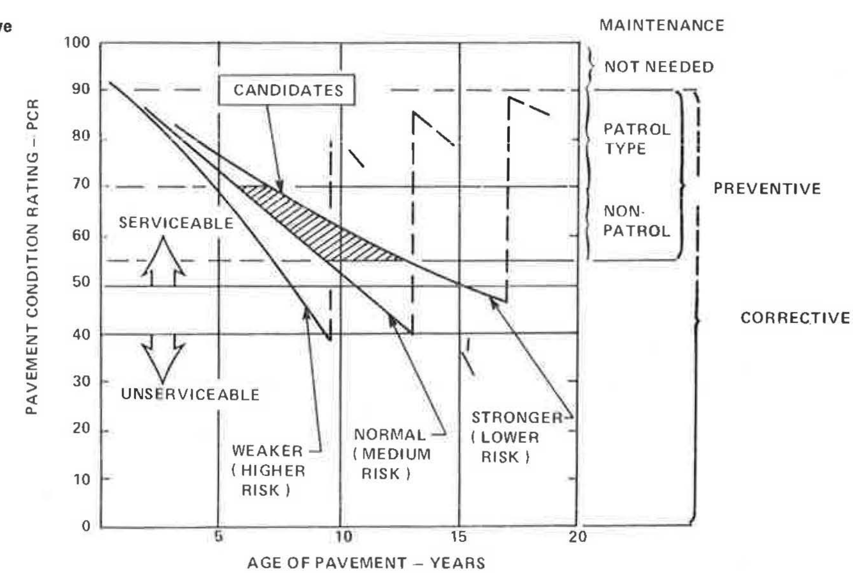

Figure 9. Identification of candidates for preventive maintenance.

REFERENCES

1. G.J. Chong, W.A. Phang, and G.A. Wrong. Manual for Condition Rating of Flexible Pavements--Distress Manifestations. Ontario Ministry of Transportation and Communications, Downsview, Aug. 1975.
2. W.A. Phang. Pavement-Condition Ratings and Rehabilitation Needs. TRB, Transportation Research Record 700, 1979, pp. 11-19.
3. G. Chong. Measurement of Road Rideability in Ontario. Ontario Ministry of Transportation and Communications, Downsview, Rept. IR29, March 1969.
4. W.A. Phang. Pavement Condition and Performance Observations--Brampton Test Road. Presented at Assoc. of Asphalt Paving Technologists meeting, San Diego, 1981.
5. W.E. Blum and W.A. Phang. Preventive Pavement Maintenance Concepts. Ontario Ministry of Transportation and Communications, Downsview, PAV-80-04, Jan. 1981.
6. G.J. Chong, W.A. Phang, and F.W. Jewer. Choosing Cost-Effective Maintenance. TRB, Transportation Research Record 800, 1981, pp. 41-47.
7. G.J. Chong, F.W. Jewer, and K. Macey. Pavement Maintenance Guidelines--Distresses, Maintenance Alternatives, and Performance Standards. Ontario Ministry of Transportation and Communications, Downsview, Rept. SP-001, Sept. 1980.
8. D.H. Kobi. ARAN Road Analyzer. Paper presented at 60th Annual Meeting, TRB, 1981.

Publication of this paper sponsored by Committee on Pavement Condition Evaluation.

Airfield Pavement Distress Measurement and Use in Pavement Management

M.Y. SHAHIN

This paper describes airfield pavement distress measurement and use procedures that were developed for the U.S. Air Force. The procedures have been implemented by the U.S. Air Force and published by the Federal Aviation Administration. Distress identification, distress data collection procedures, distress data processing, and distress data analysis and use in pavement management are discussed. The paper also describes the pavement condition index (PCI), which is computed based on distress type, severity, and amount. The PCI is measured on a scale from 0 to 100, with 100 being excellent. Both the distress data and PCI provide an invaluable tool for pavement evaluation, determination of maintenance and repair needs, and management at both the project and the network levels.

The majority of existing airfield pavements is approaching their economic design life, so a great need exists for pavement management. A primary component of pavement management is pavement condition evaluation. Figure 1 presents the major pavement condition indicators (PCIs) for airfield pavements. These indicators include roughness, skid resistance, structural integrity and capacity, and the potential for damage from foreign objects. Field experience has shown that most of these condition indicators can be measured through objective and accurate measurement of distress. Figure 1 also shows how the various distress types in asphalt pavements relate to the various pavement condition indicators. Many pavement engineers think that a distress survey should be performed before a direct measurement of the condition indicators (e.g., structural capacity) is recommended.

This paper describes airfield pavement distress measurement and use procedures that were developed for the U.S. Air Force. The procedures have been implemented by the U.S. Air Force and published by the Federal Aviation Administration (FAA).

DISTRESS IDENTIFICATION

An accurate distress characterization should include three parameters: distress type, severity, and quantity. The lack of any of these parameters will produce an unrepeatable and inconsistent distress characterization. A comprehensive distress manual, which identifies various distress types in both asphalt- and concrete-surfaced pavements, has been developed for the U.S. Air Force (1). FAA has also published the same manual in a technical report (2). Figure 2 (1,2) is an example distress definition for rutting. For each distress type a description is provided that includes the possible causes of distress. Three levels of severity are defined: low, medium, and high. Photographs of each level of severity are also provided. The use of the distress identification manual has provided accurate and consistent distress survey results.

DISTRESS DATA COLLECTION PROCEDURES

The first step in the distress data collection procedures is to divide the airfield pavements into uniform features based on construction, condition, and traffic. Figure 3 shows an airfield layout map with pavements divided into features. For the purpose of inspection each feature is divided into sample units. A sample unit is defined as approximately 5000 ft² for asphalt-surfaced pavements and approximately 20 slabs for jointed concrete-surfaced pavements. When the inspection is performed, each sample unit may be surveyed or inspection may be performed by sampling. For inspection by sampling, both the number of sample units to be surveyed and their locations should be determined. A procedure to do so has been developed and used successfully (1). The number of sample units to be inspected is a function of the level of reliability desired in the data collected. This in turn is a function of the objective of the survey (i.e., whether the survey is performed for developing a project for that pavement or only for the purpose of identifying the overall condition of the airfield pavement network). If the objective is the latter, then only a few sample units may suffice; however, if the objective is to use the distress information in developing a project, then more sample units should be surveyed.

Figure 4 shows a field data sheet for asphalt pavements that is used when surveying a sample unit. The numbers shown in circles are the distress types. In this example they are distress types 1 (alligator cracking) and 3 (block cracking). Under each distress type the quantity of distress encountered is recorded, followed by the severity level. For example, 20L indicates that there were 20 ft^2 of low-severity alligator cracking. After the field survey, the data are then totaled.

The distress data can be collected manually or by using automated methods.

Manual Distress Collection

For manual distress collection the survey is performed by a crew that usually consists of two or three persons. The crew walks the pavement and, through the use of simple tools such as a measuring wheel, straight edge or rope, and a ruler, identifies the distress types and severities that exist in each sample unit. The rope or straight edge is used to determine depths of surface deformations such as rutting and depression.

Automated Data Collection

The automated data collection procedures presented here have been used in Japan for the last 10 years. They have been developed by the Pacific Aero Survey Company, Ltd. (PASCO) (3). Two systems are presented here. The first is known as Road Recon-70. The Road Recon-70 is capable of photographing pavements at night while traveling at speeds of up to 45 mph. One advantage of using the system is that the condition of the pavement is recorded on film for future use and reference. The second system used by PASCO is the Rut Depth-75 (RDP-75). The RDP-75 [Figure 5 (3)] is used to measure rut depth at preselected intervals. It uses the same vehicle, power source unit, power control unit, and camera supporting unit as the Road Recon-70. The RDP-75, however, uses a pulse camera and a power source unit and hairline projector that are all mounted on the vehicle. The camera shutter intervals are correctly controlled through the pulse signal transmission device in accordance with the traveling speed of the vehicle. The RDP-75 system is patented in the United States and several other countries.

DISTRESS DATA PROCESSING

The distress type, severity, and amount collected for each sample unit are used to compute PCI. The PCI (Figure 6) is measured on a scale of 0-100, with

Figure 1. Relation between pavement condition indicators and distress types for asphalt airfield pavements.

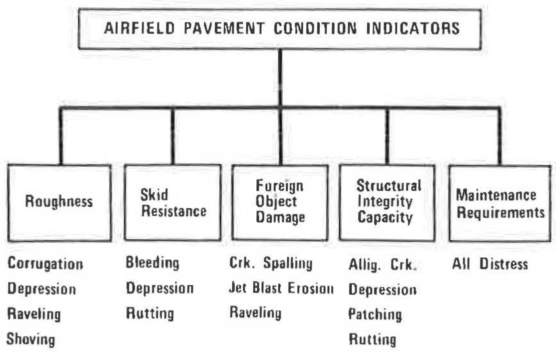

Figure 2. Example distress definition for rutting.

Name of Distress: Rutting

Description: A rut is a surface depression in the wheel paths. Pavement uplift may occur along the sides of the rut; however, in many instances ruts are noticeable only after a rainfall, when the wheel paths are filled with water. Rutting stems from a permanent deformation in any of the pavement layers or subgrade, usually caused by consolidation or lateral movement of the materials due to traffic loads. Significant rutting can lead to major structural failure of the pavement.

Severity Levels: Mean Rut Depth Criteria

Severity	All Pavement Sections
L	¼-½ inch (Figures A1-58, A1-59)
M	>½ 1 inch (Figure A1-60)
H	>1 inch (Figures A1-61, A1-62)

How to Measure: Rutting is measured in square feet of surface area, and its severity is determined by the mean depth of the rut. To determine the mean rut depth, a straightedge should be laid across the rut and the depth measured. The mean depth in inches should be computed from measurements taken along the length of the rut.

Figure 3. Airfield layout showing different pavement features.

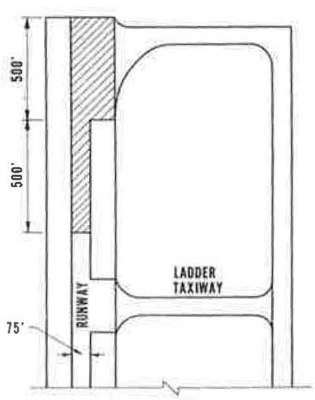

Figure 4. Sample field data sheet for asphalt pavements.

DISTRESS TYPES

1. Alligator Crack
2. Bleeding
3. Block Crack
10. Patching
11. Polished Agg
12. Raveling

	Existing Distress Types			
	1	3		
	20L	100L		
	30L	150M		
L	50	100		
M		150		
H				

100 being excellent. It is computed by using the concept of deduct values. A series of deduct values has been developed for each distress type, as shown in Figure 7. The deduct values for each distress existing in the pavement are determined from such

Figure 5. Rut depth measurement system RDP-75 used by PASCO.

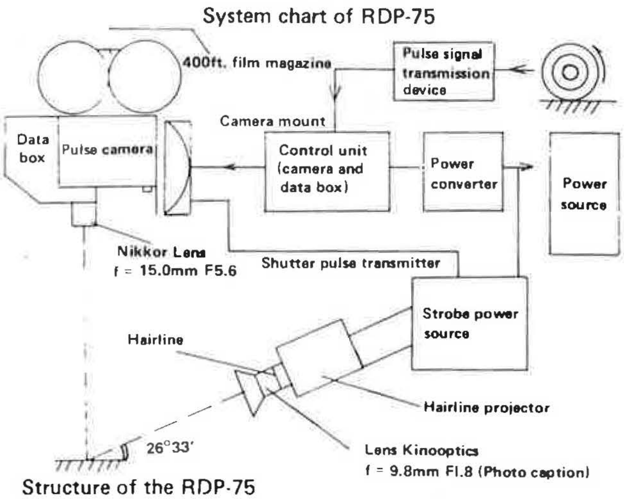

Figure 6. PCI rating system.

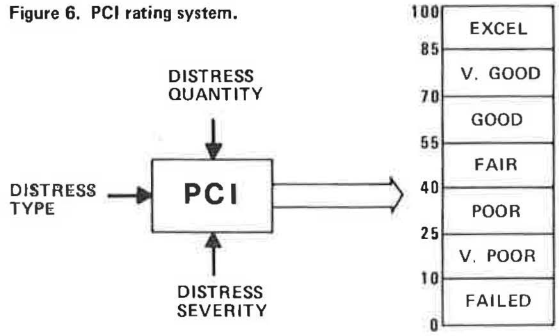

Figure 7. Example deduct values for one distress type.

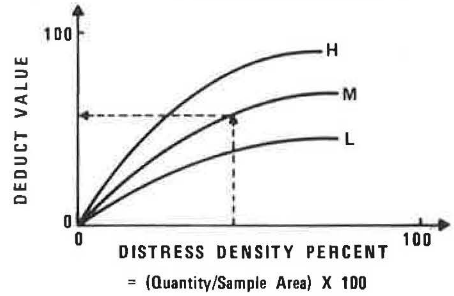

Figure 8. Corrected deduct values for asphalt- or tar-surfaced pavements.

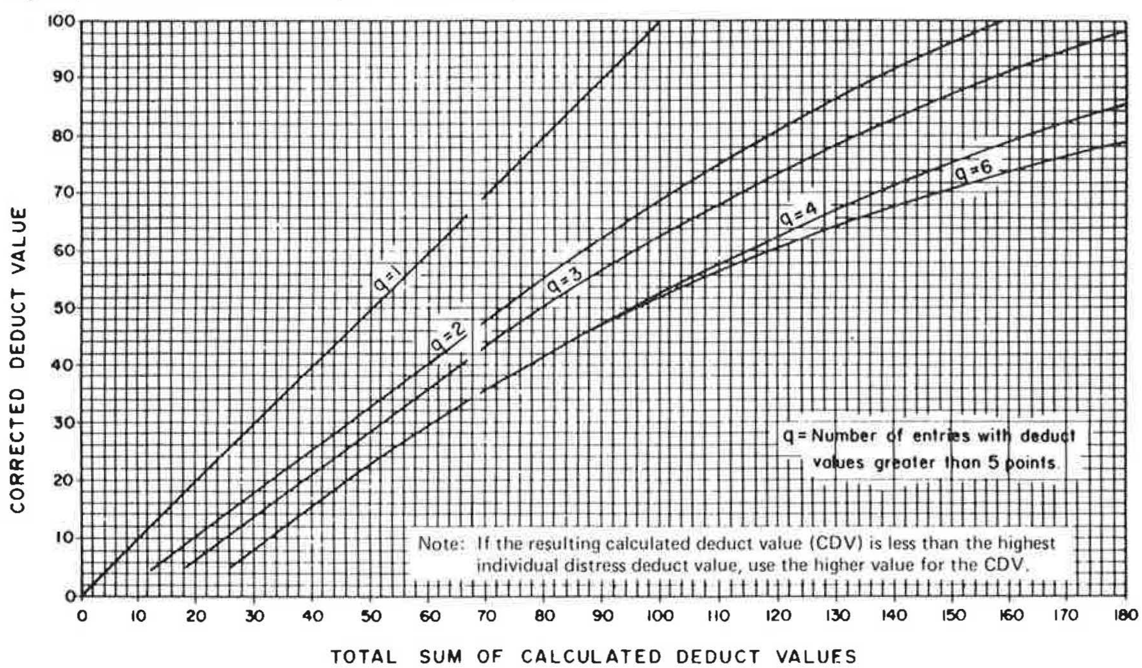

Figure 9. PCI calculation for sample unit.

DIST TYPE	DENSITY %	SEVERITY	DEDUCT VALUE
Allig. Crack	1.0	L	21
Block Crack	2.0	L	10
Block Crack	3.0	M	16
		Total =	47
		Corrected =	26
		PCI = 100–26 =	74

Figure 10. Extrapolated distress data for pavement feature.

PCI: Average PCI of Sample Units
Extrapolated Distress Data

DIST.TYPE	SEV.	QUANTITY	DENSITY	DEDUCT VALUE
Allig. Crack	L	450	0.9	20
Block Crack	L		2	10
Block Crack	M	1500	6	20

Figure 11. Example of computer output showing estimated cost based on distress data.

```
                          MRG REPORT

DATE := 82/04/22.      MAINTENANCE AND REPAIR GUIDELINES

BRANCH := TAXIWAY 7614                    BRANCH NMBR := T43A
SECTION NMBR := 1                         SECTION AREA :=     444 SY

DISTRESS       DIS   DIST-QTY     REPAIR CODE          LABOR LABOR MAT L EQUIP TOTAL
TYPE           SEV  REPAIR-QTY    REPAIR TYPE          HOURS COST$ COST$ COST$ COST$
------------------------------------------------------------------------------------
ALLIGATOR CR    M     2015  SF          2
                      2015  SF      DEEP PATCH          0.0   0.    0.    0. 22165.
ALLIGATOR CR    H       82  SF          2
                        82  SF      DEEP PATCH          0.0   0.    0.    0.   902.
L & T CR        M      145  LF          1
                       145  LF      CRACK FILLING       0.0   0.    0.    0.    73.
L & T CR        H       42  LF          1
                        42  LF      CRACK FILLING       0.0   0.    0.    0.    29.
RUTTING         H      998  SF         12
                       998  SF      SHALLOW PATCH       0.0   0.    0.    0.  1148.
------------------------------------------------------------------------------------
                                    TOTALS              0.0   0.    0.    0. 24317.
```

Figure 12. Sample computer output of PCI versus time plot.

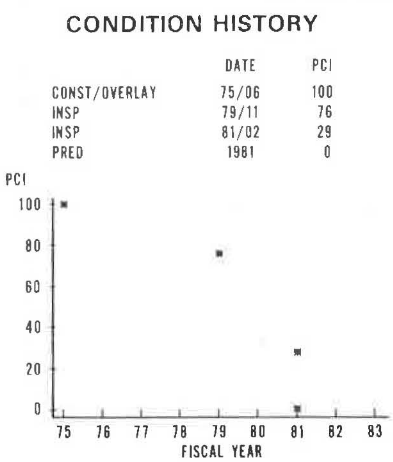

Figure 14. Relation between PCI, computed based on structural distress (PCI_{STR}), and C factor in U.S. Army Corps of Engineers design equation.

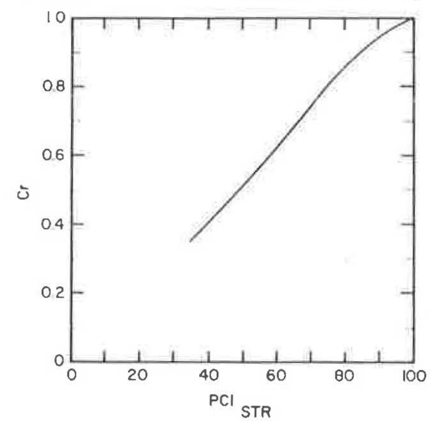

Figure 13. Sensitivity analysis of PCI prediction model, which is function of load, environment, and material thickness and properties.

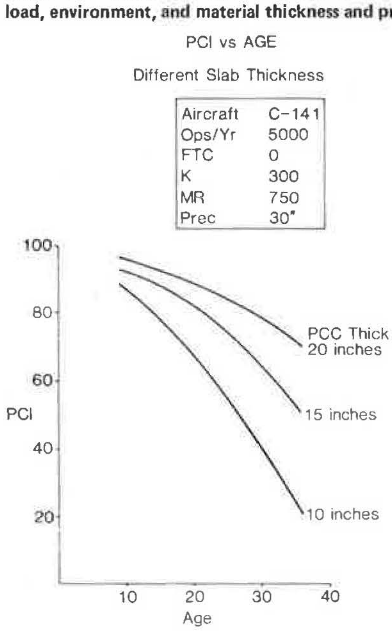

curves and totaled for the sample unit. The total deduct values are then corrected based on the number of deducts over 5 points and the total value of the deducts, as shown in Figure 8. Figure 9 is an example PCI calculation for a sample unit. The PCI for a feature is determined by averaging PCIs of the sample units inspected.

The distress for the feature is extrapolated based on the distresses determined for the sample units, as illustrated in Figure 10. To expedite the process of PCI calculations for a sample unit and a feature, a computer program has been prepared that performs these calculations in a batch or interactive mode. An important characteristic of PCI is that it agrees closely with the collective judgment of experienced pavement engineers. That was one of the objectives of its development. Another important characteristic is that it correlates closely with the needed level of maintenance and repair. This is particularly true because PCI is computed based on the distress.

ANALYSIS AND USE OF DISTRESS DATA

The distress data and PCI play an important role in pavement management at both the project level and the network level. At the project level the distress data can be used to determine the causes of failure. The calculations below show that the sum of deduct values due to alligator cracking (load caused) is 20 and due to block cracking (climate caused) is 30.

Percentage of deduct due to load = (20/50) x 100 = 40 percent

Percentage of deduct due to climate = (30/50) x 100 = 60 percent

The percentage of deduct value due to load and climate can be calculated as shown. The distress information can also be used to compute the cost of localized repair such as patching and crack filling, as shown in Figure 11. The figure shown is obtained from the PAVER pavement management system (4-6). The localized repair costs are computed based on user's identified maintenance policy and unit cost of repair. The program also computes the cost of overlay if requested.

Another important use at the project level is the determination of rate of deterioration, both for the short term and for the long term. This can be obtained by plotting the PCI versus time for the pavement, as shown in Figure 12. The consequence of various maintenance and repair alternatives is also achieved through PCI. Special mathematical models have been developed that correlate PCI deterioration with existing pavement structure, traffic, and climate. Figure 13 is a sensitivity analysis on the model for concrete pavement. The distress and PCI data also provide necessary information for overlay design. In the U.S. Army Corps of Engineers design Equation 1, C factor is computed that reflects the condition of existing pavement.

$$h_c = [h^p - C_r h_e^p]^{1/p} \tag{1}$$

where

- h_c = required concrete overlay thickness;
- h = designed concrete thickness for a new pavement;
- h_e = thickness of existing concrete pavement;
- p = 2.0 for unbonded overlay, 1.4 for partly bonded overlay, or 1.0 for fully bonded overlay; and
- C = 1.0 for existing pavement in good condition, 0.75 for existing pavement in fair condition, or 0.35 for existing pavement in poor condition.

Shahin and Darter (7) have developed a method with which the C factor can be more consistently determined by using the PCI information. The relation between PCI computed based on structural related distress only and the C factor is shown in Figure 14. Distress and PCI data are also very important at the network level. Various uses have been summarized by Shahin and Kohn (5). These include project prioritization, inspection scheduling, prediction of network condition, and budget planning.

SUMMARY AND CONCLUSIONS

A procedure for airfield pavement distress measurement and use in pavement management has been presented. The procedures are implemented by the U.S. Air Force and have been used by several states, including Illinois and Texas. In conclusion, distress provides invaluable information for management at both the project level and the network level. It is, however, important to emphasize that load-carrying capacity, roughness, and skid should also be considered, particularly at the project level.

ACKNOWLEDGMENT

The views expressed in this paper do not purport to reflect the position of the U.S. Department of the Army or the U.S. Department of Defense.

REFERENCES

1. Airfield Pavement Evaluation Program. U.S. Air Force Regulation 93-5, May 18, 1981.
2. Procedure for Condition Survey of Civil Airports. Federal Aviation Administration, Rept. FAA-RD-80-55, May 1980. NTIS: ADA 058860.
3. Road Surface Surveying System. Pacific Aero Survey Company, Ltd., Tokyo, Japan, 1977.
4. M.Y. Shahin and S.D. Kohn. Pavement Maintenance Management for Roads and Parking Lots. U.S. Army Construction Engineering Research Laboratory and U.S. Air Force Engineering and Services Center, Tech. Rept. M-294, Oct. 1981, 220 pp.
5. M.Y. Shahin and S.D. Kohn. Overview of PAVER Pavement Management System. TRB, Transportation Research Record 846, 1982, pp. 55-60.
6. S.D. Kohn and M.Y. Shahin. Economic Analysis of Field Implementation of PAVER Pavement Management. TRB, Transportation Research Record 846, 1982, pp. 61-66.
7. N.Y. Shahin and M.I. Darter. Rehabilitation Design for Airfield PCC Pavements. Proc., 2nd International Conference on Concrete Pavement Design, Indianapolis, April 1981.

Publication of this paper sponsored by Committee on Pavement Condition Evaluation.